

Pex19 and cytosolic Hsp70 are involved in the import of mitochondrial tail- anchored proteins

Dissertation

der Mathematisch-Naturwissenschaftlichen Fakultät

der Eberhard Karls Universität Tübingen

zur Erlangung des Grades eines

Doktors der Naturwissenschaften

(Dr. rer. nat.)

vorgelegt von

Bogdan Adam Cichocki

aus Warschau

Tübingen

2018

**Gedruckt mit Genehmigung der Mathematisch-Naturwissenschaftlichen
Fakultät der Eberhard Karls Universität Tübingen**

Tag der mündlichen Qualifikation:

Dekan: Prof. Dr. Wolfgang Rosentiel

1.Berichterstatter Prof. Dr. Doron Rapaport

2.Berichterstatter Prof. Dr. Gabriele Dodt

Table of contents

List of abbreviations	1
1. Summary.....	4
2. Introduction	5
2.1 Mitochondria	5
2.1.1 Origin of mitochondria.....	5
2.1.2 Structure and function of mitochondria	5
2.1.3 Dynamics of mitochondria	6
2.1.4 Protein import into mitochondria	8
2.1.4.1 Import Complexes	9
2.2 Peroxisomes - origin, function, dynamics and protein import.....	12
2.3 Tail-anchored (TA) proteins	15
2.4 Chaperones	18
2.4.1 Pex19	19
2.4.2 Heat shock proteins (HSP)	20
3. Aims of the study.....	23
4. Materials and Methods.....	24
4.1 Materials	24
4.1.1 Media.....	24
4.1.2 Buffers	26
4.1.3 Enzymes.....	29
4.1.4 Antibodies.....	30
4.1.5 Yeast and <i>E. coli</i> strains	31
4.1.6 Oligonucleotides	33
4.2 Methods	37
4.2.1 Molecular biology methods	37
4.2.1.1 Polymerase chain reaction (PCR)	37
4.2.1.2 Agarose gel electrophoresis	38
4.2.1.3 Extraction of DNA from agarose gel	38
4.2.2.4 Restriction digestion of DNA.....	38
4.2.2.5 Ligation with T4 DNA ligase	38

4.2.2.6 Preparation of chemically competent <i>E. coli</i> cells	38
4.2.2.7 Transformation of <i>E. coli</i> cells	39
4.2.2.8 Small scale plasmid isolation from <i>E. coli</i> cells (Miniprep)	39
4.2.2.9 Large scale plasmid isolation (Midiprep)	39
4.2.2 Methods in yeast genetics	40
4.2.2.1 Cultivation of yeast strains	40
4.2.2.2 Yeast transformation with the lithium acetate method	40
4.2.2.4 Construction of yeast deletion strains	40
4.2.2.5 Mating of yeast strains and tetrad analysis	41
4.2.3 Cell biology methods	41
4.2.3.1 Drop dilution assay	41
4.2.3.2 Cycloheximide treatment of yeast cells	42
4.2.3.3 Isolation of crude mitochondria	42
4.2.3.4 Isolation of pure mitochondria from yeast	42
4.2.3.5 Separation of mitochondria and peroxisomes by sucrose gradient	43
4.2.3.6 Obtaining of yeast extract	44
4.2.3.7 Fluorescence microscopy	45
4.2.4 Methods in protein biochemistry	46
4.2.4.1 Determination of protein concentration	46
4.2.4.2 Protein precipitation by trichloroacetic acid (TCA)	46
4.2.4.3 Protein precipitation by chloroform-methanol	46
4.2.4.4 Carbonate extraction	47
4.2.4.5 Proteinase K treatment	47
4.2.4.6 IASD assay	47
4.2.4.7 SDS-PAGE	47
4.2.4.8 Western blotting	49
4.2.4.9 Immunodetection of proteins	49
4.2.4.10 <i>In vitro</i> synthesis of radiolabeled proteins	49
4.2.4.11 <i>In vitro</i> import of proteins into mitochondria	51
4.2.4.12 Inactivation of Hsp40/Hsc70 complex by addition of inhibitors .	51
4.2.4.13 Autoradiography and quantification of bands	51
4.2.4.14 Overexpression and purification of GST-tagged proteins	52
4.2.4.15 Pull-down of mitochondrial proteins with purified GST-tagged proteins	53

5. Results	54
5.1 Cytosolic Hsp70s and their yeast co-chaperone Sti1 are required for Fis1 mitochondrial biogenesis.....	54
5.2 Pex19 chaperone affects mitochondrial functionality	57
5.3 Pex19 is involved in biogenesis of mitochondrial Fis1 and Gem1	59
5.4 Pex19 is contributing to Atg32-HA biogenesis	63
5.5 Peroxisomal contaminations in crude mitochondria fraction do not affect the outcome of the assays	64
5.6 Pex19 does not influence the stability of mitochondrial TA proteins	66
5.7 Pex19 is an interactor of Fis1 and Gem1	68
5.8 The TA region of Gem1 is sufficient for recognition by Pex19	69
5.9 GFP-Gem1 and GFP-Gem1(TMS) are dually localized to mitochondria and peroxisomes.....	70
5.10 Pex19 is required for import of Fis1 and Gem1 into mitochondria	72
5.11 Pex19 is localized to mitochondria.....	74
5.12 Mim1 and Tom20 are involved in the biogenesis of Atg32-HA	75
5.13 The effects of deletion of Pex19 and Sti1 are not cumulative	79
6. Discussion	81
6.1 Hsp70 chaperone complex involved in Fis1 biogenesis.....	81
6.2 Possible roles of Pex19 in the biogenesis of MOM TA proteins.....	83
6.3 Pex19 has impact on mitochondrial functionality	86
6.4 Pex19 is bound to the mitochondrial membrane	87
6.6 The biogenesis pathway of MOM TA proteins	90
6.7 Evolution of the dual-localized TA proteome.....	90
6.8 Summary	91
7. References	92
Acknowledgments	107
Curriculum Vitae	108

List of abbreviations

AA	acryl amide
AAC	ADP/ATP carrier
AMP	ampicillin
APS	ammonium peroxodisulfate
Atg32	AuTophagy related 32
ATP	adenosine triphosphate
bp	base pair
bis-AA	bis-acryl amide
Bmh1	brain modulosignalin homologue 1
CTE	C-terminal extension
BSA	bovine serum albumin
DHFR	dihydrofolate reductase
DTT	dithiotreitol
Dnm1	DyNaMin-related 1
dNTP	desoxynucleoside triphosphate
<i>E. coli</i>	<i>Escherichia coli</i>
ECL	Enhanced chemiluminescence
EDTA	ethylenediaminetetraacetic acid
ER	Endoplasmic reticulum
Fis1	Fission protein 1
Gem1	GTPase EF-hand protein of mitochondria 1
GET	Guided Entry of Tail-anchor
GFP	Green fluorescence protein
GST	Glutathione-S transferase
GTP	guanosine triphosphate
HA	heme agglutinin
HEPES	N-2 hydroxyl piperazine-N'-2-ethane sulphonic acid

Hex	hexokinase
Hsp	Heat shock protein
IASD	4-acetamido-4'-[(iodoacetyl)amino]stilbene-2,2'-disulfonic acid
IM	Inner membrane
IMS	Intermembrane space
MIM	Mitochondrial inner membrane
MIM complex	Mitochondrial import complex
MOM	Mitochondrial outer membrane
mtDNA	mitochondrial genome
OD	optical density
PAS	pre-autophagosomal structure
PCR	polymerase chain reaction
PEX	PEroXisome related
PK	Proteinase K
PMSF	Phenylmethylsulonylfluride
mPTS	Peroxisomal membrane Targeting Signal
RNA	ribonucleic acid
<i>S. cerevisiae</i>	<i>Saccharomyces cerevisiae</i>
SDS	sodium dodecyl sulfate
SND	SRP iNDependent targeting
SSa	Stress-seventy subfamily A
Ssb	Stress-seventy subfamily B
SRP	Signal Recognition Particle
Sti1	Stress inducible 1
TA	tail anchored
TEMED	N,N,N',N'-tetramethylene diamine
TMS	transmembrane segment
TPR	Tetratricopeptide
TOB complex	Topogenesis of β -barrel proteins complex

Tob55	subunit of TOB complex 55
TOM	Translocase of the outer membrane
Tris	tris-(hydroxymethyl)-aminomethane
TX-100	Triton X-100
v/v	volume per volume
w/v	weight per volume
WT	wild type

1. Summary

The Majority of mitochondrial proteins are synthesized in the cytosol and afterwards targeted to the organelle. The transport process is accompanied by cytosolic factors, which ensure targeting specificity and prevent the proteins from aggregation in the aqueous environment of the cytosol. This especially applies to tail-anchored (TA) proteins that are directed to membranes in a post-translational manner. Tail-anchored proteins are embedded into their corresponding membrane via a single transmembrane segment at their C-terminus whereas the majority of the protein is facing the cytosol. The targeting pathways of these proteins to the ER or to peroxisomes have been characterized. However, so far, cellular factors that mediate the integration of such proteins into the mitochondrial outer membrane have not been found. Equally elusive remains the existence of mitochondrial membrane insertases or receptors for TA import. Thus, it is currently postulated that import of mitochondrial TA proteins is mediated solely by unassisted insertion without the requirement of any protein factors.

Using budding yeast as a model system, we identified the cytosolic Hsp70 chaperone Ssa1, its co-chaperone Sti1, and the peroxisome import factor Pex19 as mediators of import of mitochondrial TA proteins. Accordingly, deletion of *PEX19* results in: (i) growth defect under respiration conditions; (ii) alteration in mitochondrial morphology; (iii) reduced steady-state levels of the mitochondrial single span proteins Fis1, Gem1, and Atg32; and (iv) hampered *in organello* import of the TA proteins Fis1 and Gem1. Furthermore, we demonstrate that recombinant Pex19 can bind directly the TA proteins Fis1 and Gem1 and that all three proteins share a mitochondrial and peroxisomal dual localization. Alteration in Atg32 levels are dependent on the mitochondrial receptors Mim1 and Tom20 suggesting that both can mediate Pex19 binding to mitochondria. Collectively, this work identified the first factors that are involved in the biogenesis of mitochondrial TA proteins and uncovered an unexpected function of Pex19.

2. Introduction

2.1 Mitochondria

2.1.1 Origin of mitochondria

According to the endosymbiont hypothesis mitochondria are derived from *α-proteobacteria* which were incorporated into the protoeucariotic cell in a single event over 1.5 billion years ago (Dyall et al., 2004; Gray, 2012; Martin et al., 2015). Over time, the symbiotic intracellular organism transformed into mitochondria. During this process, the genetic material was transferred into the host genome or deleted leaving only a minor part (less than 1%) of the original genome in the mitochondria. Nowadays, the mitochondrial genome (mtDNA) encodes proteins mainly of the the respiratory chain (13 in mammals and 8 in *Saccharomyces cerevisiae*) as well as 2 ribosomal RNAs (rRNA) and several transfer RNAs (tRNA) involved in the mitochondrial translation system. Additionally, in *Saccharomyces cerevisiae* the 9S component of the RNAase P and the ribosomal protein Var1 are encoded in the mtDNA (Chen and Butow, 2005; Freel et al., 2015; Westermann, 2014). The remaining mitochondrial proteins, around 1000 in yeast and 1500 in mammals, are encoded in the nucleus (Morgenstern et al., 2017; Palmfeldt and Bross, 2017)

2.1.2 Structure and function of mitochondria

In contrast to other organelles, mitochondria are composed of two membranes. These two membranes enclose and isolate the inner of the mitochondria and divide it into two additional compartments such as the inter-membrane space (IMS) between the two membranes, and the matrix as the inner most compartment (Wiedemann and Pfanner, 2017). Due to this unique structure, mitochondria are able to generate energy from oxidative phosphorylation. The IMS is in part impenetrable for small ion compounds including protons allowing, by pumping protons from the matrix into the IMS, the creation of an electrochemical potential across the membrane, described as the membrane

potential. The resulting flux of protons into the matrix through a designated protein machinery called the ATPase synthase is believed to generate energy required for the synthesis of ATP (Nunnari and Suomalainen, 2012). The separation of the mitochondrial inner compartments from the cell environment allows the mitochondria to participate in other metabolic functions like β -oxidation of fatty acids, tricarboxylic acid cycle, the generation of iron-sulfur clusters, amino acids and, heme cofactors (Ahn and Metallo, 2015; Lill, 2009; Osellame et al., 2012). In higher eukaryotes mitochondria function is expanding to regulatory functions in apoptosis, autophagy, and aging (Youle and Karbowski, 2005).

2.1.3 Dynamics of mitochondria

Mitochondria are dynamic organelles, which constantly divide and fuse. The plasticity of the organelle significantly influences a broad range of mitochondrial features including mitochondrial DNA stability, respiratory capacity, stress-response, apoptosis and mitophagy. Dysfunction of mitochondrial dynamics can lead to severe disorders including neurodegenerative disease (Chan, 2012). Fusion and fission of mitochondria are regulated by proteins belonging to the dynamin family. This protein family, known to function in vesicle trafficking, possesses a GTPase effector domain. After oligomerization of dynamin-like proteins the GTP hydrolysis by the GTPase domain generates the force required for scissoring lipid membranes or merging them (van der Bliek et al., 2013). In yeast cells, fusion of the mitochondrial membranes is achieved by two factors such as the MOM protein Fzo1 and the IM protein Mgm1. Fzo1 facilitates the fusion of the MOM whereas Mgm1 of the MIM. IM fusion is always coordinated and subsequent to the MOM fusion (Chan, 2012).

In contrast to fusion, the dynamin homolog involved in fission is a cytosolic protein, Dnm1. To bind the membrane, it needs to interact with its adaptor proteins Mdv1 or Caf4, which in turn associate with the tetratricopeptide domain of Fis1. Fis1 is bound via a single transmembrane segment (TMS) to the MOM and consequently allows the oligomerization of Dnm1 in a ring around the fission site. Later constriction of this ring upon GTP hydrolysis leads to scission of the membrane (Chan, 2012; Merz et al., 2007). In mammals, more membrane

receptors for the adaptor proteins are found including Mff, GDAP1, Mid49, and Mid51 (Palmer et al., 2011).

The placement of the scission is dependent on the location of fission factors but also on the inter-organelle interaction with the ER. The latter has been noticed to wrap around the fission site before recruitment of Drp1 (human homolog Dnm1) and so it determines the place of fission. Similarly, Mff is recruited to ER-Mitochondria contact sites before Drp1 binding (Friedman et al., 2011). The exact reason for the involvement of ER in the fission process is not well understood. It has been proposed that the ER might, via contact sites, alter the lipid composition of the MOM to recruit additional fission factors to the construction site (Friedman and Nunnari, 2014). Lipid transport to the mitochondria is facilitated mainly by the ERMES (ER-mitochondria encounter structure) contact site (Dimmer and Rapaport, 2017). Surprisingly, in yeast the formation of the ERMES is regulated by Gem1, a rho GTPase which has been proposed to alter mitochondrial morphology and determine the distribution of daughter mitochondria after fission (Kornmann et al., 2011; Murley et al., 2013). Similarly, the human homologs of Gem1 (Miro1 and Miro2) function in mitochondrial trafficking (Fransson et al., 2006). Thus, it has been suggested that Gem1 functions in the fission process as part of the tether between mitochondria and ER (Friedman and Nunnari, 2014; Merz et al., 2007).

Mitochondrial dynamics play an important role in autophagy and mitophagy. Mitochondrial fission enhances the catabolic processes whereas fusion acts in contrary, inhibiting mitochondrial degradation (Youle and Karbowski, 2005). Especially in mitophagy, fission is believed to allow segregation of damaged mitochondrial proteome from functional mitochondria and to direct it so to lysis (Müller et al., 2015). One of the key regulators of mitophagy is the mitochondrial protein Atg32. Atg32 is composed of a cytosolic N-terminal region, a C-terminal IMS region and a single TMS anchoring it to the MOM. Upon mitochondrial damage the N-terminal region of Atg32 recruits the autophagy factors Atg11 and later Atg8, which in turn recruits mitochondria to the pre-autophagosomal structure (PAS) preceding the creation of the autophagosome (Kondo-Okamoto et al., 2012). Atg11 was demonstrated to

interact with Dnm1 and accordingly is suggested to promote mitochondrial fission after mitophagy induction (Mao et al., 2013).

2.1.4 Protein import into mitochondria

The majority of mitochondrial proteins is encoded in the nucleus and synthesized on cytosolic ribosomes. In comparison to mtDNA coded proteins, synthesis in the cytosol generates a number of physiological obstacles for the mitochondria proteins, especially the membrane proteins, which the cell has to overcome. The two main ones are the mislocalization of proteins to other organelles and the aggregation of hydrophobic proteins in the cytosolic aqueous environment. To prevent these unfavoured events, an extensive network of protein factors was evolved to escort mitochondrial proteins from their time of synthesis in cytosol till their incorporation into the right mitochondrial compartment. The role of cytosolic chaperones in this process is described in section 2.4

Mitochondrial import is facilitated by coordinated work of specific receptors and complexes in the mitochondrial membranes (Fig. 2.1). About 70% of all mitochondrial proteins are synthesized with a cleavable presequence which serves as the targeting factor to mitochondria (Vögtle et al., 2009). Pre-sequences are variable in size ranging from 10 to 100 residues. A characteristic feature of presequences is their ability to form an amphipathic α -helix containing one hydrophobic face and positively charged surface recognized by mitochondrial receptors (Wiedemann and Pfanner, 2017). The remaining mitochondrial proteins, including all outer membrane proteins, some IMS proteins, and proteins with internal targeting signal, possess non-cleavable targeting signals (Chacinska et al., 2009)

For many years it was believed that all mitochondrial proteins are imported in post-translational fashion. However, co-translational import is an efficient way of preventing aggregation of hydrophobic proteins like in the case of the SRP-pathway for ER insertion (Nyathi et al., 2013). Recently, some mitochondrial proteins, including mainly IM proteins, have been suggested to be imported co-translationally (Williams et al., 2014). Ribosome association with mitochondria

has been confirmed with electron microscopy and messenger RNA (mRNA) enrichment on mitochondria has been demonstrated for human and yeast (Gadir et al., 2011; Gold et al., 2017). Ribosomes are believed to associate with mitochondria via the translocase of outer membrane (TOM) complex. The linking tether between the two machineries was found to be the nascent chain translated from the ribosome (Gold et al., 2017).

2.1.4.1 Import Complexes

Protein import into mitochondria is facilitated by seven import machineries. Two translocases of the inner membranes (TIMs) import presequence-carrying proteins (TIM23) and IM proteins with internal targeting signal (TIM22). Import of proteins with cysteine rich motifs is dependent on Mia40. The TOB complex of the MOM is required for biogenesis of β -barrel proteins whereas another MOM complex (MIM) inserts helical single- and multispan proteins. The biogenesis of all the aforementioned protein classes is dependent on the TOM complex (Wiedemann and Pfanner, 2017). The two biogenesis pathways unrelated to the TOM complex are the Oxa1-mediated insertion of mitochondrially encoded proteins into the IM and the integration into the OM of some tail-anchored proteins (Chacinska et al., 2009).

The TOM complex consists of four receptors (Tom70, Tom71, Tom20, Tom22), the protein channel Tom40 and three small subunits (Tom5, Tom6 and Tom7). Tom22 is believed to form the central receptor, which receives the precursor proteins from Tom20 and Tom70/71 and passes them to the import pore Tom40 (Neupert and Herrmann, 2007). Tom20 specifically recognizes the presequence-containing proteins, whereas the receptors Tom70 and Tom71 recognize non-cleavable precursors like carrier proteins. However, all three receptors have partially overlapping substrate specificities (Yamano et al., 2008). Likewise, all three of them are believed to be involved in β -barrel protein import (Jores et al., 2016). The small Tom subunits are dispensable for the function of the TOM complex although they are involved in the assembly and stability of the complex. Tom6 and Tom5 promote the assembly of the complex, whereas Tom7 stimulate the dissociation of the complex, most likely by titrating Mdm10,

a β -barrel protein required for biogenesis of Tom22 (Dembowski et al., 2001; Yamano et al., 2010). Additionally, Tom5 is believed to mediate transfer of precursors from Tom22 to Tom40 (Chacinska et al., 2009).

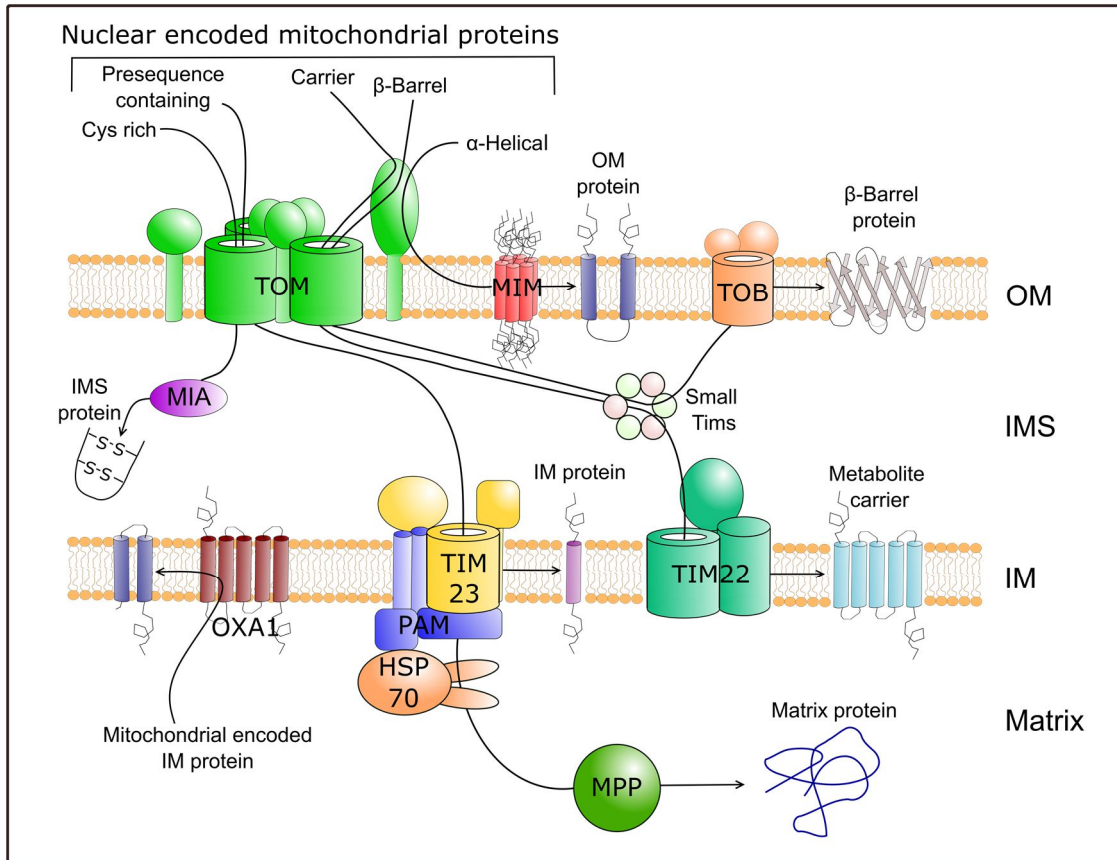


Fig 2.1 Import machineries of yeast mitochondria. Almost all nuclear encoded mitochondrial proteins are passing through the TOM complex during their biogenesis. α -helical proteins are passed from the surface receptor Tom70 to the MIM complex before insertion into the OM. The remaining mitochondrial proteins are transported by TOM import pore to the IMS. Cysteine rich proteins are oxidized by the MIA complex trapping the proteins in the IMS. β -barrel proteins are escorted by the small Tim chaperones in the IMS and inserted through the TOB complex in the OM. Similarly, carrier proteins require the small Tim chaperones for their biogenesis but are inserted into the IM by the TIM22 complex. Presequence containing proteins are passed from the TOM pore to the TIM23 complex, which either inserts them into the IM or translocates them through the IM membrane. Translocation to the matrix is dependent on the PAM complex and mtHsp70, which generate the force necessary for pulling the presequence protein through TIM23. After the presequence proteins reach the matrix they are processed by the mitochondrial processing peptidase (MPP) resulting in the formation of a mature matrix protein.

In order to facilitate import of precursors, the TOM complex has to work in cooperation with chaperones and other insertases. As such, Tom40 hands presequence-containing precursor proteins to the TIM23 complex, which transports them either to the matrix or releases them to the IM (van der Laan et al., 2007; Neupert and Herrmann, 2007). The pulling force for matrix import is generated by the membrane potential across the IM and a ATP dependent chaperone motor based on the mitochondrial chaperone Hsp70 (mtHsp70) (Chacinska et al., 2005; Kang et al., 1990).

Similarly, import of IMS proteins is Tom40 dependent. Import of proteins with cysteine rich motifs is facilitated by passing of such precursor proteins from Tom40 to the IMS protein Mia40. Mia40 oxidizes the cysteine residues of the imported protein leading to formation of intramolecular disulfide bonds. The subsequent folding prevents the protein from leaving the IMS back to cytosol (Chacinska et al., 2004).

IM proteins with internal targeting signal or β -barrel proteins are transported initially via the pore of Tom40 before their engagement by the small Tim chaperones (Tim9 and 10) in the IMS. These small chaperones in turn, transfer the internal targeting signal proteins to the Tim22 insertase complex which finally releases them to the IM. β -barrel proteins are routed from the small Tims to the MOM where the TOB complex mediates their integration into the membrane (Wiedemann and Pfanner, 2017).

Cooperation of Tom70 with the MIM complex leads to import of multispan proteins (Becker et al., 2011). The MIM complex itself is composed of two proteins with single TMS: Mim1 and Mim2, which together are believed to form a membrane pore in the MOM (Dimmer et al., 2012; Krüger et al., 2017). Surprisingly, the import of Mim1 itself is dependent on the cytosolic co-chaperones Djp1 and the Tom70 receptor (Papic et al., 2011).

MIM was similarly demonstrated to facilitate the import of α -helical membrane proteins with a single TMS (Becker et al., 2008). Accordingly, MIM regulates the membrane insertion of the signal-anchored proteins Tom20 and Tom70 and their assembly with the TOM complex (Popov-Celeketić et al., 2008).

Another class of α -helical proteins which biogenesis is dependent on MIM are the tail-anchored (discussed in Chapter 2.3) small TOM subunits (Becker et al., 2010; Dembowski et al., 2001; Waizenegger et al., 2005). The import of single span proteins is one of the few examples of mitochondrial protein import where a clear involvement of the TOM complex was not demonstrated.

2.2 Peroxisomes - origin, function, dynamics and protein import

Similarly to mitochondria, the peroxisomes were believed to have an endosymbiotic origin (de Duve, 1969). This view was based on the fact that both organelles are able to self-replicate in the cellular environment. Moreover, phylogenetic analysis of the peroxisomal proteome revealed that 33-38% of its proteins have prokaryotic or archaeal ancestry (Gabaldón et al., 2006). Mitochondria were selected as a possible origin for peroxisomes, since many mitochondrial proteins are dual-localized and both organelles are functionally related (Mohanty and McBride, 2013). Additionally, peroxisomes share the same division machinery with mitochondria. However, studies over the last decade have demonstrated that peroxisomes can be formed *de novo* from ER, a mechanism which is not known for mitochondria nor chloroplast (Dimitrov et al., 2013). These studies reasoned that peroxisomes origin from the ER and its genesis is not connected to an endosymbiont (Schliebs et al., 2010). This view was questioned when recently mitochondria were shown to be involved in peroxisomal generation *de novo* (Sugiura et al., 2017).

Peroxisome main function is assigned to β -oxidation of fatty acids. In yeast, this process is solely performed by peroxisomes whereas in mammals it is shared with mitochondria. Peroxisomal biogenesis is greatly enhanced if cells are fed by fatty acids (such as oleate). Aside from β -oxidation, the second main function of peroxisomes is the reduction of reactive oxygen species (Smith and Aitchison, 2013). A plethora of additional metabolic functions are catabolized in the peroxisomal lumen like biotin and penicillin synthesis or amino acid degradation (Meijer et al., 2010; Tanabe et al., 2011). However, peroxisomes are evolutionary plastic and harbor various functions across diverse species (Smith and Aitchison, 2013). In humans, a further function shared between mitochondria

and peroxisomes includes the recruitment of both organelles in antiviral signaling which is dependent on the insertion of the TA protein MAVS into both organelles (Dixit et al., 2010).

Peroxisomal functionality is strictly connected to its biogenesis. The biogenesis of peroxisomes is controlled by proteins called peroxines that are encoded by PEX genes, which were initially identified in yeast. Loss of function in humans of one of 13 PEX genes leads to peroxisomal biogenesis disorders (PBDs). As peroxisomes in humans are involved in the biosynthesis of plasmalogen, PBDs cause severe neural defects including the lethal Zellweger syndrome (Gould and Valle, 2000; Matsuzono et al., 1999; Waterham et al., 2016). Additionally, these disorders are not only characterized by peroxisome dysfunction but also result in functional alteration in mitochondria (Baumgart et al., 2001; Dirkx et al., 2005; Ferrer et al., 2005).

New peroxisomes are created in two ways, either by growth and division or by *de novo* formation from the ER (Hoepfner et al., 2005; Lazarow and Fujiki, 1985). Formation from the ER is believed to be the main pathway of peroxisome generation in yeast (van der Zand et al., 2010). In this pathway, peroxisomal membrane proteins (PMP) are imported to the ER and distributed to specific subdomains, which later will bud off and fuse with each other to form mature peroxisomes (van der Zand et al., 2012). Peroxisome replication is facilitated first by import of proteins and lipids and later fission, which resembles the fission process of mitochondria. Both processes require pre-constriction of the membrane leading to local requirement of scission factors. Similarly to mitochondria, peroxisomes in mammalian cells recruit to the fission site membrane proteins like Fis1, Mff, and GDAP1, whereas in yeast cells the adaptor proteins Mdv1 and Caf4 and the dynamin-like protein Dnm1/DLP1 are assembled at the fission site (Gandre-Babbe and van der Bliiek, 2008; Huber et al., 2013; Koch et al., 2005; Schrader et al., 2016). In contrast to mitochondria, peroxisomal division is regulated by an additional peroxin family Pex11, which is believed to deform the peroxisomal membrane at pre-constriction sites, interact and recruit Fis1 and Mff to the membrane, and stimulate Dnm1/DLP1 GTPase activity

leading to oligomerization of the scission ring (Koch and Brocard, 2012; Williams et al., 2015; Yoshida et al., 2015).

Interestingly, similar to mitochondria, peroxisomal membrane dynamics are linked to autophagy (Mao et al., 2014). Likewise, the pexophagy is regulated by Atg11, Atg8 and PAS (Motley et al., 2012). The size of the peroxisome is a limiting factor for the engulfment of the compartment by the autophagosome. Thus, during induction of phagocytosis, Atg11 recruits to the peroxisomal membrane Dnm1 and Vps1 which in turn can mediate fission. Of note, this complex assembly seems to occur only at peroxisome-mitochondria contact sites (Mao et al., 2014). Atg11 recruitment to peroxisomes is facilitated by the peroxisomal protein Atg36 in contrast to mitochondria where it is mediated by Atg32 (Müller et al., 2015).

Peroxisomal fission as well as *de novo* synthesis is dependent on import of PMPs to the new forming organelles. Interestingly, for both processes PMP import is believed to be facilitated by the general peroxisome targeting chaperone Pex19, its membrane receptor Pex3, and additionally in mammals PMP receptor Pex16 (Hoepfner et al., 2005, 2005; Schmidt et al., 2012). PMPs harbor one or multiply specific peroxisomal membrane targeting signals (mPTS) built of positively charged residues close to their TMS (Honsho and Fujiki, 2001; Jones et al., 2001). The mPTSs can be divided into two classes dependently whether the PMP can bind to Pex19 (Honsho and Fujiki, 2001). Proteins carrying the mPTS1 signal require Pex19 binding for their targeting whereas mPTS2-harboring proteins do not. So far, except for some yeast peroxisomal TA proteins, which import can be Pex19 independent, Pex3 and Pex22 are the only verified proteins with mPTS2 (Buentzel et al., 2015; Giannopoulou et al., 2016).

According to the semi-autonomous peroxisome biogenesis model, Pex19 supports peroxisomal protein biogenesis in two different ways (Mayerhofer, 2016). It either delivers them to the peroxisomes directly and transfers them to Pex3, which in turn inserts the proteins to the membrane, or Pex19 promotes together with Pex3 early peroxisome budding from ER subdomains (Hoepfner et al., 2005; Jones et al., 2004; Matsuzono and Fujiki, 2006). The latter has been suggested to occur via recruitment of a budding machinery to the ER subdomains

which is catalyzed by the Pex3-Pex19 interaction (Mayerhofer, 2016). The mechanism of import of mPTS2 proteins is unknown although in mammals, it has been suggested that Pex16 can facilitate the direct import of Pex3 into peroxisomes and dedicated subdomains in the ER (Aranovich et al., 2014).

Recently, a second *de novo* synthesis pathway for peroxisomes has been demonstrated. In this pathway peroxins Pex3 and Pex14 in an event of pexophagy are targeted to mitochondria where they initiate formation of pre-peroxisomes similarly to the one found in the ER. These pre-peroxisomes are subsequently budding of mitochondria and fusing with ER derived peroxisomes containing Pex16 in order to form fully import competent mature peroxisomes. Interestingly, although the Pex3 receptor is one of the proteins located in mitochondria pre-peroxisomes, import of peroxines and budding of the peroxisome-mitochondria compartment could not be inhibited by knock-down of Pex19 (Schrul and Kopito, 2016).

2.3 Tail-anchored (TA) proteins

Tail-anchored (TA) proteins comprise 3-5% of all eukaryotic membrane proteins (Hegde and Keenan, 2011). They are characterized by a single TMS at their C-terminus that serves as a targeting signal and as the anchor of the protein to the membrane, leaving the N-terminal part exposed to the cytosol. TA proteins participate in a broad range of processes from organelle fission, contact site formation, protein import, and apoptosis to vesicle targeting and anti-viral response (Borgese and Fasana, 2011; Krumpke et al., 2012; Schrader et al., 2015; Sherman et al., 2005). As the TMS of TA proteins is synthesized as the last part of the protein, the targeting of these proteins is performed after the TMS dissociates from the ribosomes and therefore is post-translational (Hegde and Keenan, 2011). In order to prevent the TA proteins from aggregation, various cytosolic factors are ensuring their proper folding and delivery to the right compartment (Chio et al., 2017). TA proteins are inserted from the cytosol to peroxisomes, mitochondria, or to the ER from which they are distributed to the plasma membrane or other compartments of the secretory pathway (Borgese and Fasana, 2011).

In *S. cerevisiae*, targeting of TA proteins to the ER is mainly ensured by the GET pathway. However, alternative routes such as the Hsp40-Hsp70 complex, the SRP pathway, or the recently discovered SND pathway were also reported. Peroxisomal targeting is believed to be facilitated by the aforementioned chaperone Pex19 (Abell et al., 2004; Aviram et al., 2016; Rabu et al., 2008; Schuldiner et al., 2008).

The GET pathway is the most studied pathway of TA insertion and consists of membrane bound receptors Get1/Get2 and cytosolic recognition complex formed of Get3, Get4, Get5 and their co-chaperone Sgt2. After GET client TA proteins are released from ribosomes, they are captured by the co-chaperone Sgt2, which passes them to Get3 in a process catalyzed by the Get4/5 complex. An ATP hydrolysis-dependent process releases Get3 together with the substrate from Get4/5. Next, the TA protein is inserted into the ER membrane through interaction with the Get1/2 receptor complex. The multistep insertion process of the protein to the ER membrane ensures a mechanism of substrate selection in which each Get factor contributes to the targeting specificity by acting as a selection filter (Rao et al., 2016). Although the Get pathway is believed to be the main entry gate for TA proteins to the ER, loss of its functionality does not lead to complete abolishment of TA insertion. This is most likely because the alternative SND and SRP routes can compensate for the loss of the Get pathway (Haßdenteufel et al., 2017). Moreover, some ER TA proteins were demonstrated to insert into liposomes independently of any targeting factors (Brambillasca et al., 2005).

Despite extensive knowledge regarding the delivery of TA proteins to other compartments, targeting factors for mitochondrial TA proteins have not been identified yet. Previous reports raised many questions regarding the existence of targeting and receptor/insertion machineries. On the one side, levels of yeast mitochondrial TA proteins such as the small Tom subunits, Tom5, 6 and 7, were found to be dependent on Mim1, Mas37/Sam37 and Tom receptors (Becker et al., 2008; Horie et al., 2002; Setoguchi et al., 2006; Stojanovski et al., 2007; Thornton et al., 2010). In yeast and mammals, Tom5 levels also rely on Tom40 abundance. Additionally, import of Bak in mammalian cells is dependent on the

mitochondrial pore VDAC2 whereas the Tom subunits are dispensable for its import. On the other side, import in mammals of other TA proteins like Omp25 and Bcl-XL was completely independent of the Tom subunits and any protease accessible protein on the surface of the mitochondria (Horie et al., 2003; Setoguchi et al., 2006). Likewise, in yeast Fis1 import was unaffected by deletion of TOM or TOB/SAM subunits and digestion of any protease accessible protein at the mitochondria outer membrane (MOM). This raised doubts about the necessity of membrane receptors for insertion of TA proteins into the MOM and suggests that the small TOM subunits might follow a unique import pathway (Kemper et al., 2008).

In vitro import assays of MOM TA proteins demonstrated that Fis1 can insert spontaneously into liposomes (Kemper et al., 2008). Studies on the early stages of the import of mitochondrial TA proteins in mammalian cells suggested that TA proteins do not need any cytosolic factors for insertion although some level of folding seem to be required (Itakura et al., 2016; Setoguchi et al., 2006). Taken together, these observations led to a hypothesis that mitochondrial TA proteins are able to integrate into the mitochondria lipid bilayer in an unassisted manner but cytosolic factors are likely necessary to keep the hydrophobic TMS in an import competent state (Borgese and Fasana, 2011). Such spontaneous insertion could be facilitated by the specific lipid composition of the mitochondria. For example, these organelles contain low ergosterol levels. Accordingly, reduction of ergosterol levels in ER membranes were shown to lead to mislocalization of the MOM TA proteins Gem1 and Fis1 to ER (Krumpe et al., 2012).

However, the hypothesis of spontaneous insertion of MOM TA proteins leaves some unanswered questions. First is the aforementioned requirement of cytosolic chaperones in the process. Since some mitochondrial proteins are known to require Hsp70/90 chaperones (only Hsp70 in yeast) involvement in their import, it has been suggested that Hsp70 chaperone complexes could fulfill this role also for mitochondrial TA proteins (Borgese and Fasana, 2011; Humphries et al., 2005; Young et al., 2003). Second, MOM TA proteins have to be able to distinguish among the specific compartment of the cells in order to avoid

mislocalization to other organelles. Segregation between the various pathways is believed to be achieved via different composition of the TMS. The TMS and the flanking residues of sole MOM TA is less hydrophobic and has less helical content than in ER TAs (a signal which is recognized by the GET pathway) and its C-terminal element (CTE) is less charged than of peroxisomes TA proteins (a signal which is recognized by Pex19) (Chio et al., 2017; Costello et al., 2017; Rao et al., 2016).

Surprisingly, many of the MOM proteins (not related to the small Tom complex) are shared between organelles, especially with the peroxisomes (Ast et al., 2013). TA proteins comprise a significant part of the proteins that are dually-localized to both mitochondria and peroxisomes. In humans OMP25, Bcl-2, Bcl-XL, MAVS, GDAP1, Mff, Fis1 and the Gem1 homologs Miro1 and Miro2 have been identified in both compartments (Costello et al., 2017). In yeast, such extensive studies were not performed leaving Fis1 as the only TA protein identified in both peroxisome and mitochondria (Motley et al., 2008; Mozdy et al., 2000). Of note, the signal anchored protein Msp1/ATAD1, which is involved in removal of mistargeted TA proteins, is also dual localized to both compartments, further underscoring the importance of correct proteostasis of TA proteins in the organelles membranes (Chen et al., 2014b; Okreglak and Walter, 2014).

2.4 Chaperones

Cells grow optimally in a narrow niche of conditions and deviations from these conditions are regarded as stress. In order to tolerate the changing environment, cells have developed various adaptation mechanisms. One of these mechanisms are the molecular chaperones called also heat shock proteins (HSP), as historically the first chaperones were identified to be induced by elevated temperature. However, nowadays chaperones are known to function also in native conditions (Ellis, 1987; Verghese et al., 2012). Chaperones protect proteins from aggregation, unfold protein aggregates, refold damaged proteins or direct them for degradation, and participate in biogenesis of proteins. To facilitate such diversity of functions, cells encode many families of chaperones destined to

different activities. However, growing evidence demonstrates that these proteins cooperate in multi-chaperone networks (Gong et al., 2009).

2.4.1 Pex19

Pex19 targets PMPs to peroxisomes and is involved in their membrane integration. In addition, it also functions as a chaperone by binding mPTS1 proteins and stabilizing them in the cytosol before their delivery to the membrane (Chen et al., 2014a; Jones et al., 2004). Pex19 is composed of two domains: a disordered N-terminal domain necessary for Pex3 binding and a globular C-terminal domain required for substrate binding (Chen et al., 2014a). Pex19 contains at its very C-terminus a CAAX motif box known to serve as a recognition site for farnesylation. All peroxisome containing species carry at least one Pex19 copy and the CAAX box is conserved among nearly all Pex19 sequences (Giannopoulou et al., 2016). Farnesylation of Pex19 was demonstrated to be dispensable for peroxisome biogenesis however, it enhances by allosteric regulation the substrate binding to Pex19 (Emmanouilidis et al., 2017; Rucktäschel et al., 2009). Recently, an additional function of Pex19 was discovered. Pex19 in cooperation with Pex3 promotes hairpin protein UBXD8/FaF2 (FAS-associated factor 2) routing from ER to lipid droplets. Surprisingly, this function is dependent on the farnesylation of Pex19 leading to a hypothesis that Pex19 post-translational modifications regulate Pex19 shift among its different functions (Fig. 2.2) (Schrul and Kopito, 2016). In accordance to the newly found function of Pex19, a recent study suggested lipid droplets and peroxisomes formation to be spatially connected at specific ER subdomains whereas another study demonstrated that Pex19 and Pex3 can additionally facilitate posttranslational import of other hairpin proteins, belonging to the reticulon homology domain family, to ER (Joshi et al., 2017; Yamamoto and Sakisaka, 2018).

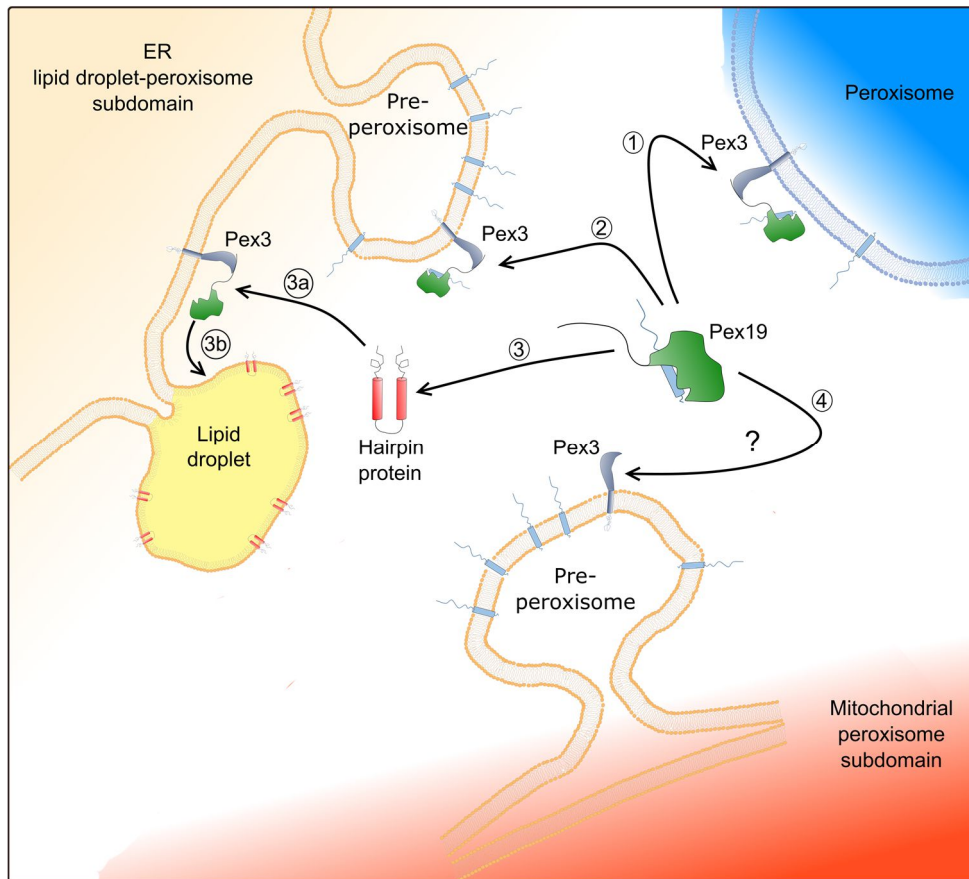


Fig. 2.2 Model of Pex19 function in diverse biogenesis pathways. (1) Pex19 induces peroxisome biogenesis by direct delivery of PMPs to the Pex3 receptor on peroxisomes. (2) Alternatively, Pex19 and Pex3 can promote pre-peroxisome budding from ER by recruitment of budding factors. (3) Additionally to peroxisome biogenesis, Pex19 and Pex3 inserts hairpin protein to lipid droplets at pre-peroxisome-lipid droplets biogenesis sites at the ER. (4) Similarly, Pex3 is required for pre-peroxisomes formation at mitochondria, however the role of Pex19 in this process is not clarified.

2.4.2 Heat shock proteins (HSP)

HSP protein families are the most abundant classes of chaperones in a cell. They are originally classified according to their molecular size, from which Hsp70s (70 kDa), Hsp90s (90 kDa), or Hsp40s (40 kDa) families are the most distinguished (Whitley et al., 1999).

The Hsp70 family is one of the most conserved chaperone classes. Members of this group are found from bacteria till humans and in many cellular compartments including mitochondria. Hsp70 primary function is to ensure proper

folding of proteins usually carrying hydrophobic patches, which are prone to aggregation. In yeast, cytosolic Hsp70s include proteins of Ssa, Ssb and Sse families as well as the Ssz1 protein (Verghese et al., 2012). The Ssa family is involved in general folding of proteins (James et al., 1997). It is comprised of four chaperones: the constitutively expressed Ssa1 and Ssa2 as well as Ssa3 and Ssa4, which are induced upon cell stress. The Ssa family is essential for viability of yeast cells, although due to functional redundancy among its members, viability can be recovered by even one Ssa chaperone (Werner-Washburne et al., 1987). In contrast, the Ssb family and Ssz1 function in cooperation with ribosomes ensuring folding of nascent peptide chains (Gautschi et al., 2001; Pfund et al., 1998). The Sse family is believed to function as dis-aggregases (Mattoo and Goloubinoff, 2014). Yeast cytosolic Hsp70s are known to participate in the biogenesis of mitochondrial proteins. The Ssa family was demonstrated to deliver carrier proteins to the Tom70 receptor for their optimal import. A similar activity was reported for Hsp70 and Hsp90 in mammals (Young et al., 2003). Additionally, Ssz1 was shown to stimulate the import of presequence-containing precursor proteins upon their synthesis on mitochondria-associated ribosomes (Gautschi et al., 2001).

Hsp70s are formed by two domains: the C-terminal substrate binding domain (SBD) and the N-terminal nucleotide-binding domain (NBD). The SBD contains a substrate-binding pocket and α -helical "lid" of this pocket whereas the NBD is known to bind ATP. A interdomain linker between the two domains transmits allosteric information from the NBD, depending on the state of ATP binding, to the SBD (Vogel et al., 2006a). Hsp70s act in a chaperone cycle where ATP hydrolysis leads to conformational changes of the SBD "lid" trapping the substrate in the binding pocket and so increasing the binding affinity. ADP release opens the lid and reduces the substrate binding affinity allowing the cycle to repeat (Mayer and Bukau, 2005; Vogel et al., 2006b).

Since the NBD domain has only a marginal ATPase activity, the ATP hydrolysis has to be stimulated by Hsp70 co-chaperones. One of these co-chaperone families are the Hsp40s called also J-domain proteins. The Hsp40s bind Hsp70s at the NBD thus, inducing conformational changes necessary for

ATP hydrolysis. This feature has significant impact on Hsp70 activity and thus Hsp40s determine and regulate the function of the complex (Greene et al., 1998).

In *S. cerevisiae*, there are thirteen identified Hsp40 chaperones functioning in diverse cellular processes from general protein folding to specific processes like ER protein degradation, maturation of ribosomes, or vesicle trafficking (Sahi and Craig, 2007). The deletion of the Hsp40 Ydj1 together with Ssa1 was demonstrated to affect translocation of precursor protein into mitochondria (Becker et al., 1996). Of note, Ydj1, similarly to Pex19, is post-translationally farnesylated at its C-terminus, allowing Ydj1 to bind intracellular membranes (Caplan et al., 1992). Another Hsp40 chaperon Djp1 was shown to affect the import of Mim1 and Mim2 preventing their aggregation and guiding them to the Tom70 receptor. Interestingly, Djp1 deletion additionally severely affects import of peroxisomal lumen proteins.

Another commonly found Hsp family known to interact with Hsp70s is the Hsp90 family. Hsp90 acts downstream of Hsp70 at the end of the maturation process of proteins. Thus, its substrates are more specific than Hsp70s and are termed “client” proteins. Hsp90 functions as a dimer but similar to Hsp70s, Hsp90s act in an ATP-dependent cycle, which is regulated by co-chaperones. The most important Hsp90 co-chaperone in yeast is Sti1, known as HOP (Hsp90/Hsp70 organizing protein) in mammalian cells. Interaction of Sti1 allows the assembly of the ternary multi-chaperone complex composed of Hsp90, Sti1 and Hsp70, which promotes client maturation and its transfer to Hsp90. To achieve this, Sti1 first inhibits the ATPase activity of Hsp90 stabilizing the chaperone in an open conformation. Then, Sti1 binds simultaneously via two TPR domains to Hsp70 and Hsp90. This brings the proteins into close proximity and enhances client transfer.

3. Aims of the study

Despite the importance of TA proteins for many mitochondrial functions, the targeting and insertion mechanisms of these proteins into the MOM remains elusive. Previous reports and the requirement for chaperones in the import of TA proteins to other organelles suggest that cytosolic factors are probably involved also in the biogenesis of mitochondrial TA proteins. My aim was to characterize the biogenesis of mitochondrial TA proteins by addressing the following questions:

- I. Are cytosolic factors required for the biogenesis of the mitochondrial TA proteins Fis1 and Gem1? If yes, what factors are those?
- II. What is the role of these cytosolic factors in the biogenesis process?
- III. Is the biogenesis of Atg32, a non-canonical TA protein, dependent on the same factors?

4. Materials and Methods

4.1 Materials

4.1.1 Media

All media, carbon source and amino acid stock solutions were autoclaved prior to use. Carbon source such as glucose, sucrose, and glycerol were added to a final concentration of 2% (v/v). For synthetic media, YNBGO and YNBO, amino acids (from 100x stock) were added dependent on the required type of specific auxotrophic selection markers. The tables below list the components of the media that were used in this study.

Table 1: Media for *S. cerevisiae*

Media	Composition
YP	2% (w/v) bacto peptone, 1% (w/v) yeast extract, 2% (v/v) carbon source, pH adjusted to 5.5 with NaOH
YP agar	YP liquid medium supplemented with 1.5% (w/v) agar
S media (Synthetic medium)	0.19% (w/v) yeast nitrogen base without ammonium sulfate, 0.5% (w/v) ammonium sulfate, 0.0055% (w/v) adenine sulfate, 0.0055% (w/v) uracil, 2% (v/v) carbon source, 1% (v/v) amino acid stock solution, pH adjusted to 5.5 with NaOH
S media (Synthetic medium) agar	S liquid media supplemented with 1.5% (w/v) agar
YNBGO	0.1% (w/v) yeast extract, 0.17% (w/v) yeast nitrogen base without ammonium sulfate, 0.5% (w/v) ammonium sulfate, 0.1% (w/v) glucose, 0.1% (v/v) oleic acid, 0.00002% (w/v) uracil, 0.00002% (w/v) adenine

4. MATERIALS AND METHODS

	sulfate, 1% (v/v) tergitol, 1% amino acid stock solution, pH adjusted to 6.0 with KOH
YNBO	0.1% (w/v) yeast extract, 0.17% (w/v) yeast nitrogen base without ammonium sulfate, 0.5% (w/v) ammonium sulfate, 0.1% (v/v) oleic acid, 0.00002% (w/v) uracil, 0.00002% (w/v) adenine sulfate, 1% (v/v) tergitol, 1% amino acid stock solution, pH adjusted to 6.0 with KOH
YNBO agar	YNBO liquid medium supplemented with 1.5% (w/v) agar
D-Glucose stock solution	40% (w/v) D-glucose
Glycerol stock solution	100% glycerol
Sucrose stock solution	40% (w/v) sucrose
100 × stock amino acid	0.2% (w/v) arginine, 0.4% (w/v) tryptophan, 1% (w/v) leucine, 0.4% (w/v) lysine, 0.2% (w/v) histidine, 0.6% (w/v) phenylalanine, 0.2% (w/v) methionine

Table 2: Media for *E. coli*

Media	Composition
LB	1% (w/v) bacto-tryptone, 0.5% (w/v) yeast extract, 0.5% (w/v) NaCl, pH 7.0
LB agar	Liquid LB medium supplemented with 1.5 % (w/v) agar
LB medium with ampicilin	LB media (liquid or agar) supplemented with 100 µg/ml ampicillin

4.1.2 Buffers

Table 3: Buffers for agarose gel electrophoresis

Buffer	Composition
1x TAE-buffer	40 mM tris-base, 0.114 % (v/v) acetic acid, 1 M EDTA, pH 8
10x DNA loading buffer	10% (v/v) glycerol, 0.2% (w/v) Orange G

Table 4: Buffers for small scale isolation of plasmid DNA from *E. coli* cells

Buffer	Composition
E1	50 mM Tris-HCl, 10 mM EDTA, 100 µg/ml RNase A
E2	200 mM NaOH, 1% (w/v) SDS
E3	3 M potassium acetate, pH adjusted to 5.5 with acetic acid

Table 5: Buffers for polymerase chain reaction

Buffer	Composition
10x <i>Taq</i> buffer with (NH ₄) ₂ SO ₄	200 mM (NH ₄) ₂ SO ₄ , 0.1% (v/v) Tween20, 750 mM Tris, pH adjusted to 8.8 with HCl
10x <i>Pfu</i> buffer with MgSO ₄	100 mM (NH ₄) ₂ SO ₄ , 100 mM KCl, 1% (v/v) Triton X-100, 1 mg/ml BSA, 20 mM MgSO ₄ , 200 mM Tris, pH adjusted to 8.8 with HCl

Table 6: Buffers for preparation of electrocompetent *E. coli* cells

Buffer	Composition
Tfb1 buffer	30 mM potassium acetate, 100 mM RbCl, 100 mM CaCl ₂ , 50 mM MnCl ₂ , 15% (v/v) glycerol, pH adjusted to 5.8 with acetic acid
Tfb2 buffer	100 mM MOPS, 75 mM CaCl ₂ , 10 mM RbCl, 15% (v/v) glycerol, pH adjusted to 6.5 with NaOH

Table 7: Buffers for isolation of mitochondria

Buffer	Composition
Resuspension buffer	100 mM Tris, 10 mM DTT
Spheroplasting buffer	1.2 M sorbitol, 20 mM potassium phosphate, pH 7.2
Homogenization buffer	0.6 M sorbitol, 1 mM EDTA, 1 mM PMSF, 0.2% (w/v) fatty acid-free BSA, 10 mM Tris pH adjusted to 7.4 with HCl
SEM buffer	250 mM sucrose, 1 mM EDTA, 10 mM MOPS, pH adjusted to 7.4 with KOH

Table 8: Buffers for isolation of peroxisomes and sucrose gradient

Buffer	Composition
Buffer A1	50 mM potassium phosphate, 1 mM EDTA pH 7.5
Buffer B	5 mM MES, 1 mM EDTA, 1 mM KCl, pH 5.5
Buffer A plus	Buffer A, 1.2 M sorbitol
Buffer B plus	Buffer B, 1.2 M sorbitol
Buffer 2B plus	Buffer B, 0.25 M sorbitol
XY% sucrose	XY% sucrose (w/w) in Buffer B

Table 9: Buffers for SDS-PAGE, Western-blot and immunodecoration

Buffer	Composition
2x Lämmli buffer	4% (w/v) SDS, 20% (v/v) glycerol, 0.02% (w/v) bromophenol blue, 5% (v/v) β -mercaptoethanol, 160 mM Tris, pH adjusted to 6.8 with HCl
SDS running buffer	50 mM Tris, 1.61 M glycine, 0.1% (w/v) SDS
SDS running buffer for UREA gels	25 mM Tris, 190 mM glycine, 0.1% (w/v) SDS
Blotting buffer	20 mM Tris, 150 mM glycine, 0.02% (w/v) SDS, 20% (v/v) ethanol

4. MATERIALS AND METHODS

Ponceau staining solution	3.06% (v/v) TCA, 3 mM Ponceau
TBS buffer	10 mM Tris, 154 mM NaCl, pH adjusted to 7.5 with HCl
TBST buffer	TBS buffer, 0.05% (v/v) Tween20
Blocking buffer	5% (w/v) powdered skim milk in TBS buffer
ECL	0.2 mM p-coumaric acid, 1.25 mM Luminol, 100 mM Tris, pH adjusted to 8.5 with HCl. 0.03% (v/v) H ₂ O ₂ were added before usage to the ECL solution

Table 10: Buffers for isolation of yeast extract and *in vitro* translation

Buffer	Composition
Buffer A	30 mM HEPES–KOH pH 7.6, 100 mM KOAc pH 7.0, 0.3 mM MgOAc pH 7.0, 0.3 M DTT
Buffer A + mannitol	Buffer A, 8.5% mannitol (v/v)
10x Energy Mix	200 mM HEPES-KOH pH 7.6, 10 mM ATP, 1 mM GTP, 200 mM creatine phosphate, 20 mM DTT
10U Creatine phosphokinase	10 mM HEPES-KOH pH 7.6, 50 mM KOAc, Creatine phosphokinase 10 U/ μ l, 50% glycerol

Table 11: Buffers for *in vitro* transcription and import of proteins into mitochondria

Buffer	Composition
Transcription buffer	40 mM Tris-HCl pH 7.5, 10 mM NaCl, 6 mM MgCl ₂ , 2 mM spermidine
F5-import buffer	250 mM sucrose, 10 mM MOPS, 80 mM KCl, 5 mM MgCl ₂ , 0.5% (w/v) fatty acid free BSA, pH adjusted to 7.2 with KOH
SEM-K⁸⁰ buffer	SEM buffer with 80 mM KCl

Labeling buffer	0.6 M sorbitol, 20 mM HEPES, 50 mM Tris, 4 M Urea, 1 mM DTT, pH adjusted with KOH to 7.4
IASD buffer	5 mM 4-acetamido-4'-[(iodoacetyl) amino]stilbene-2,2'-disulfonic acid (IASD) in Labeling-buffer
IASD buffer + TX-100	5 mM IASD in Labeling buffer + 1% (v/v) Triton X-100

Table 12: Buffers for purification of GST-tagged proteins and pull-down assays

Buffer	Composition
GST-basic buffer	20 mM HEPES, 100 mM NaCl, 1.5 mM MgCl ₂ , pH adjusted with NaOH to 7.25
GST-lysis buffer	0.2 mg/ml lysosome, 2 mM PMSF, 1 mM DTT, 3 mM EDTA, 1x cOmplete protease inhibitor in GST-basic buffer
GST-elution buffer	15 mM reduced L-glutathione in GST-basic buffer, pH adjusted to 7.25 with NaOH
Wash buffer	0.6 M sorbitol, 10 mM Tris, pH 7.4

Table 13: Microscopy buffer

Buffer	Composition
PBS	137 mM NaCl, 2.7 mM KCl, 10 mM Na ₂ PO ₄ , 1.8 mM KH ₂ PO ₄

4.1.3 Enzymes

If applicable, enzymes were used with buffers provided by the manufacturer according to the manufacturer's recommendation.

Table 14: Enzymes used in this study

Enzyme	Source
T4-DNA-Ligase	Fermentas
Taq DNA polymerase	Genaxxon
Pfu DNA polymerase	Fermentas
Q5 DNA polymerase	New England Biolabs
ExactRun DNA polymerase	Genaxxon
SP6 RNA polymerase	Promega
RNase A	Applichem
Lysozyme	Serva
Miccococal nuclease	Roche
Creatine phosphokinase	Roche
Proteinase K	Roche
Restriction enzymes	New England Biolabs
Zymolase 20T	Seikagaku Biobusiness

4.1.4 Antibodies

All antibodies were diluted in blocking buffer and stored at -20°C except for the Pex19 antibody, which was stored at 4°C. All used antibodies were raised in rabbit except for anti-HA and anti-GFP which were raised in rat and mouse, respectively.

Table 15: Primary Antibodies

Name	Dilution	Cellular localization of antigen
α-Fis1	1:1000	MOM
α -Porin	1:1000	MOM
α-Tom70	1:1000	MOM
α-Tob55	1:1000	MOM
α-Tom40	1:1000	MOM
α-Tom22	1:1000	MOM
α-Tom20	1:1000	MOM

α -Mim1	1:1000	MOM
α -Om14	1:1000	MOM
α -Fum1	1:1000	Cytosol/IMS
α -Pic1	1:6000	IM
α -Mge1	1:1000	Matrix
α -Aco	1:1000	Matrix
α -Pex19	1:5000	Cytosol/Peroxisomes
α -Pex14	1:5000	Peroxisomes
α -Bmh1	1:2000	Cytosol
α -Hexo	1:5000	Cytosol
α -Sti1	1:2000	Cytosol
α -GFP	1:1000	n.a.
α -GST	1:2000	n.a.
α -DHFR	1:500	n.a.
α -HA	1:2000	n.a.

Table 16: Secondary antibodies

Name	Dilution	Manufacture
Goat anti-rabbit IgG (H+L)-HRP conjugate,	1:10000	Bio-Rad
Goat anti-rat IgG (H+L)-HRP conjugate,	1:2000	abcam
Goat anti-mouse IgG (H+L)-HRP conjugate,	1:2500	Bio-Rad

4.1.5 Yeast and *E. coli* strains

Table 17: Yeast Strains

Strain	Genotype	Reference
W303a/ α	<i>MATa/α; ade2-1, can1-100, his3-11, leu2-3, 112, trp1-1, ura3-1</i>	Strain collection, Rapaport group

4. MATERIALS AND METHODS

<i>pex19Δ</i>	W303a; <i>pex19::KANMX4</i>	This study
<i>sti1Δ</i>	W303α, <i>sti1::HIS3</i>	Strain collection, Rapaport group
<i>sti1Δ</i>	W303a, <i>sti1::KANMX4</i>	Strain collection, Rapaport group
<i>sti1Δ/pex19Δ</i>	W303α; <i>pex19::KANMX4</i> ; <i>sti1::HIS3</i>	This study
<i>tom20Δ</i>	W303α, <i>tom20::KanMX4</i>	Papic et al., 2011
<i>mim1Δ</i>	W303α, <i>mim1::KanMX4</i>	Dimmer et al., 2012
BY4741	<i>MATa</i> ; <i>his3Δ1</i> ; <i>leu2Δ0</i> ; <i>met15Δ0</i> ; <i>ura3Δ0</i>	Euroscarf, Frankfurt a. M., Germany
<i>pex19Δ</i>	<i>BY4741</i> , <i>pex19::KANMX4</i>	Euroscarf, Frankfurt a. M., Germany
<i>pex14Δ</i>	<i>BY4741</i> , <i>pex14::KANMX4</i>	Euroscarf, Frankfurt a. M., Germany
JSY7452	<i>MATa</i> ; <i>ade2-1</i> , <i>leu2-3</i> , <i>his3-11.15</i> , <i>trp1-1</i> , <i>ura3-1</i> , <i>can1-100</i>	Kondo-Okamoto et al., 2006
<i>tom70/71Δ</i>	JSY7452, <i>tom70::TRP1</i> , <i>tom71::HIS3</i>	Kondo-Okamoto et al., 2006
<i>ssa2-4Δ+SSA1</i> wt	JN516; <i>MATa leu2-3,112</i> ; <i>his3-11</i> ; <i>ura3-52</i> ; <i>trp1Δ1 lys2</i> ; <i>Ssa1 ssa2::LEU2 ssa3::TRP1</i> ; <i>ssa4::LYS2</i>	Ophry Pines
<i>ssa2-4Δ+SSA1</i> ts	JB67; <i>MATa leu2-3,112</i> ; <i>his3-11</i> ; <i>ura3-52</i> ; <i>trp1Δ1 lys2</i> ; <i>ssa1-45 ssa2::LEU2 ssa3::TRP1</i> ; <i>ssa4::LYS2</i>	Ophrey Pines

Table 18: *E.coli* strains

Name	Source
XL10-Gold	Agilent
BL21	Stratagene

4.1.6 Oligonucleotides**Table 19: List of oligonucleotides**

Name	Sequence	Remarks
pex19delF2	5' GTA TTG ACG GAA AGA AGA AAT GCC AAA CAT ACA ACA CGA AGT AAT GCG TAC GCT GCA GGT CGA CGG ATC C 3'	Amplification of KanMX4 or HISMX6 cassette
pex19delR2	5' ATC ATA AAT ATA TAT ACC TTA TTG TTG TTT GCA ACC GTC GGT TAA TTC CTA TCA TCG ATG AAT TCG AGC TCG TT 3'	Amplification of KanMX4 or HISMX6 cassette
Pex19inF	GCT CTA GAA GAG GCA GCT AAA GTA C 3'	Verification of deletion by PCR
PEx19inR	5' TCT TGA AAC CAA ACA CCG AAC TCA C 3'	Verification of deletion by PCR
Pex19testF	5' CTA CTT ACC TTT CTT CCT GAA GA 3'	Verification of deletion by PCR
Pex19testR	5' GTA TCA TGA CGA AGG ACT TGG CT 3'	Verification of deletion by PCR
Pex19gench eckF2	5' GCA CCT ACA AGA GGC AAT TTA AT 3'	Verification of deletion by PCR
Pex19gench eckR2	5' CTG TCT TCA CAT TAT TCT CGT TA 3'	Verification of deletion by PCR

NGFPGem1 FOR	5' TGA ACT ATA CAA AGA ATT CAC CAT GGA TCC GAC TAA AGA AAC GAT TCG GGT AGT TAT TTG 3'	Amplification of GEM1 ORF. 5'contains BamHI restriction site
NGFPGem1 REV	5' AC GGA TAC CCG GGT CGA CGC GTA AGC TTA TTT TGA GAA TTT TGA TGA TTT G 3'	Amplification of GEM1 ORF. 5'contains HindIII restriction site
NGFPGem1 TMDF	5' TGA ACT ATA CAA AGA ATT CAC CAT GGA TCC GAC GGC TCT CAT TTT TGG GTC CAC 3'	Amplification of the TMD sequence of Gem1. 5'contains BamHI restriction site
XmaIGem1F	5' GGG CCC GGG ACT AAA GAA ACG ATT CGG GTA G 3'	Amplification of GEM1 ORF. 5'contains XmaI restriction site
HindIIIGem1 R	5' CCC AAG CTT TTA TTT TGA GAA TTT TGA TGA TTT GAA TAA TTT CAT 3'	Amplification of GEM1 ORF. 5'contains HindIII restriction site
InterGem1F or	5' AAG AAA CGA TTC GGG TAG 3'	Sequencing of pYX132-GFP-GEM1

Table 20: List of plasmids used in this study

Plasmids	Promotor	Selection marker	Reference
pRS426-TPI	TPI	Ura, Amp	Laboratory stock
pRS426-Pex19	TPI	Ura, Amp	Thesis of K. Krumpe
pRS426-GFP- Fis1	TPI	Ura, Amp	Krumpe et al., 2012

4. MATERIALS AND METHODS

pRS426-mts-GFP	TPI	Ura, Amp	Laboratory stock
pRS316-Fis1pr-HA-Gem1-Fis1T	Fis1	Ura, Amp	Daniela Vitali
pRS316-Atg32-HA	Atg32	Ura, Amp	Okamoto et al., 2009
pYX142	TPI	Leu, Amp	Laboratory stock
pYX142-Pex19	TPI	Leu, Amp	This study
pYX142-GFP-Gem1	TPI	Leu, Amp	This study
pYX142-GFP-Gem1-TMD	TPI	Leu, Amp	This study
pYX142-HA-Gem1	TPI	Leu, Amp	K.S. Dimmer
pYX142-eGFP	TPI	Leu, Amp	Jores et al., 2016
pYX132	TPI	Trp, Amp	Laboratory stock
pYX132-GFP-Gem1	TPI	Trp, Amp	This study
pYX132-GFP-Gem1-TMD	TPI	Trp, Amp	This study
pYX132-Pex19	TPI	Trp, Amp	Thesis of K. Krumpe
pYX122-HA-Gem1	TPI	His, Amp	This study
pGem4-Fis1-TMC	SP6	Amp	Kemper et al., 2008
pGem4-Gem1	SP6	Amp	Daniela Vitali
pGem4-pSu9-DHFR	SP6	Amp	Pfanner et al., 1987
pGem4-AAC	SP6	Amp	Mayer et al., 1993
pGex4T	Tac	Amp	Amersham Biosciences

4. MATERIALS AND METHODS

pGex4T-Pex19	Tac	Amp	Thesis of K. Krumpe
pAD54-PTS1- RFP	Tac	Leu	Maya Schulinder
pFA6a-KanMX4		G418	Wach et al., 1994

4.2 Methods

4.2.1 Molecular biology methods

4.2.1.1 Polymerase chain reaction (PCR)

For amplification of genetic material, the polymerase chain reaction (PCR) was used (Saiki et al., 1988). A standard PCR reaction mix is shown in Table 21. The *Taq*, *Q5*, *Pfu*, or *ExactRun* polymerase were added for the reaction. PCR was performed in a thermocycler (Biometra) with the program described in Table 22.

Table 21: PCR reaction mix

Reaction component	Volume (50 μ l)
Template	1 μ l (1-10ng)
dNTP mix (10 mM)	1 μ l
10x or 5x enzyme buffer	1x
5' primer (5 pmol)	1 μ l
3' primer (5 pmol)	1 μ l
Polymerase	1 μ l
H ₂ O	till 50 μ l

Table 22: General PCR program used in this study

Step	Temperature	Time and cycles
1	96°C	5'
2	96°C	1'
3	65°C	1'(-1°C each cycle)
4	72°C	1'→ step 2 x 10
5	96°C	1'
6	55°C	1'
7	72°C	1'→ step 5 x 25
8	72°C	10'
9	4°C	Pause

4.2.1.2 Agarose gel electrophoresis

To separate DNA fragments according to their molecular masses, agarose gel electrophoresis was performed. Separation took place on 0.5 - 2% (w/v) gels prepared in TAE buffer (Table 3) with either 3% (v/v) midori green or 2% gel red (Biotium). DNA samples were pre-mixed with 10xOrange G prior to loading onto the gel. To determine the size of the DNA fragments, a 1 kb DNA ladder (Fermentas, Gene Ruler™) was loaded in parallel. Electrophoresis was performed at a voltage of 50 V to 120 V in TAE buffer and the bands were visualized by UV light.

4.2.1.3 Extraction of DNA from agarose gel

After gel electrophoresis, DNA bands of interest were cut out and isolated using Fast gene™ extraction kit (NIPPON Genetics) according to the manufacturer's manual.

4.2.2.4 Restriction digestion of DNA

Restriction digestion of the genetic material was performed using high-fidelity endonucleases (New England Biolabs) with the buffers recommended by NEB. Reaction volume was set to 20 µl and the restriction reaction was incubated at 37°C for one hour or overnight. If necessary, the enzyme was inactivated at 60°C for 30 min.

4.2.2.5 Ligation with T4 DNA ligase

For ligation of DNA fragments, a 20 µl reaction with 1 Weiss U T4 DNA Ligase and 1x ligation buffer was set up. The insert and vector were ligated in 1:3 (w/w) ratio, left on ice in room temperature overnight. On the next day, the reaction mixture was transformed into competent XL10 gold cells.

4.2.2.6 Preparation of chemically competent *E. coli* cells

Chemo-competent cells were prepared from XL10-gold or BL-21 *E. coli* strains. The cells were inoculated for overnight culture at 37°C in LB medium with chloramphenicol and the next day diluted in 400 ml of fresh LB medium to an OD₆₀₀=0.1 and grown to OD₆₀₀=0.5. The cells were sedimented by centrifugation

(3000 g, 5 min, 4°C) in pre-cooled sterile tubes and the cell pellet was resuspended in 160 ml of pre-cooled TfbI buffer (Table 6) and incubated on ice for 15 min. The cell suspension was harvested by centrifugation (4000 g, 10 min, 4°C), the pellet was resuspended in 16 ml pre-cooled TfbII buffer and kept on ice for 15 min. Afterwards, the competent cells were divided into aliquots of 100 µl and snap frozen.

4.2.2.7 Transformation of *E. coli* cells

The DNA of interest was transformed into XL-10 or BL21 *E. coli* cells by adding it to the cells, incubating them for 30 min on ice, subjecting them to heat-shock at 42°C for 90 sec and cooling them down for 2 min on ice. Afterwards, cells were left to recover for 1-2 hrs in LB medium at 37°C, pelleted for 1 min at 5000 g and plated on LB-agar plates to incubate them overnight at 37°C.

4.2.2.8 Small scale plasmid isolation from *E. coli* cells (Miniprep)

For small scale plasmid isolation the alkaline lysis method was used (Birnboim and Doly, 1979). Transformed single *E. coli* colonies were picked and shaken in 4 ml LB+Amp at 30°C overnight. The next day, 2 ml of the cells were harvested (5000 g, 5 min) and resuspended in 300 µl buffer E1 (Table 4) and subjected to lysis by adding 300 µl of buffer E2 and inverting the tube 5 times. The lysis was stopped by neutralization of buffer E2 with 300 µl of buffer E3 and inverting the tube 5 times. DNA was collected by centrifugation (15000 g, 15 min, 2°C), then the supernatant was taken into a new tube and precipitated with 96% isopropanol (15000 g, 15 min, 2°C). The pellet was washed with 70% ethanol and again centrifuged as above. Finally, the pellet was resolved in 30 µl of H₂O and stored at -20°C.

4.2.2.9 Large scale plasmid isolation (Midiprep)

The midiprep was performed from a 100 ml LB+Amp overnight shaken (37°C) *E. coli* culture. To isolate the plasmid, a PureYield Plasmid Midiprep System (Promega) was used according to the instructions of the manufacturer. DNA concentration was determined with the NanoDrop (Thermo Fisher Scientific) and the DNA was stored at -20°C.

4.2.2 Methods in yeast genetics

4.2.2.1 Cultivation of yeast strains

Liquid culture of yeast strains were grown at 24°C, 30°C, or 37°C with 120 rpm shaking in complete (YP) or synthetic (S) medium. Carbon sources used for the medium were either fermentable (glucose, sucrose) or non-fermentable (glycerol or lactate). Cells grown on solid media were incubated at 15°C, 30°C, or 37°C on synthetic or YNBO medium.

4.2.2.2 Yeast transformation with the lithium acetate method

For transformation of yeast cells, the lithium acetate method was adopted (Gietz et al., 1995). Yeast cells were centrifuged (3000 g, 5 min) from a fresh culture grown overnight at 30°C, washed with water and centrifuged again. The cell pellet was resuspended in 1 ml of 100 mM lithium acetate and pelleted down (6000 g, 20 sec). Afterwards, the pellet was again resuspended in a mixture of 240 µl of 50 % (w/v) polyethylene glycol, 5 µl salmon sperm DNA, 36 µl 1 M lithium-acetate and 1 µg of the transformed plasmid. The mixture was then incubated for 30 min at 37°C followed by incubation for 25 min at 42°C. After the heat-shock, the cells were centrifuged (6000 g, 20 sec), resuspended in 100 µl water, streaked on the appropriate selective plate, and grown at 30°C till single colonies could be selected.

4.2.2.4 Construction of yeast deletion strains

The *PEX19* gene has been deleted by the homologous recombination approach (Wach et al., 1994). The *PEX19* ORF has been replaced by a Kanamycin cassette which was previously PCR amplified using the pFA6a-*KanMX4* plasmid and primers (Table 19) carrying complementing sequences to *PEX19* regions. After transformation of the cassette into a W303a strain, colonies harboring the deletion were selected by growing them on SD+G418 plates at 30°C. The deletion was confirmed by colony PCR with specific primers (Table 19).

4.2.2.5 Mating of yeast strains and tetrad analysis

Creation of the *sti1Δ/pex19Δ* double-deletion strain was achieved by mating the *sti1Δ::HIS3 MAT α* and *pex19Δ::KANMX4 MAT α* yeast strains. Both strains were streaked on separate YPD plates as parallel lines and grown overnight at 30°C. Next, both plates were replica plated on a single YPD plate so that the parallel lines were crossed and the plate was incubated at 30°C. The growing yeast diploids generated in the places of the crossed lines were replica plated on SD-HIS+G418 plates, grown at 30°C, and selected again on a SD-HIS+G418 plate. Afterwards, the cells were streaked on a sporulation plate and incubated for a couple of days at 24°C in order to force the diploids to sporulate. Sporulation was monitored microscopically and subsequently a small amount of diploids was picked from the plate to digest the cell wall for 10 min at 30°C with 100 μ g/ml zymolyase resuspended in 1.2 M sorbitol. A drop of the ascus suspension was pipetted on YPD plate. Tetrad dissection was performed with micromanipulator (ZEISS, Axioscope 40). The asci were ripped and the spore transported to certain separate positions on the plate by the needle of the micromanipulator. Afterwards, the plate was incubated at 30°C and single colonies of the haploid cells were re-streaked on selective medium in order to select the double deletion cells. The mating type of single colonies was determined by mating-type PCR (Huxley, 1990).

4.2.3 Cell biology methods

4.2.3.1 Drop dilution assay

Cells for the drop dilution assay were pre-grown in SD-URA medium at 30°C and re-cultured a day before the assay in YNBGO-URA medium at 30°C. On the next day the strains were diluted to OD₆₀₀=0.2 and grown to OD₆₀₀=1.0. Afterwards, cells were harvested by centrifugation (3000 g for 5 min), washed with 1 ml H₂O and the pellet was resuspended in water to reach an OD₆₀₀=2.0. The cell suspension was diluted in five series of a fivefold dilution and 5 μ l of each dilution were spotted on the selective solid medium plates. The plates were then grown at 15°C, 30°C, or 37°C for up to two weeks.

4.2.3.2 Cycloheximide treatment of yeast cells

To address the question of protein stability, the translation process in yeast cytosol was inhibited by cycloheximide. A 50 ml yeast culture was grown overnight at 30°C, diluted the next day to OD₆₀₀=0.3 and grown to OD₆₀₀=1.0. Then, cycloheximide was added to a concentration of 100 µg/ml and 10 ml of the culture were collected into a Falcon™ tube, spined down (3000 g, 5 min), and washed with 10 ml of water. Such 10 ml fractions were later collected from the cultures at 1, 2, and 4 hour time points after adding the inhibitor. Cell pellets were stored at -20°C and later subjected to whole cell lysis.

4.2.3.3 Isolation of crude mitochondria

Yeast cell cultures were grown overnight in a 50 ml medium and diluted the next day in 100 ml medium to OD₆₀₀ of 0.1-0.3. After the cultures reached an OD of 1.0-1.5 for synthetic medium or 1.0-2.5 for full media the cells were harvested (3000 g, 5 min). The pellet was washed and stored at -20°C. For mitochondria isolation, the pellet was thawed and resuspended with SEM buffer (Table 7) so that the cell suspension had a density of approximately an OD₆₀₀=270. Cell solutions were added to a 2 ml tube with glass beads. The weight of the glass beads was calculated to match a ratio of one mg of glass beads to each 2/3 ml of the SEM buffer volume used for the culture. The cells were broken by vortexing them eight times with the glass beads for 30 sec, with 30 sec of cooling on ice after each vortex. The lysate was centrifuged at 1000 g to remove cell debris and after protein concentration determination with Bradford method (section 4.2.4.1), the supernatant was centrifuged (15400 g, 10 min) in a new tube in order to pellet mitochondria. The pellet was then dissolved in 1.4 µl of 2xLaemmli per 1 µg mitochondria and heated for 5 min either at 50°C (for mitochondria from HA-Gem1, Gem1-HA and Atg32-HA expressing strains) or 95°C (for the rest of isolated crude mitochondria). If required, the post mitochondrial supernatant was kept for further analysis.

4.2.3.4 Isolation of pure mitochondria from yeast

Pure mitochondria were isolated according to a previously described method (Daum et al., 1982). Buffers used for pure isolation of mitochondria are listed in

Table 7. Yeast cells were grown in the appropriate medium in 2 l volume to an OD_{600} of 1.5. The culture was harvested (3000 g, 5 min), washed with 100 ml sterile H_2O and weighed. Afterwards, the cell pellet was re-suspended in a ratio of 2 ml of resuspension buffer per g of cells, shaken for 10 min at $30^\circ C$ and centrifuged at 3000 g for 5 min. Cell pellet was resuspended in 100 ml of 1.2 M sorbitol and reisolated again (3000 g, 5 min). Then, the cells were mixed with 6.6 ml of spheroblasting buffer containing zymolyase in a ratio of 3 mg per 1 g of harvested cells. The cells were shaken at $30^\circ C$ for one hour to digest the cell wall. The generated spheroblasts were pelleted (2000 g, 5 min), resuspended in 6.6 ml of homogenization buffer per g of cells and transferred into a douncer. Spheroblasts were opened by douncing the suspension 20 times in an ice-bath. The douncer was rinsed with homogenization buffer and the wash, together with the dounced solution, were pooled together and centrifuged twice (2000 g, 5 min) to get rid of cell debris. The supernatant was then harvested (18000 g, 12 min) and the isolated mitochondria were resuspended in 30 ml SEM buffer to be again centrifuged twice (2000 g, 5 min) in order to get rid of the remaining cell debris. At last, the mitochondria were pelleted (17500 g, 12 min), dissolved in samples of 500 μl of SEM buffer and snap-frozen in liquid nitrogen. Determination of protein concentration was performed with the Bradford assay (section 4.2.4.1).

4.2.3.5 Separation of mitochondria and peroxisomes by sucrose gradient

For isolating and later separating mitochondria and peroxisomes on sucrose gradient, a peroxisome isolation approach has been adopted (Distel and Kragt, 2006). A starting culture has been pre-grown in 50 ml YPD overnight at $30^\circ C$, next day diluted to $OD_{600}=0.2$ grown to $OD_{600}=2.5$, diluted again to $OD_{600}=0.05$ in 100 ml YPD and grown again overnight at $30^\circ C$. In the morning, the culture has been again diluted to $OD_{600}=0.2$ in 200 ml YPD and grown to $OD_{600}=2.5$. This culture then could be used to inoculate the main 2 l culture in YNBO media which has been grown overnight at $30^\circ C$. The cells were harvested (3000 g, 5 min), the pellet weighed, dissolved in resuspension buffer and incubated for 15 min at $30^\circ C$. Then the cells were harvested, resuspended in buffer A1 (Table 8) with 1.2 M sorbitol and centrifuged down (3000 g, 5 min). The pellet was then resuspended in buffer A1 with 1.2 M sorbitol in ratio of 1 ml buffer to 0.125 g cell

pellet. Zymolyase was added to the mix in a ratio of 3 mg of zymolyase per 1 g of cell pellet and the suspension was incubated for one hour at 30°C. During incubation, the degree of spheroblasting was monitored microscopically by looking at the cell wall remnants.

The cells were harvested and carefully resuspended in buffer B (Table 8) with 1.2 M sorbitol. This step and all the subsequent were performed at 4°C. The cell suspension was re-centrifuged and washed twice with the same buffer. Again, pellet was resuspended in buffer B with sorbitol and 1 mM PMSF. In order to lyse the spheroblasts, buffer B with 0.25 mM sorbitol and 1 mM PMSF was added to the cells till a final concentration of 0.65 M sorbitol. Afterwards, the lysate was homogenized additionally by douncing it 5 times with a loosely fitting glass homogenisator and 10 times with a tightly fitting glass homogenisator. Lysis was monitored microscopically. The homogenate was centrifuged (2000 g, 10 min). The pellet was resuspended in buffer B with 0.65 M sorbitol and later spined down (2000 g, 10 min) but before that the supernatant was saved. Both supernatants of the last and previous centrifugation step were pooled together and spined again (2000 g, 10 min). Finally, the supernatant was centrifuged (18000 g, 35 min) to sediment the mitochondria and peroxisomes.

Isolated organelles were subjected to sucrose gradient centrifugation by resuspending them in 30% sucrose (Table 8) to a concentration of approximately 5 mg/ml and loading 700 µl on top of the gradient. Each gradient consisted of 1.8 ml 60% sucrose, 4.33 ml 46% sucrose, 4.33 ml 44% sucrose and 1.8 ml 40% sucrose in open top tubes. The gradient and organelles were overlaid with 20% sucrose. Separation of organelles was performed by ultracentrifugation (34500 g, 21 hrs) in a SW-40Ti swing-out rotor (Beckman). After centrifugation, fractions of 1 ml were collected with a pipette.

4.2.3.6 Obtaining of yeast extract

Wild type and *pex19Δ* cells were grown in 1 l YPD medium to $OD_{600}=1-2$ and harvested (1500 g, 5 min, 4°C). Cells were resuspended in 20 ml ice-cold buffer A + mannitol (Table 10) and centrifuged (1000 g, 5 min, 4°C). This step was repeated four more times. After the last resuspension, the pellet was spined down

(2000 g, 5 min), its weight determined and resuspended again in buffer A + mannitol + 0.5 mM PMSF in a ratio of 1.5 ml of buffer per 1 g of cells. Next, 6 g of glass beads per 1 g of cell pellet were added and cells were opened by manually shaking them in the cold room five times for 1 min with 1 min pause in-between. Cell debris and glass beads were removed by spinning the lysate (120 g, 3 min, 4°C). The supernatant was carefully taken by a Pasteur pipette and centrifuged two times (16000 g, 6 min, 4°C). Subsequently, a PD10 column (GE Healthcare) was equilibrated with 25 ml of buffer A containing 0.5 mM PMSF and the ribosome-containing supernatant was separated on it. Fractions each containing 0.5 ml were collected. The ribosome concentration in the fraction has been measured at 260 nm with a NanoDrop (Thermo Fisher Scientific). The fractions richest in rRNA (containing at least 75% of the highest absorbance of the fractions) were pooled together and CaCl₂ was added to the extract to a final concentration of 1mM and micrococcal nuclease to a final concentration of 50 U/ml. The reaction was incubated for 10 min in a water bath and stopped by adding EGTA to a final concentration of 2.5 mM. The yeast extract was snap frozen in liquid nitrogen and stored at -80°C.

4.2.3.7 Fluorescence microscopy

Yeast strains expressing fluorescent markers were pre-cultured overnight in 50 ml flasks in selective medium and diluted the next day to OD₆₀₀=0.2. The cells were grown to an OD₆₀₀ of 0.8-1.0 and 1 ml of the cultures was harvested (3000 g, 3 min). Prior to microscopy, the cells were resuspended in 1x PBS buffer (Table 13) and 5 µl of it were mixed on a microscopy glass with 5 µl of 1% low-melting point agarose (Roth) and sealed with a cover slip glass.

Fluorescent microscopy was performed with Zeiss Axio Examiner.Z1 equipped with a CSU-X1 real-time confocal system (Visitron), VS-Laser system, and SPOT Flex CCD camera (Visitron Systems). Two laser emission wavelengths were used: 488 nm (GFP) and 561 nm (mCherry). Images were analysed with VisiView software (Visitron).

4.2.4 Methods in protein biochemistry

4.2.4.1 Determination of protein concentration

For protein concentration determination the Bradford (Bradford, 1976) method was applied. 10 µl of protein solution were mixed with 1 ml Roti-Quant Bradford solution and incubated for 5 min. Absorbance of the sample was measured at 595 nm with a photometer (Eppendorf®, BioPhotometer®). Standard curve was determined by a series of dilutions (200-1000 µg/ml) of BSA in 1 ml Roti-Quant Bradford solution. The protein concentration was estimated according to the calibration plot.

4.2.4.2 Protein precipitation by trichloroacetic acid (TCA)

Precipitation of proteins from solutions was achieved by adding 72% TCA to a final concentration of 12%. The samples were vortexed and then incubated on ice for 30 min or overnight at -80°C. The solution was centrifuged (30000 g, 20 min, 2°C), washed in 1 ml of 90 % acetone (30000 g, 5 min, 2°C) and the pellet was dried at 45°C for 10 min. Subsequently, the pellet was resuspended in 2x Lämmli buffer and boiled at 95°C for 5 min.

4.2.4.3 Protein precipitation by chloroform-methanol

Proteins of post-mitochondria fraction were precipitated with chloroform and methanol precipitation method (Wessel and Flügge, 1984). For this method first four times sample volume of methanol, later three sample volumes of chloroform, and then three sample volumes of water were added to the samples and vortexed thoroughly after each addition of the solvent. The solution was separated (16000 g, 1 min) into two phases and the upper phase was discarded. Three volumes of methanol were added to the lower phase and the mixture was vortexed. Precipitated protein was pelleted (16 000 g, 2 min), dried at 45°C for 10 min and resuspended in 2x Laemmli. The loading solution was incubated at 95°C for 5 min.

4.2.4.4 Carbonate extraction

Carbonate extraction was performed according to a published procedure (Fujiki et al., 1982). Isolated mitochondria (40 µg) were mixed with 100 µl of 0.1 M sodium carbonate in SEM buffer. Then, they were incubated on ice for 30 min and centrifuged (120000 g, 1 h, 2°C). The pellet was dissolved in 40 µl Laemmli buffer and boiled at 95°C for 5 min.

4.2.4.5 Proteinase K treatment

Isolated mitochondria (40 µg) were resuspended in 100 µl SEM buffer and supplemented with 2.5 µl (2 mg/ml) of Proteinase K (PK). The mitochondria solution was incubated on ice for 15 min, the reaction was stopped by adding 2 mM PMSF and incubation for another 10 min on ice. Mitochondria were afterwards sedimented (20000 g, 15 min, 2°C), resuspended in 40 µl Laemmli buffer and heated at 95°C for 5 min.

4.2.4.6 IASD assay

For testing the membrane integration of Fis1-TMC, a modified assay with the 4-acetamido-4'-[(iodoacetyl) amino] stilbene-2,2'-disulfonic acid (IASD) was used (Kemper et al., 2008). Three mitochondrial pellets coming from the same split import reaction were resuspended in 30 µl of labeling buffer, IASD buffer (5 mM IASD), or IASD buffer + 1% TX-100 and incubated for 30 min on ice, followed by a second incubation step for 20 min at 25°C. Mitochondria with the added IASD buffer or IASD were re-isolated by centrifugation (20000 g, 20 min, 2°C). Samples containing Triton X-100 were precipitated with TCA. All pellets were dissolved in 30 µl 2x Laemmli buffer and incubated for 5 min at 95°C. Samples were further analyzed by SDS-PAGE and autoradiography.

4.2.4.7 SDS-PAGE

To analyze protein samples, the SDS-PAGE method has been applied. SDS-PAGE was performed using the commercially available PeqLab system Perfect Blue®. Samples were run under denaturing conditions in 10-23.5% SDS-PAGE gels. Gels were cast between two glass plates with 0.8 mm spacing in between. If necessary, prior to casting the running gels, a bottom gel was separately poured

to avoid leakage. The composition of bottom, running, and stacking gel are described in Table 22, and buffer composition in Table 9. The protein samples were prepared in 2x Lämmli buffer with a concentration of 0.715 µg/µl (15-100 µg). Electrophoresis was performed at 30-40 mA per gel, for approximately 3 hrs until the dye front reached the end of the running gel. A protein ladder (PAGE Ruler™, Fermentas) was used as a molecular weight markers. In cases where a separation of proteins with small mass differences was required, high-Tris urea gels were cast (Table 23). These gels were run at a power output of 40-60 mA for approximately 9 h.

Table 22: List of Acrylamide Gels used in this study

Components	Bottom gel	Running gel		Stacking gel
	15%	10%	12.5%	
40% AA/bis-AA (29:1)	3.75 ml	3.13 ml	3.91 ml	563 µl
1M Tris pH 8.8	3.75 ml	4.69 ml	4.69 ml	-
1M Tris pH 6.8	-	-	-	625 µl
Water	2.39 ml	4.55 ml	3.77 ml	3.76 ml
10% APS	100 µl	125 µl	125 µl	50 µl
TEMED	8 µl	10 µl	10 µl	4 µl
Total volume	10 ml	12.5 ml	12.5 ml	5 ml

Table 23: Composition of high-Tris urea gel

Components	60% aa, 0.8% bis-aa	1.825 M Tris-HCl + 1 mM NaCl pH 8.8	0.6 M Tris-HCl pH 6.8	urea	water	10% SDS	10% APS	TEMED
Running gel	4.9 ml	6 ml	-	5.46 g	-	152 µl	100 µl	20 µl
Stacking gel	500 µl	-	1.25 ml	2.16 g	60 µl	2.62 ml	30 µl	10 µl

4.2.4.8 Western blotting

For western blotting, the semi-dry blotting method was applied as described previously (Kyhse-Andersen, 1984; Towbin et al., 1979). A sandwich was constructed on the bottom of the apparatus consisting of three filter papers (Whatman, 3 mm) followed by a nitrocellulose membrane, the gel, three further filter papers and the top of the apparatus. Filter papers, membrane and gel were shortly soaked in blotting buffer before assembly. Transfer of proteins was performed for 1.5 hr at 220 mA (app. 1.2 mA/cm² membrane). Efficiency of the protein transfer was assessed by incubating the membrane in Ponceau staining solution for 1-2 min till visible protein bands appeared followed by washing the membrane in water several times.

4.2.4.9 Immunodetection of proteins

Before antibody decoration, the membrane was incubated with 5% skim-milk in TBS buffer for 30-120 min to block unspecific binding sites on the membrane. Then, membranes were briefly washed with TBS before incubating them with primary antibodies at 4°C overnight or at room temperature for 2 h. The membranes were then washed twice with TBS and once with TBST before their incubation at room temperature with secondary antibodies in 5% skim-milk for 1 h. Secondary antibodies were conjugated to HRP to allow detection of specific antibodies bound to the primary antibody. A chemiluminescence signal was obtained upon interaction of HRP with ECL and H₂O₂, which were added to the membrane. This signal was detected by X-ray films (Super RX, Fuji) which were developed by an X-ray film developing machine (SRX-101A, Konica Minolta). Quantification of bands was performed using AIDA image analyzer tool.

4.2.4.10 *In vitro* synthesis of radiolabeled proteins

In vitro synthesis of proteins required two steps: transcription to obtain mRNA and translation of the mRNA into protein. Transcription was performed from a pGEM4 plasmid carrying the gene of interest. A typical transcription mixture is listed in Table 24. This mixture was incubated at 37°C for 1 h, and the synthesized mRNA was precipitated by adding 5 µl of 10 M LiCl and 150 µl 96% ethanol and incubating the solution overnight at -80°C. The mRNA was further isolated by

centrifugation (37000 g, 20 min, 2°C) and washed with 500 µl ice-cold 70% ethanol. The mRNA pellet was resuspended in 37 µl H₂O with 2 µl RNase inhibitor, and used for the translation reaction or snap frozen and stored at -80°C.

Proteins were either translated in rabbit reticulocyte lysate (Promega) or in yeast extract. A typical mixture for translation in reticulocyte lysate is listed in Table 25. The composition of the translation reaction in yeast extract is listed in Table 26. For translation of Fis1-TMC and Gem1 in yeast extract, 5 µl of 0.4 M spermidine were added instead of H₂O. Translation reactions in reticulocyte lysate were incubated for 1 hr at 30°C whereas those in yeast extract for 40 min at 26°C. Both reactions were stopped by cooling them on ice and adding 6 µl of 58 mM methionine and 12 µl of 1.5 M sucrose. The solutions were clarified from ribosomes and aggregates by centrifugation (90000 g, 50 min, 4°C).

Table 24: Composition of transcription reaction

Component	Volume
Transcription buffer	10 µl
0.1 M DTT	5 µl
RNase inhibitor (Promega)	2 µl
2.5 mM rNTP-mix (GE Healthcare)	10 µl
7 methyl- G (5') ppp (5') G cap (Amersham)	2.6 µl
SP6 Polymerase	3.8 µl
DNA Plasmid (1 µg/ml)	5 µl
H ₂ O	11.6 µl
Total	50 µl

Table 25: Composition of rabbit reticulocyte lysate translation reaction

Component	Volume
Transcribed mRNA	12.5 µl
15 mM Mg-acetate	3.5 µl
1 mM Amino-acid without methionine	1.75 µl
20 U/µl RNase inhibitor (Promega)	0.5 µl
Rabbit reticulocyte lysate (Promega)	50 µl
10 µM ³⁵ S-Methionine	6 µl
Total	74.25 µl

Table 26: Composition of yeast extract translation reaction

Component	Volume
10x Energy mix	10 μ l
10U Creatine Phosphokinase	0.6 μ l
15mM KAc	2.5 μ l
1 mM Amino-acid without methionine	1.0 μ l
10 μ M Met- ³⁵ S	5 μ l
20 U/ μ l RNase inhibitor (Promega)	0.5 μ l
10-15 mM MgAc ₂	10 μ l
Yeast extract	50 μ l
H ₂ O	7 μ l
Total	100 μ l

4.2.4.11 *In vitro* import of proteins into mitochondria

To allow protein import, 30-40 μ g of the organelles were diluted in 100 μ l of import buffer. The mitochondria solution was mixed prior to import with the translation reaction (rabbit reticulocyte lysate or yeast extract) and NADH and ATP were added to a final concentration of 1 or 2 mM, respectively. Import of precursor proteins was performed at 25°C for pSU9-DHFR and at 4°C for Fis1 and Gem1. Import reaction was stopped by diluting the import mixture with 400 μ l of SEM-K₈₀ (Table 11), cooling it on ice and centrifuging the mitochondria (20000 g, 15 min, 4°C). Import of Fis1-TMC was performed in the triple reaction volume if the samples were later subjected to IASD treatment (see section 4.2.4.6).

4.2.4.12 Inactivation of Hsp40/Hsc70 complex by addition of inhibitors

The activity of chaperones of the Hsp70 family can be inhibited by addition of small molecule reagents (Fewell et al., 2004; Rabu et al., 2008; Wright et al., 2008). The inhibitors Mal3-101 or DMT002220 were solubilized in DMSO to a final concentration of 5 mM and added to the radiolabeled proteins in rabbit reticulocyte lysate translation mixture to a final concentration of 250 μ M. A corresponding volume of DMSO was added as a control. All the mentioned reactions were incubated for 10 min at 25°C.

4.2.4.13 Autoradiography and quantification of bands

The radiolabeled proteins were subjected to SDS-PAGE, transferred on a nitrocellulose membrane and detected by exposure to a X-ray film (Kodak Bio

Max MM). The exposure to the film varied from 2 to 30 days. Bands were quantified as described in 4.2.4.9.

4.2.4.14 Overexpression and purification of GST-tagged proteins

Buffers used for the purification of GST-tagged proteins are listed in Table 12. XL10 *E. coli* cells expressing either GST alone or GST-Pex19 encoded by the pGEX-4T plasmid were cultivated overnight at 37°C in 100 ml LB media. The next day, the culture was diluted to an OD₆₀₀ of 0.1 in 2 l LB media and grown at 37°C to an OD₆₀₀=0.5. At this point, protein expression was induced with IPTG (final concentration 1 mM) and the cells were grown at 37°C for another 5 h. Cells were harvested (3000 g, 10 min, 4°C), washed with water (3000 g, 10 min, 4°C), and resuspended in 40 ml GST lysis buffer. Lysis mixture was rolled at 4°C for 45 min and afterwards the cells were homogenized 20 times with a tight fitting glass douncer. The homogenate was additionally lysed with a French press (EmulsiFlex-C5) with running cycles of 500-1000 psi. Lysate was centrifuged (15000 g, 15 min, 4°C) and the GST-tag containing supernatant filtered with a filtropur S 0.2 µM filter.

The solution was loaded with the sample valve and re-cycled overnight at 4°C on a 1 ml GSTrap® 4B (GE Healthcare) column on a ÄKTA Start system (GE Healthcare). In advance, the GSTrap® 4B was pre-washed with 5 column volumes of distilled and degassed H₂O and 5 column volumes of degassed GST-Basic Buffer. The next day the column was washed with 20 ml GST-Basic buffer and the bound proteins were eluted with 10 ml GST Elution buffer. One ml fractions were collected with the fraction collector and fractions containing the high protein levels were pooled. To reduce the content of glutathione in the solution, purified GST-Pex19 was concentrated in a Pierce® Protein Concentrator PES, 30K MWCO (Thermo Scientific) and GST in Amicon Ultracel 10K (Millipore). Protein concentration was measured by Bradford assay and the purified proteins were snap frozen and stored at -80°C. To check for purity of the samples, aliquots of the input and wash samples were analyzed together with the elution fractions by SDS-PAGE.

4.2.4.15 Pull-down of mitochondrial proteins with purified GST-tagged proteins

Mitochondrial TA proteins were pulled-down with the purified GST-tagged proteins. To achieve this, 30 μ l of Glutathione Sepharose 4B slurry was washed 3 times with 1 ml GST Basic buffer (500 g, 1 min, 4°C). Subsequently, 7 nmol of GST or GST-Pex19 were resuspended in 1 ml GST basic buffer supplemented with 1x protease inhibitor cocktail (Roche) and added to the beads. The mixture was incubated for 2 hrs at 4°C on an overhead-shaker and the beads were spun down (500 g, 1 min, 4°C). Four percent of the GST-tagged protein input and of the supernatant after spinning down were collected and mixed with 40 μ l Laemmli solution. Unspecific sites on the Glutathione Sepharose beads were blocked with 3% BSA in wash buffer (Table 12) supplemented with 1x protease inhibitor cocktail (Roche), incubated for 2 hrs at 4°C on an overhead-shaker and sedimented (500g, 1 min, 4°C). In the meantime, mitochondria were resuspended in 600 μ l of 0.5% Triton X-100 in GST basic buffer supplemented with 1x protease inhibitor cocktail (Roche) and lysed by incubating them for 1 hr at 4°C on an overhead-shaker. The generated lipid waste was spun down (30000 g, 20-25 min, 4°C) and the supernatant with solubilized proteins was loaded on the beads. A small sample (4%) of the supernatant was diluted in 40 μ l Laemmli buffer. The pull-down solution was incubated for 4 hrs at 4°C on an overhead-shaker. The beads were centrifuged (500 g, 1 min, 4°C) washed twice with Wash buffer and 4% of the wash fraction was kept and resuspended in 80 μ l Laemmli buffer. The sedimented beads were resuspended in 80 μ l Laemmli and boiled with the other Laemmli samples at 50-95°C for 5 min.

5. Results

5.1 Cytosolic Hsp70s and their yeast co-chaperone Sti1 are required for Fis1 mitochondrial biogenesis

A direct interaction of Hsp70 chaperones with Fis1 has been previously suggested based on *in vivo* site directed crosslinking. Analysis of crosslinked samples revealed that the yeast homologs of cytosolic Hsp70s- Ssa1 and/or Ssa2 were bound to Fis1. The high sequence similarity between the two proteins did not allow a unique identification of the cross-linked adduct. Subsequently, the influence of Hsp70s on Fis1 biogenesis was demonstrated (K. Krumpke, PhD thesis). In order to verify these aforementioned results, we repeat these experiments.

To that end, we monitored the steady-state levels of Fis1 in cells harboring compromised cytosolic Hsp70s. The Ssa chaperones are redundant in function but at least one functional member of the family is required for viability. To estimate the relevance of the interaction of Ssas with Fis1 for its biogenesis, we used a triple SSA deletion strain (*ssa2-4Δ*) harboring either a native Ssa1 (*ssa2-4Δ+SSA1wt*) or a temperature sensitive allele of this gene (*ssa2-4Δ+SSA1ts*) (Becker et al., 1996). These strains were grown initially at 24°C (permissive conditions) and later shifted to 37°C (non-permissive conditions). An increase in the expression of Fis1 at elevated temperatures was observed in both strains. However, this increase was nearly threefold lower for *ssa2-4Δ+SSA1ts* as compared to *ssa2-4Δ+SSA1wt*, supporting the importance of Ssa chaperones for Fis1 biogenesis (Fig. 5.1A and B). As a control, the levels of the MOM protein Porin were similar at both temperatures and in both strains. Of note, the levels of mitochondrial matrix protein Aconitase were slightly reduced in *ssa2-4Δ+SSA1ts* strain upon heat shock. Aconitase import might thus partially depend on cytosolic Hsp70s, similarly to some other presequence-containing mitochondrial proteins (Deshaies et al., 1988). Taken together, these results suggest that the yeast Hsp70 chaperones Ssa1/2 are interacting with Fis1 and are required for its biogenesis.

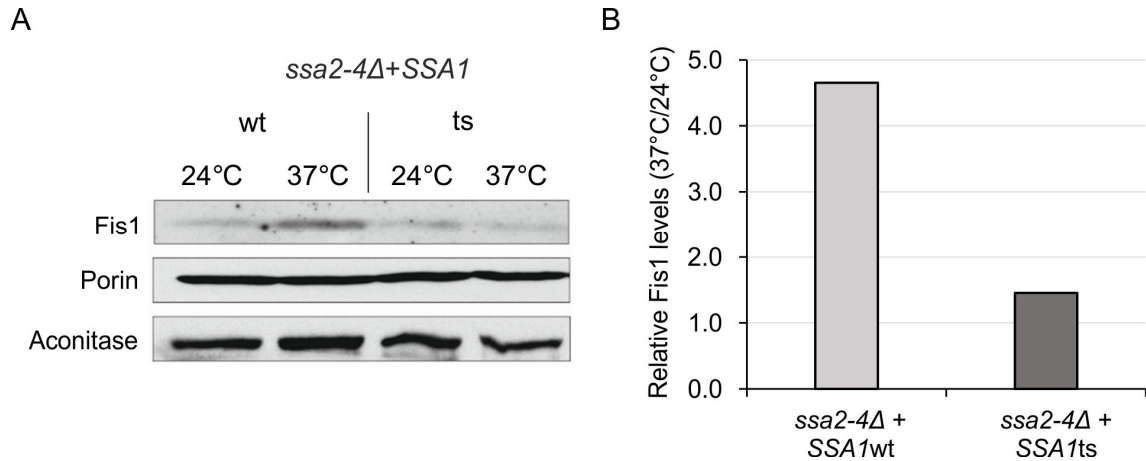


Figure 5.1: Mitochondrial steady state levels of Fis1 are reduced upon inactivation of cytosolic Hsp70s. (A) *ssa2-4Δ + SSA1wt* and *ssa2-4Δ + SSA1ts* cells were cultivated at 24°C and then were either left at 24°C or were shifted for 4 hrs to non-permissive conditions (37°C). Crude mitochondria were isolated and subjected to SDS-PAGE analysis followed by immunoblotting with antibodies against the indicated proteins. The mitochondrial protein Porin was used as a loading control. (B) Quantitative analysis of Fis1 steady-state levels. The intensities of bands from three independent experiments as that described in part (A) were quantified and the increase of Fis1 signal at 37°C as compared to 24°C for each strain was calculated.

To confirm that Hsp70 chaperones are required for mitochondrial Fis1 import, an established assay for the *in organello* import of radiolabeled Fis1 synthesized in reticulocyte lysate has been employed (Kemper et al., 2008). To monitor for a potential involvement of Hsp70, we added to the import reaction a known inhibitor of Hsp70, Mal3-101, which is a small molecule that inhibits Hsp70 ATPase activity (Fewell et al., 2004). In our assay, a Fis1 variant with a cysteine residue within the TMS (Fis1-TMC) was incubated with the sulfhydryl modifier IASD in order to distinguish between correctly membrane-integrated (unmodified) and nonintegrated (modified) Fis1 molecules. Hampering of Hsp70 with Mal3-101 led to a ca. 30% decrease in the import efficiency of unmodified Fis1-TMC and the known Hsp70 substrate, Aac (Fig. 5.2A, C and D) (Asai et al., 2004). Thus, the fact that both proteins Fis1 and Aac were similarly affected by Hsp70 inhibition indicates that inhibition of Hsp70 activity by Mal3-101 is impairing Fis1 import into the MOM. In contrast, import of pSu9-DHFR, which is not known to require the assistance of any chaperones, was unaffected (Fig. 5.2C and D).

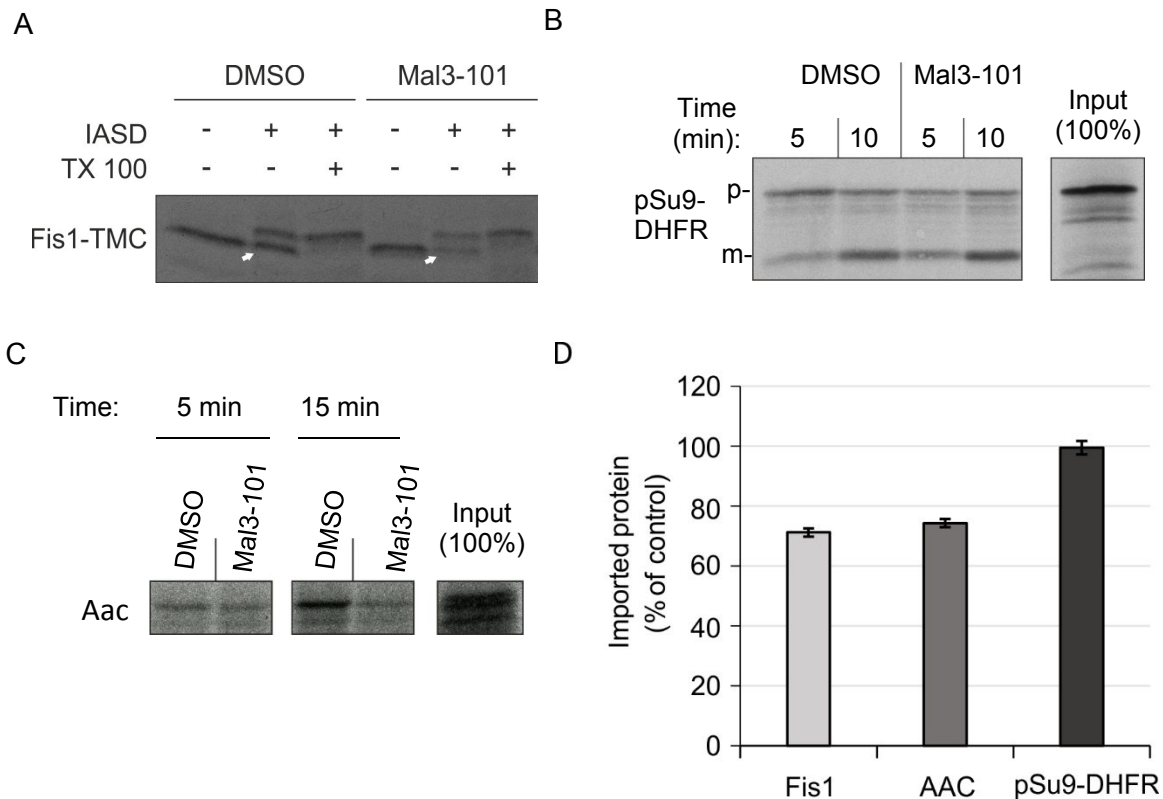


Figure 5.2: *In vitro* import of Fis1 is hampered by Hsp70 inhibition. Radiolabeled Fis1-TMC (**A**), pSU9-DHFR (**B**), and Aac (**C**) were imported into isolated WT mitochondria in the presence or absence of 250 μ M of Hsp70 inhibitor (Mal3-101) or DMSO as a control. Import reactions were analyzed by SDS-PAGE and autoradiography. Mitochondria after Fis1 import were treated with IASD in the presence or absence of TX 100. Bands representing correctly integrated Fis1-TMC are marked by a white arrow. (**D**) Import efficiencies of Fis1-TMC, Aac and pSU9-DHFR in the presence of Mal3-101 were evaluated as described in the Methods section. Import efficiency in control reactions was set to 100%. Error bars represent \pm s.d. (n=9).

To further confirm the involvement of Hsp70 in Fis1 biogenesis, the effect of deletion of the Hsp70 co-chaperone Sti1 on the mitochondrial Fis1 levels was examined. Previously, we observed reduced Fis1 levels in whole cell lysate of *sti1* Δ cells (Hoseini et al., 2016). Analysis of mitochondria isolated from either *sti1* Δ or WT cells revealed that at both normal (30°C) and elevated temperature (37°C), the levels of Fis1 are significantly reduced in the organelle from the mutated cells (Fig. 5.3A and B). In contrast, Tob55 levels were unaffected in the deletion strain and levels of Tom70, which is a potential membrane receptor for Sti1, were only slightly reduced (Fig. 5.3A) (Hoseini et al., 2016). Thus, we conclude that the Hsp70-Sti1 complex is involved in Fis1 biogenesis.

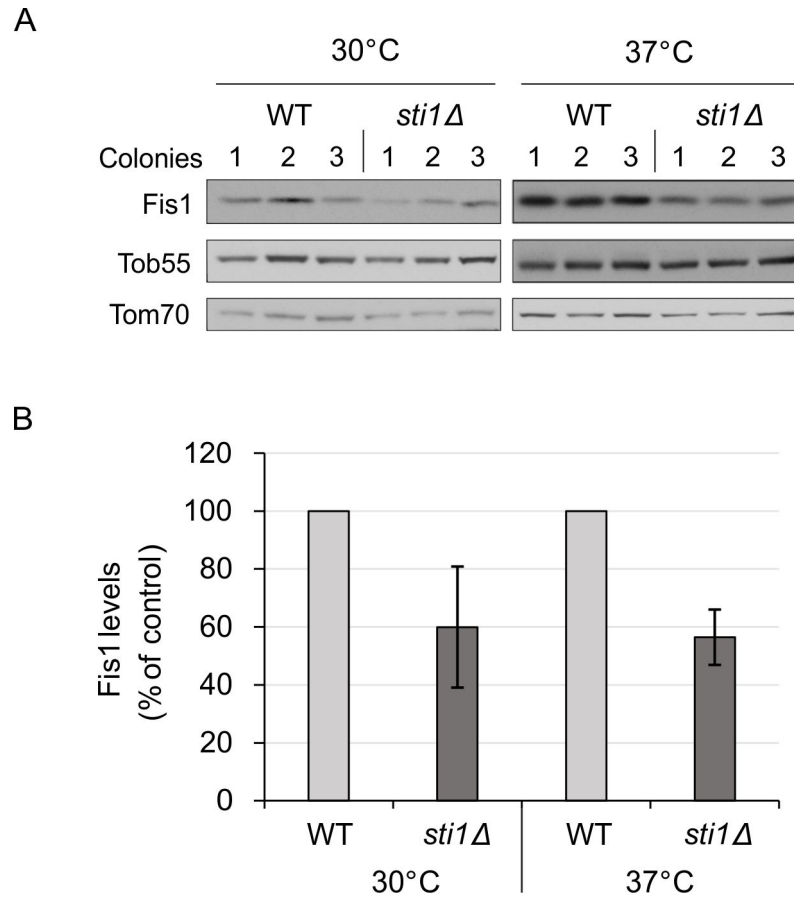


Figure 5.3: Mitochondrial steady-state levels of Fis1 are hampered in *sti1Δ* cells. (A) WT and *sti1Δ* cells were cultivated at either 30 °C or 37 °C. Crude mitochondria were isolated and subjected to SDS-PAGE followed by immunoblotting with antibodies against the indicated proteins. Tob55 was used as a loading control. (B) Quantitative analysis of Fis1 steady-state levels. The intensities of bands from three independent experiments as described in part (A) were quantified and the protein levels in WT cells were set to 100%. Error bars represent \pm s.d. (n=9).

5.2 Pex19 chaperone affects mitochondrial functionality

Since only a partial reduction of the mitochondrial Fis1 levels upon hampering Hsp70s' function was observed, we hypothesized that there is probably an alternative pathway to stabilize newly synthesized mitochondrial TA proteins. Pex19 is known to bind TA proteins shared between mitochondria and peroxisomes like Fis1 (Ast et al., 2013; Delille and Schrader, 2008).

The involvement of Pex19 in mitochondrial function is unknown. Therefore, we evaluated the effects of Pex19 deletion on mitochondrial morphology and functionality. Fluorescence microscopy analysis of mitochondria stained with mitochondrially targeted GFP (mtGFP) revealed that the number of abnormally shaped mitochondria is significantly increased in *pex19Δ* cells (Fig. 5.4A and B)

when compared to WT. In many cases, the shape of this abnormal mitochondria resembled the morphology of mitochondria with impaired fission.

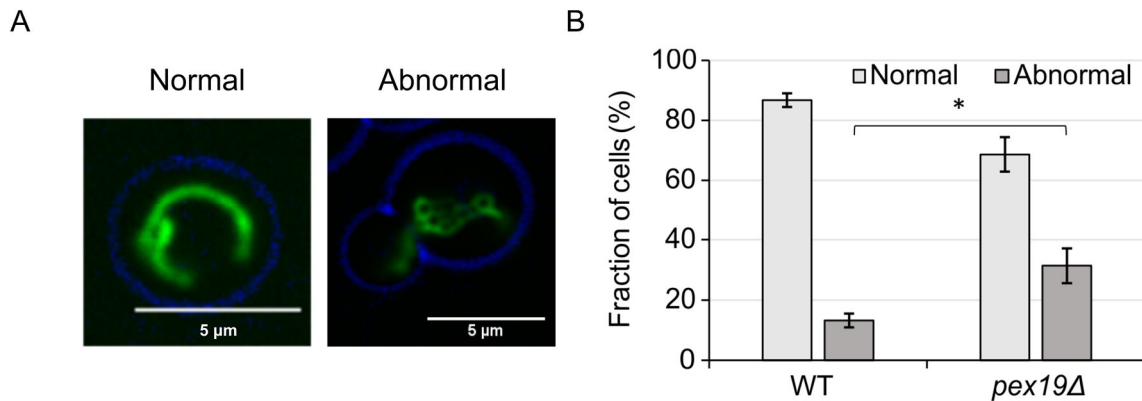


Figure 5.4: Deletion of *PEX19* causes alterations in mitochondrial morphology. (A) WT and *pex19Δ* cells expressing mitochondrial targeted GFP (mtGFP) were analyzed by fluorescence microscopy. Representing images of cells with either normal or abnormal mitochondrial morphology are shown. (B) Analysis of the cells described in (A). Average values with S.D. bars of six independent experiments with at least $n=100$ cells in each experiments are shown. * $p < 0.002$.

Additionally, growth test of the *pex19Δ* deletion strain showed growth defects of the strain on non-fermentable carbon source (glycerol or lactate) when respiration and the presence of an intact mitochondrial genome are essential (Fig. 5.5).

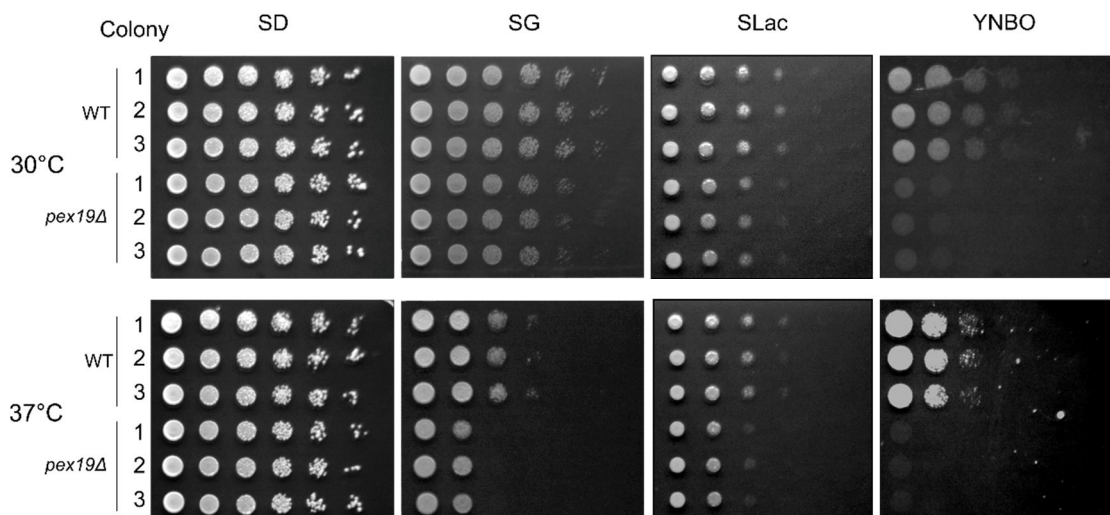


Figure 5.5: Deletion of *PEX19* causes respiratory growth defect. WT and *pex19Δ* cells were analyzed by drop dilution assay on synthetic medium containing glucose (SD), glycerol (SG), lactate (Lac) or oleate (YNBO) at either 30°C or 37°C. Three colonies from each strain are shown.

This growth impairment was even more severe at elevated temperature indicating that it is the chaperone-like function of Pex19 that is required for correct mitochondria activity. Of note, growth of the mutated strain on fermentable (glucose) carbon source was normal. As expected for a protein required for proper peroxisome biogenesis, the absence of Pex19 resulted in a severe growth defect on media containing the fatty-acid oleate as a carbon source (Fig. 5.5). Collectively, these experiments demonstrate the requirement of Pex19 for normal mitochondrial function and morphology.

5.3 Pex19 is involved in biogenesis of mitochondrial Fis1 and Gem1

To determine if Pex19 could be directly involved in mitochondrial protein biogenesis, we measured the steady state levels of Fis1 and a HA-tagged TA protein Gem1 (Gem1-HA). Protein levels were monitored in whole cell extract and mitochondria of WT, *pex19Δ* and a Pex19 overexpression strain (WT+Pex19[↑]). Of note, protein levels of mitochondrial β -barrel proteins Tob55, Tom40 and Porin, mitochondrial receptor Tom70 and Tom22 or cytoplasmic Bmh1 were not affected by Pex19 alterations (Fig. 5.6A and C, Fig. 5.8A, Fig. 5.17C). Surprisingly, although the levels of Fis1 were not reduced in whole cell extract of cells lacking Pex19 (Fig. 5.6A and B), they were significantly decreased in mitochondria isolated from these cells (Fig. 5.6C and D, 5.8A).

Next, we extend our investigation to another model mitochondrial TA protein, Gem1. Similar results as those obtained for Fis1 were observed for Gem1-HA levels in *pex19Δ* mitochondria. However, in contrast to the situation with Fis1, we observed already in whole cell extracts lower levels of Gem1-HA in cells lacking Pex19 and slightly higher, although not significant, in cells harboring elevated amounts of Pex19 (Fig. 5.7A and B). This trend was even clearer when isolated mitochondria were analyzed (Fig. 5.7C and D). The levels of the control MOM proteins Porin and Tob55 were not affected by the alterations in Pex19 amounts (Fig. 5.7A and C, Fig. 5.8B). Importantly, the reduction in the Gem1 steady-state levels was independent of the terminus that was tagged. N-terminally tagged GFP-Gem1 displayed similar compromised steady state levels

in mitochondria isolated from *pex19Δ* cells (Fig. 5.9). Thus, we conclude that the biogenesis of Gem1, similar to that of Fis1, is influenced by Pex19.

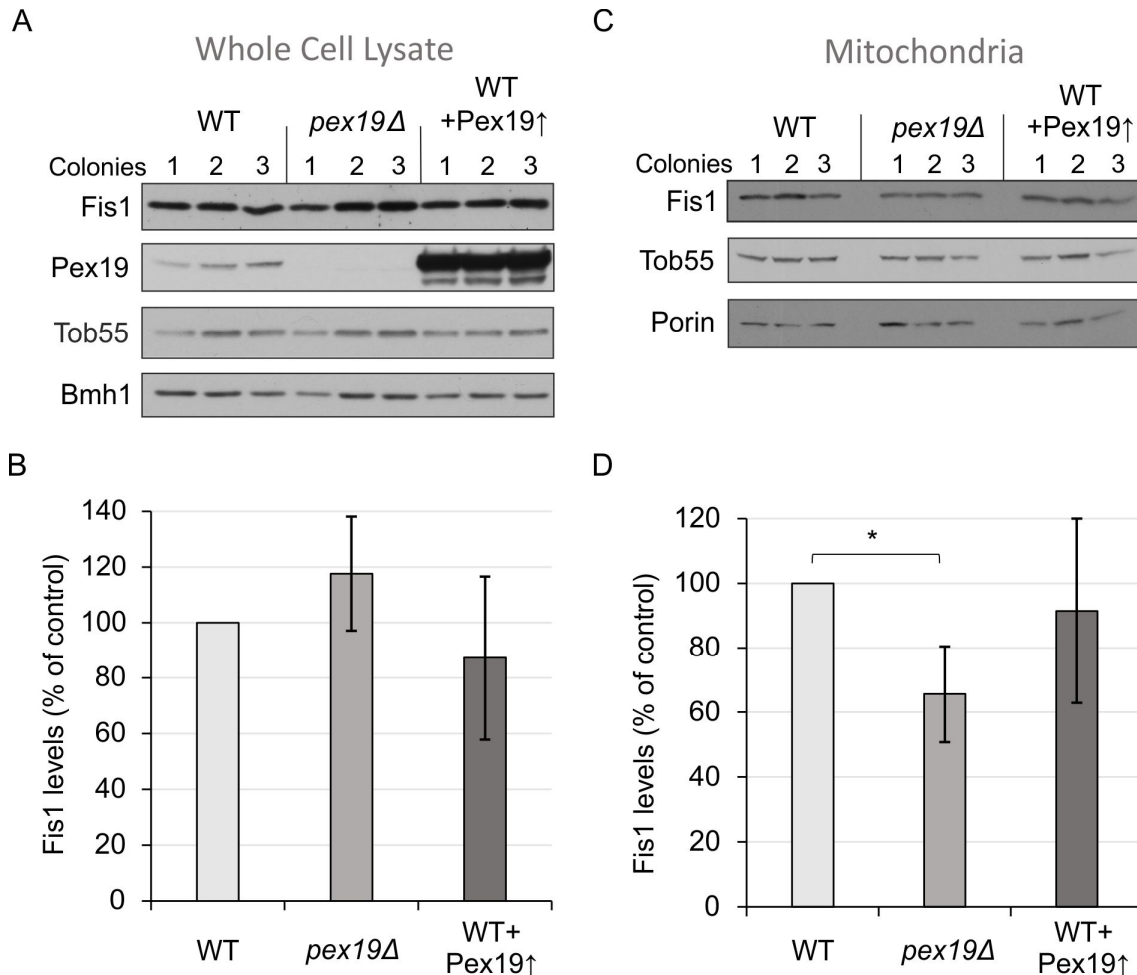


Figure 5.6: Mitochondrial from *pex19Δ* cells have impaired steady-state levels of Fis1. Whole cell lysates (A) or crude mitochondria fractions (C) of 3 colonies of WT, *pex19Δ*, or a strain overexpressing Pex19 (WT-Pex19↑) were analysed by SDS-PAGE and immunodecoration with the indicated antibodies. (B, D) The intensity of the Fis1 bands from three independent experiments as those presented in (A and C) are presented as mean percentages of their levels in whole cell lysate (B) (n=9) and mitochondria (D) of WT cells (n=15). Error bars represent \pm s.d. * $p < 0,0005$.

Accordingly, the trend remained similar when the model TA proteins levels were measured upon *PEX19* deletion or overexpression in a different yeast genetic background (W303a as opposed to BY4741). Fis1 levels were reduced in mitochondria from *pex19Δ* cells in the W303a background like they were in BY4741 background (Fig. 5.8A). Along the same line, overexpression of Pex19

in W303a background resulted in a clear increase in the mitochondrial Gem1-HA steady state levels (Fig. 5.8B). Taken together, these findings further underscore the involvement of Pex19 in mitochondrial TA biogenesis.

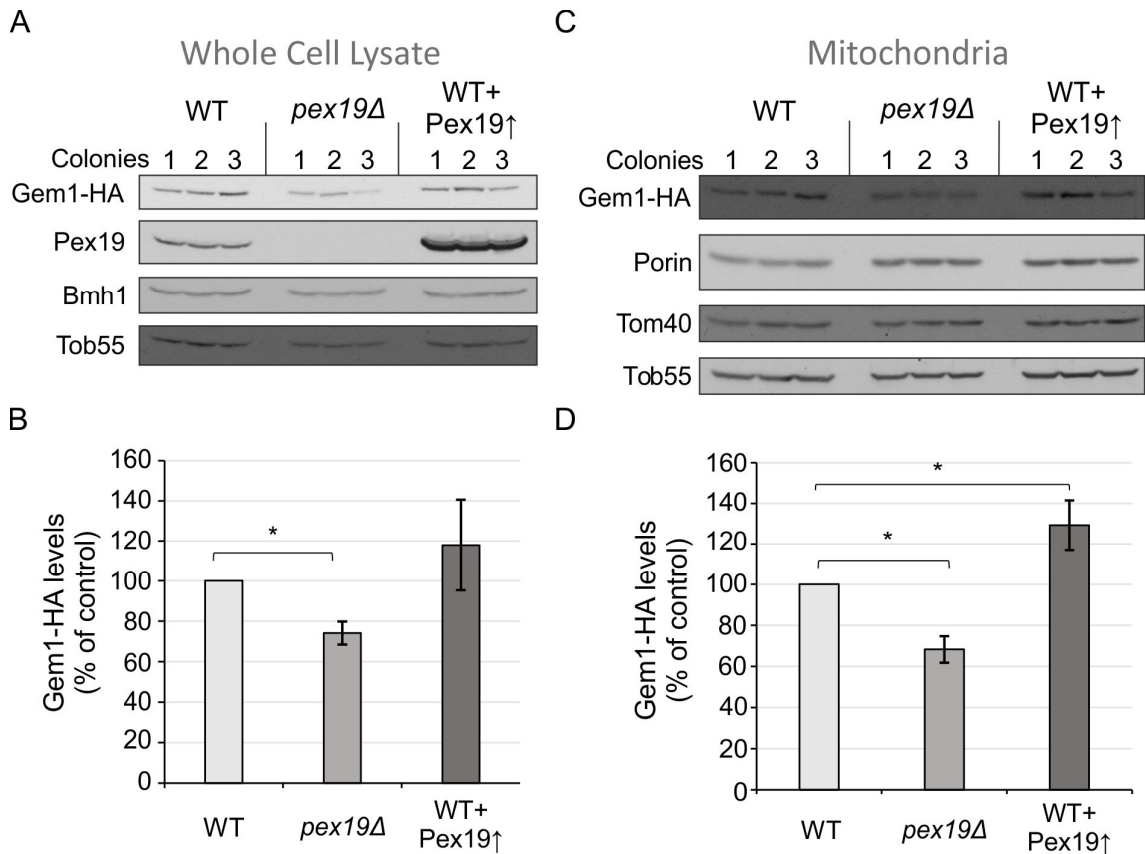


Figure 5.7: Alterations of the levels of Pex19 affect the cellular amounts of Gem1. (A, C) Whole cell lysates **(A)** or crude mitochondria fractions **(C)** of three colonies of WT, *pex19Δ*, or a strain overexpressing Pex19 (WT-Pex19↑) were analysed by SDS-PAGE and immunodecoration with the indicated antibodies. **(B and D)** The intensities of the Gem1-HA from three independent experiments as those presented in (A and C) are presented as mean percentages of their levels in whole cell lysate (B) and mitochondria (D) of WT cells (n=9).

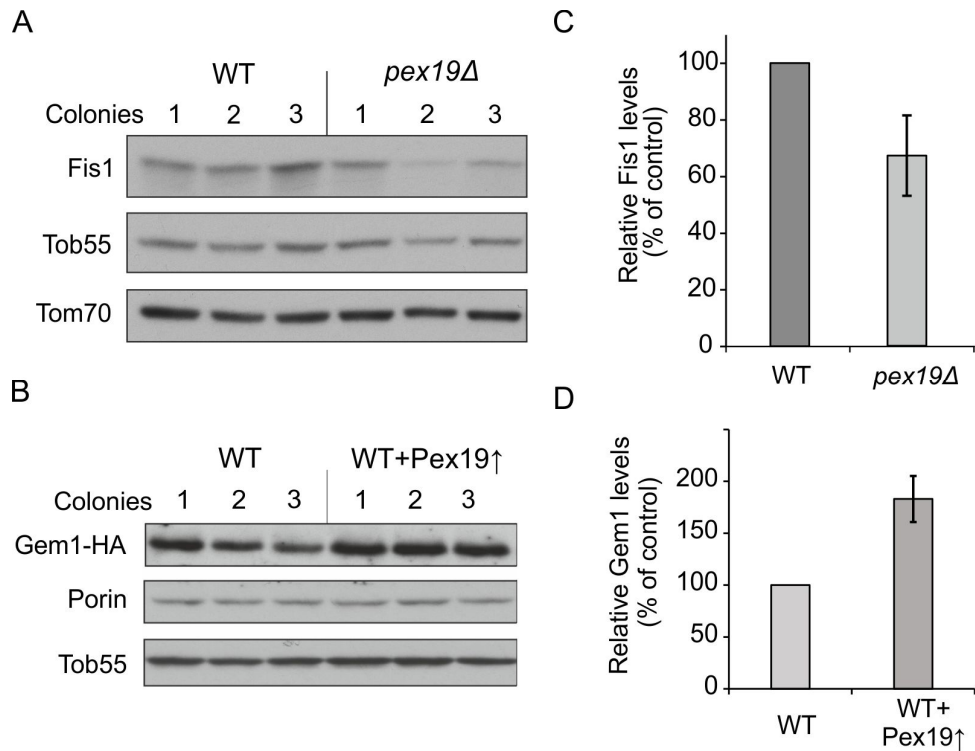


Figure 5.8: The amounts of mitochondrial TA proteins in the W303a background are affected by alteration of Pex19 levels. Crude mitochondria were isolated from three independent colonies of WT (W303a), *pex19Δ* cells (A) or cells overexpressing Pex19 (WT+Pex19↑) (B). Mitochondrial proteins were analysed by SDS-PAGE and immunodecoration with the indicated antibodies. The intensity of the Fis1 (C) or Gem1-HA (D) bands from three independent experiments as those presented in (A) and (B) are depicted as mean percentages of their levels in control mitochondria. Error bars represent \pm s.d. (n=9).

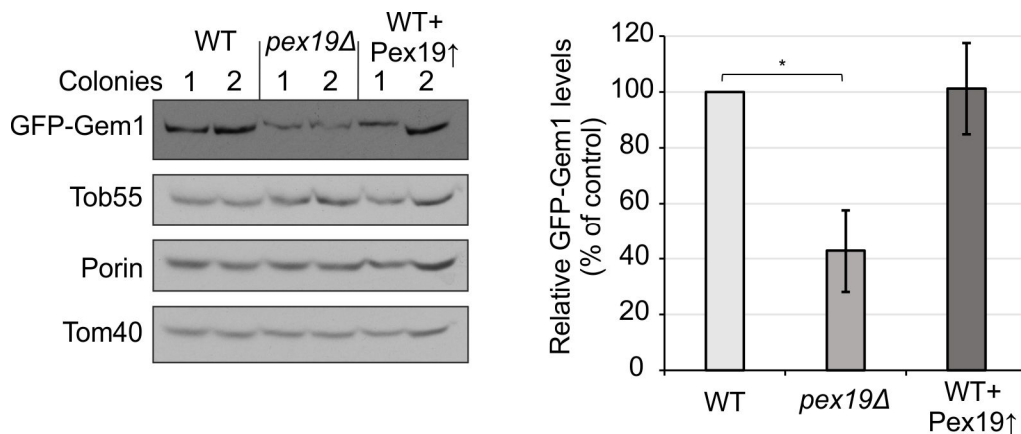


Figure 5.9: GFP-Gem1 levels are decreased in mitochondria from *pex19Δ* cells. (A) Crude mitochondria fractions of two colonies of WT, *pex19Δ* or WT+Pex19↑ cells were analysed by SDS-PAGE and immunodecoration with the indicated antibodies. (B) The intensity of the GFP-Gem1 signal from three independent experiments as those presented in (A) are depicted as mean percentages of their levels in control mitochondria. Error bars represent \pm s.d. (n=9). *, $p < 0.00027$.

5.4 Pex19 is contributing to Atg32-HA biogenesis

Since Pex19 is known to bind to different classes of membrane proteins, we wondered whether it can additionally affect biogenesis of other single span membrane proteins like Atg32, which are topologically similar to TA proteins. To evaluate if Pex19 can interact with Atg32, we searched for peroxisomal targeting motif mPTS1 consensus sequences in the Atg32. Align of the Atg32 sequence with the consensus motif revealed that the protein possess two mPTS1 sites indicating possible binding between Pex19 and Atg32 (Fig 5.10).

```

30  MVLEYQQREGKGSSSSKSMPPDSSSTTIHTC
60  SEAQTGEDKGLLDPHLSVLELLSKTGHSPS
90  PMGQNLVTSIDISGNHNVNDSISGSWQAIQ
120 PLDLGASFIPERCSSQTTNGSILSSSDTSE
150 EEQELLQAPAADIINI KQGQEGANVVSPS
180 HPFKQLQKIISLPLPGKEKTPFNEQDDDGD
210 EDEAFEDSVTITKSLTSSSTNSFVMPKLSL
240 TQKNPVFRLLILGRTGSSFYQSIPKEYQSL
270 FELPKYHDSATFPQYTGIVII FQELREMVSL
300 LNRIVQYSQG KPVIPICQPGQ VIQVKNV LK
330 SFLRNKLV KLLFPPVVVTN KRDL KKMFQRL
360 Q DLSL EYG EDVN EEDN DDEAI TKRSYCR
390 N KA ENS KKKSP KSN KKP KRKKQ KFFTSWF
420 TWGISITIGISFGCCVTYFVTAAYEHQTVK
450 SLSL RPSILASLLSL DSSS DTINTPATASP
480 SST EQFLWF DKGTLQINF HSDGFIM KSLTI
510 KETWG KMNTFVL HALS KPLKFL ENLN KSSE
540 FS DESN RILALGYILL

```

Figure 5.10: Protein sequence of Atg32. Positive (green) and negative (red) charges flanking the putative TMS are displayed. The two identified mPTS motifs are highlighted in yellow. The putative transmembrane segment of Atg32 is underlined and in bold letters.

Next we monitored the steady state levels of internally HA-tagged Atg32 (Atg32-HA) in mitochondria and whole cell lysate. Despite structural difference between Atg32 and Gem1, Atg32 was similarly affected by alterations in Pex19 levels as Gem1. Atg32-HA levels were significantly decreased in whole cell extract of *pex19Δ* cells and mitochondria isolated from these cells (Fig. 5.11 A, B, C, and D). Accordingly, upon Pex19 overexpression, Atg32-HA levels were increased both in whole cell extract and mitochondrial fraction (Fig 5.11 A, B, E and F). Thus, we conclude that Pex19 influences the biogenesis of Atg32.

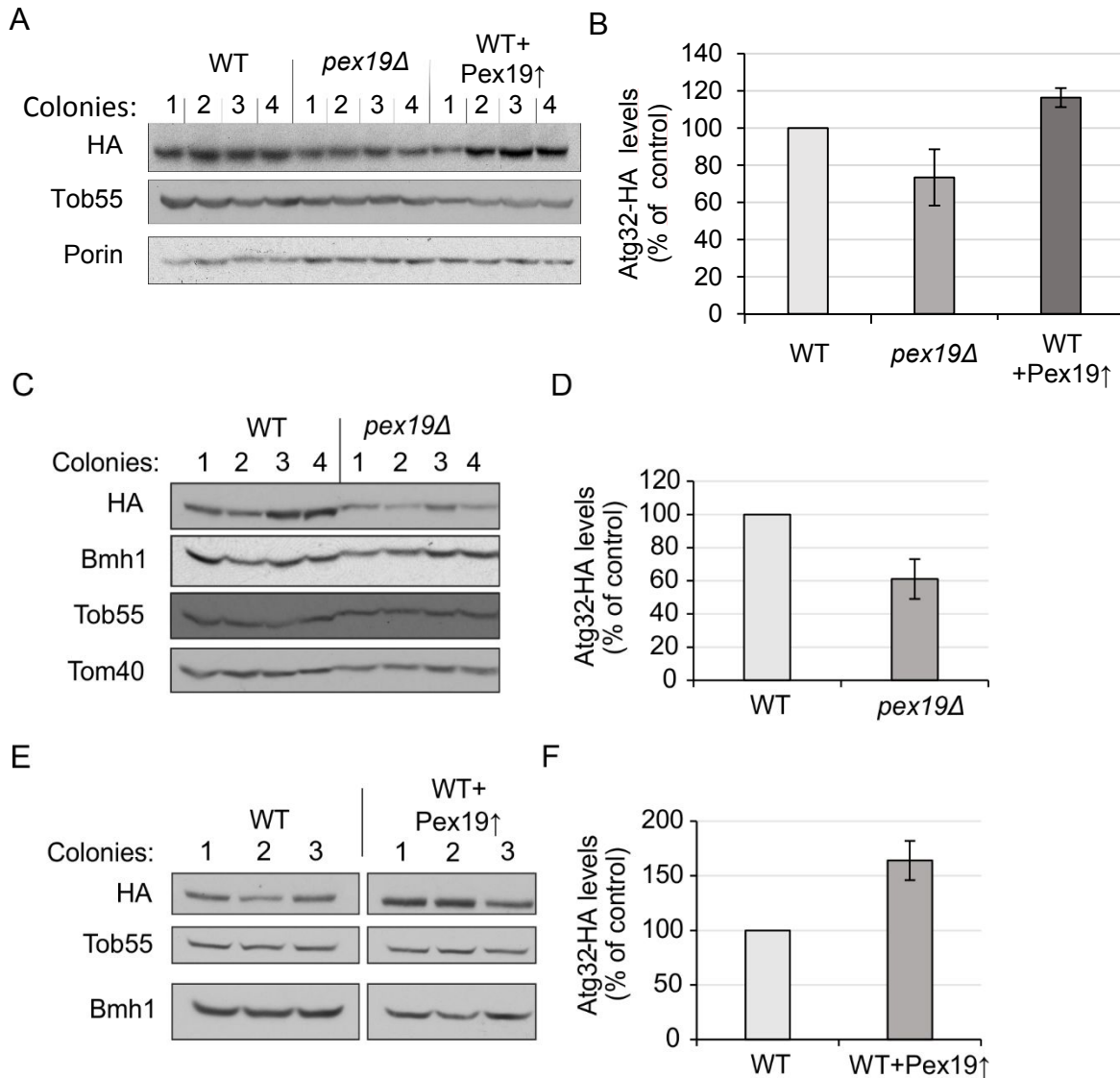


Figure 5.11: Atg32-HA levels are reduced in *pex19Δ* cells and increased in WT+Pex19↑ mitochondria. Crude mitochondria fractions (A) or whole cell lysates (C and E) of three or four colonies of WT, *pex19Δ*, or WT overexpressing Pex19 (WT+Pex19↑) strain were analyzed by SDS-PAGE and immunodecoration with the indicated antibodies (HA = Atg32-HA). The intensity of the Atg32-HA from three independent experiments as those illustrated in (A), (C) and (E) are presented as mean percentages of their levels in mitochondria (B) and whole cell lysate (D and F). Error bars represent \pm s.d. (n=9).

5.5 Peroxisomal contaminations in crude mitochondria fraction do not affect the outcome of the assays

To assure that our results are not biased by massive contamination of the mitochondrial fraction by peroxisomes, we monitored the purity of the isolated mitochondria under differential centrifugation conditions (from 2000g to 15000g). Since the density of peroxisomes is slightly lower than that of mitochondria, we

observed that the content of peroxisomes in the pelleted fraction is increasing with elevated centrifugation speed (Fig 5.12). Pelleting mitochondria by 2000g centrifugation results in a very poor yield but in relatively less peroxisome contamination.

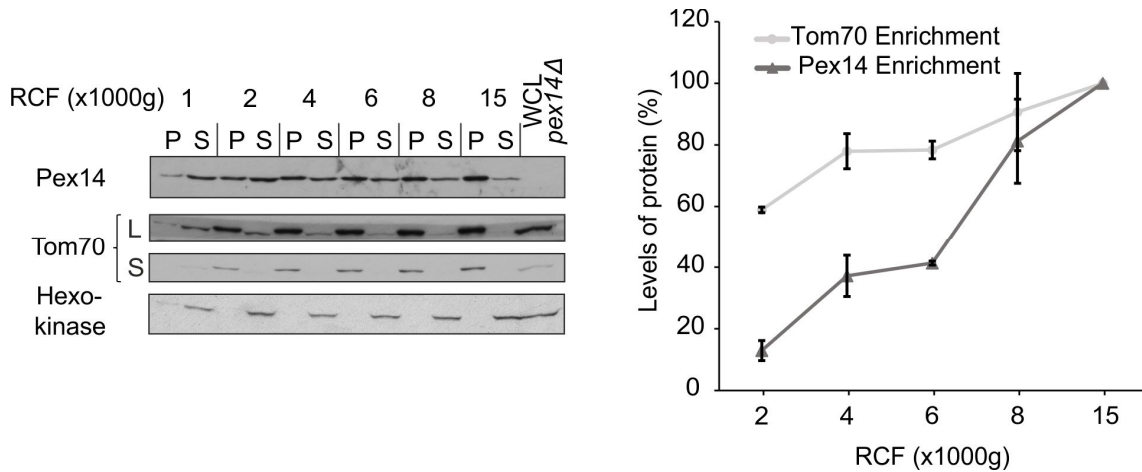


Figure 5.12: Pelleting at lower centrifugation speeds results in reduced peroxisomal contamination in mitochondria fraction. Left panel: crude membrane fractions (pellet, P) and the corresponding supernatant (S) were collected after centrifugation at the indicated force. Samples were analysed by SDS-PAGE and immunodecorated with the indicated antibodies. For Tom70, long (L) and short (S) exposures are presented. Right panel: the intensities of Tom70 and Pex14 from the different membrane fractions of three independent experiments as those presented in the left panel were quantified and presented as mean percentages of their levels in the 15×10^3 g fraction ($n=9$). Error bars represent \pm sd. ($n=3$).

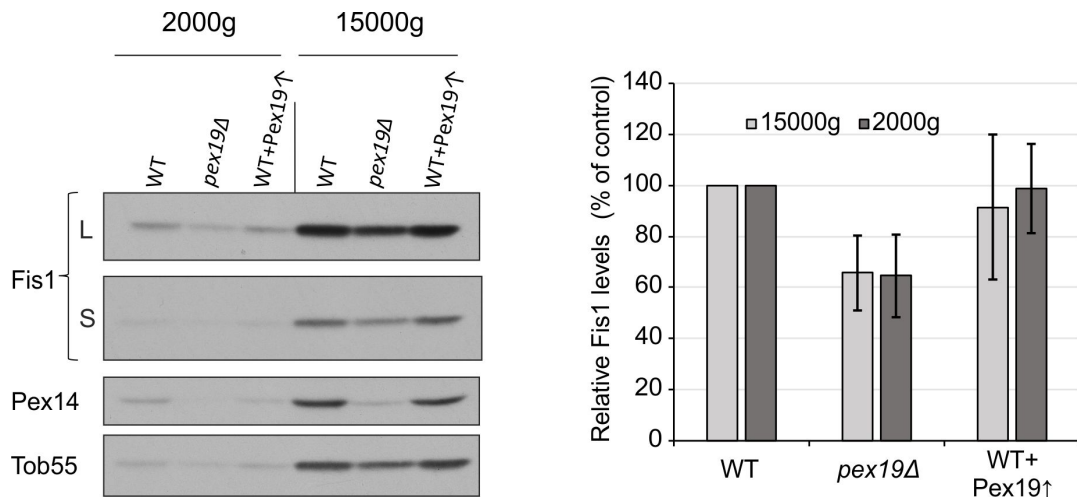


Figure 5.13: Pex19 influence on mitochondrial Fis1 levels is independent of peroxisomal contaminations in the fractions. The crude mitochondria fractions of WT, *pex19Δ*, or WT overexpressing Pex19 (WT+Pex19 \uparrow) strains were collected either at 2000g or 15000g and analysed by SDS-PAGE and immunodecoration with the indicated antibodies. For Fis1, long (L) and short (S) exposures are presented. Right panel: the intensities of Fis1 from eight experiments were quantified and the signal of WT cells was set as 100%. Error bars represent \pm s.d. ($n=8$).

Of note, also under these conditions, we observed reduced amounts of Fis1 in the *pex19Δ* mitochondrial fraction (Fig. 5.13). These findings indicate that the observed reduction of Fis1 in mitochondria from *pex19Δ* cells is independent of peroxisome contamination.

5.6 Pex19 does not influence the stability of mitochondrial TA proteins

Previous studies demonstrated that in absence of Pex19 peroxisomal membrane proteins are either mislocalized to mitochondria or degraded (Sacksteder et al., 2000). However, when we analyzed protein stability by translation inhibition assays with cycloheximide in *pex19Δ* we did not find evidence that mitochondrial Fis1, Gem1-HA or Atg32-HA levels are decreased due to fast turnover of MOM TA proteins. The stable protein Bmh1 was taken as a control. Fis1 levels in whole cell extract declined after halting of translation, similar to Tob55 and Tom22, but were not significantly altered in *pex19Δ* strains when compared to WT (Fig. 5.14A and B).

The levels of Gem1-HA and Atg32-HA turned out be much more sensitive to cycloheximide addition than Fis1 but were similarly not altered between *pex19Δ* and WT. Moreover, overexpression of Pex19, although significantly increases the amount of Gem1-HA and Atg32-HA, did not change the stability of both membrane proteins (Fig 5.14B and C). Interestingly, independently if Gem1-HA and Atg32-HA were expressed in WT, *pex19Δ* or WT+Pex19[↑] strains, after translation inhibition takes place, in all three strains the TA proteins undergo degradation to the same basal levels.

Thus, we conclude that Fis1 is neither mislocalized from peroxisomes to mitochondria, which would lead to an increase of its mitochondrial levels, nor degraded in the absence of Pex19. Likewise, we demonstrate that Gem1 and Atg32-HA stabilities are unaffected by alteration of Pex19 levels, although they are significantly more unstable than Fis1.

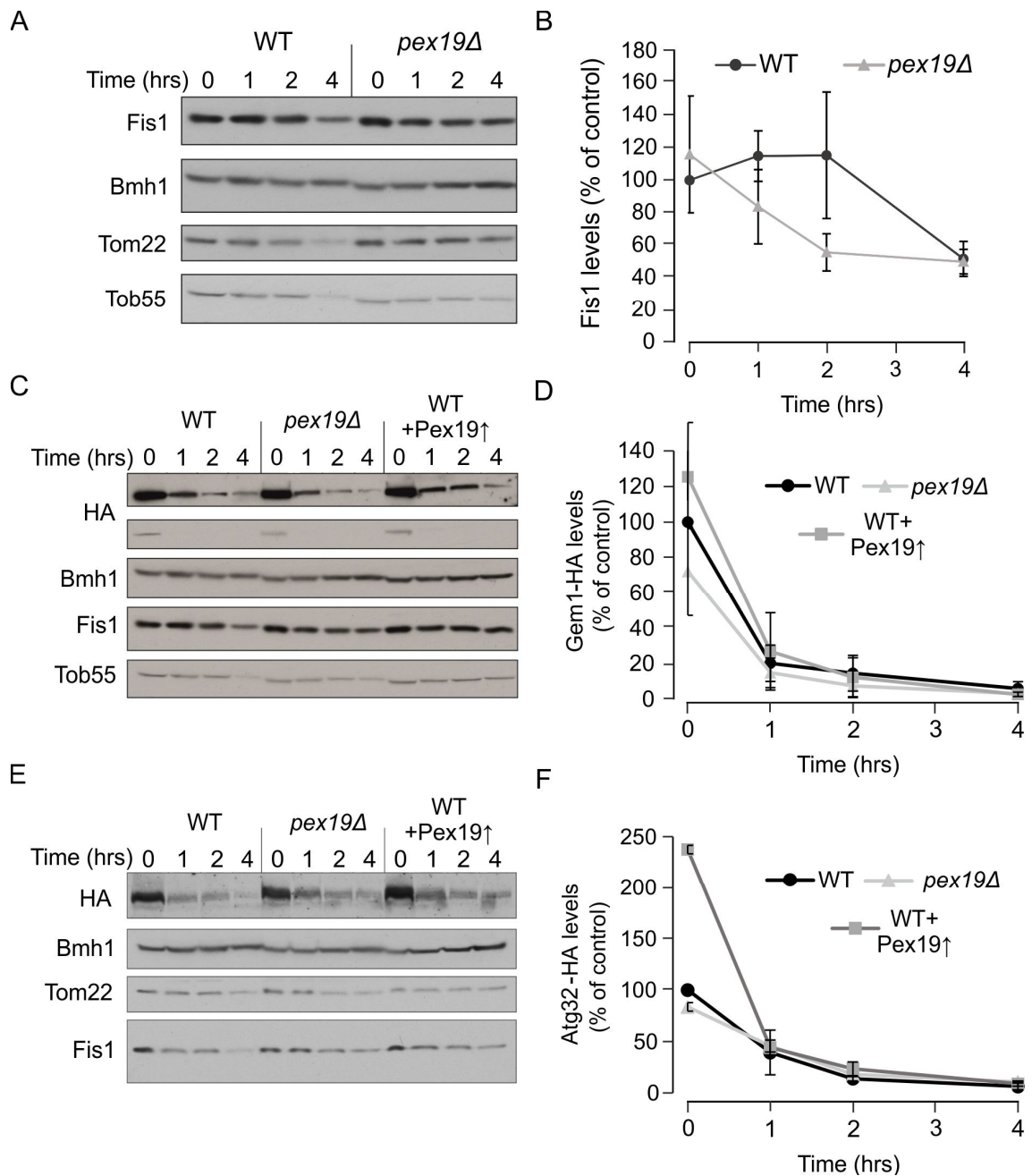


Figure 5.14: Pex19 does not affect significantly the stability of mitochondrial TA proteins. The stability of Fis1 (A) Gem1-HA (C) or Atg32-HA (E) was tested in a cyclohexamide decay experiment in either WT or *pex19Δ* cells. Fractions were collected in the indicated time points. Later, whole cell extract was obtained and analyzed by SDS-PAGE and immunodecoration. Fis1 (B), Gem1-HA (D) or Atg32-HA (F) intensities from three experiments were quantified. The signal from WT at time point 0' was set as 100%. Error bars represent \pm s.d. (n=3).

5.7 Pex19 is an interactor of Fis1 and Gem1

Data from biochemical methods indicated that alteration of Pex19 levels affect mitochondrial Fis1 and Gem1 biogenesis. To test whether this can be a result of direct interaction of Pex19 with the MOM TA proteins, we performed pull-down assays of Fis1 and Gem1 with Pex19. Fis1 and N-terminally tagged HA-Gem1 were affinity purified from lysed mitochondria using GST-tagged Pex19 as a bait (Fig. 5.15A and B). While the TA proteins were eluted with the bait protein bound to glutathione-sepharose beads, other MOM proteins like Porin or Tom22 were not. Moreover, none of the proteins was bound to GST alone although more GST was bound to the beads than GST-Pex19. These findings demonstrate that Pex19 is directly interacting with Fis1 and Gem1.

Taken together, the fact that MOM TA levels depend on the abundance of Pex19 and our observation that Pex19 can directly interact with the affected proteins suggests that Pex19 is directly involved in the biogenesis of MOM TA proteins.

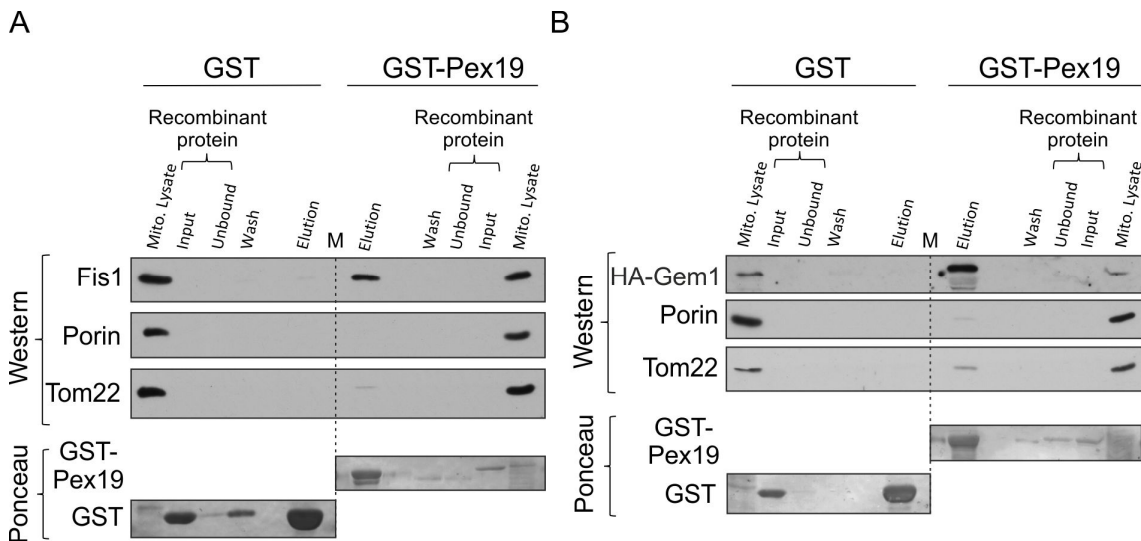


Figure 5.15: Fis1 and Gem1 interact directly with Pex19. (A and B) Mitochondria isolated from WT cells (A) or cells expressing HA-Gem1 (B) were lysed with Triton X-100 and incubated with recombinant GST alone or GST-Pex19, prebound to glutathione beads. After washing, bound material was eluted and proteins were analyzed by SDS-PAGE, blotting onto a membrane, and either detection with the indicated antibodies or Ponceau staining. Mito. Lysate, 1% of mitochondrial lysate used for binding; Wash, 0.5% of washed material; Elution, 20% of bound material; M, a lane with molecular size marker proteins. In lanes indicated 'recombinant protein', the input of the recombinant proteins added to the beads and the unbound material are shown.

5.8 The TA region of Gem1 is sufficient for recognition by Pex19

The tail-anchor segment of TA proteins is necessary and sufficient for the proper biogenesis of these proteins. Therefore, we asked whether this segment is sufficient for the recognition by Pex19. To that aim, we expressed the TMS of Gem1 fused to GFP (GFP-Gem1(TMS)) in cells lacking Pex19 or in those with elevated amounts of the protein. Similar to the full-length Gem1, GFP-Gem1(TMS) was found in reduced amounts in both whole cell lysates and isolated mitochondria of *pex19* Δ cells (Fig. 5.16A, B, C and D).

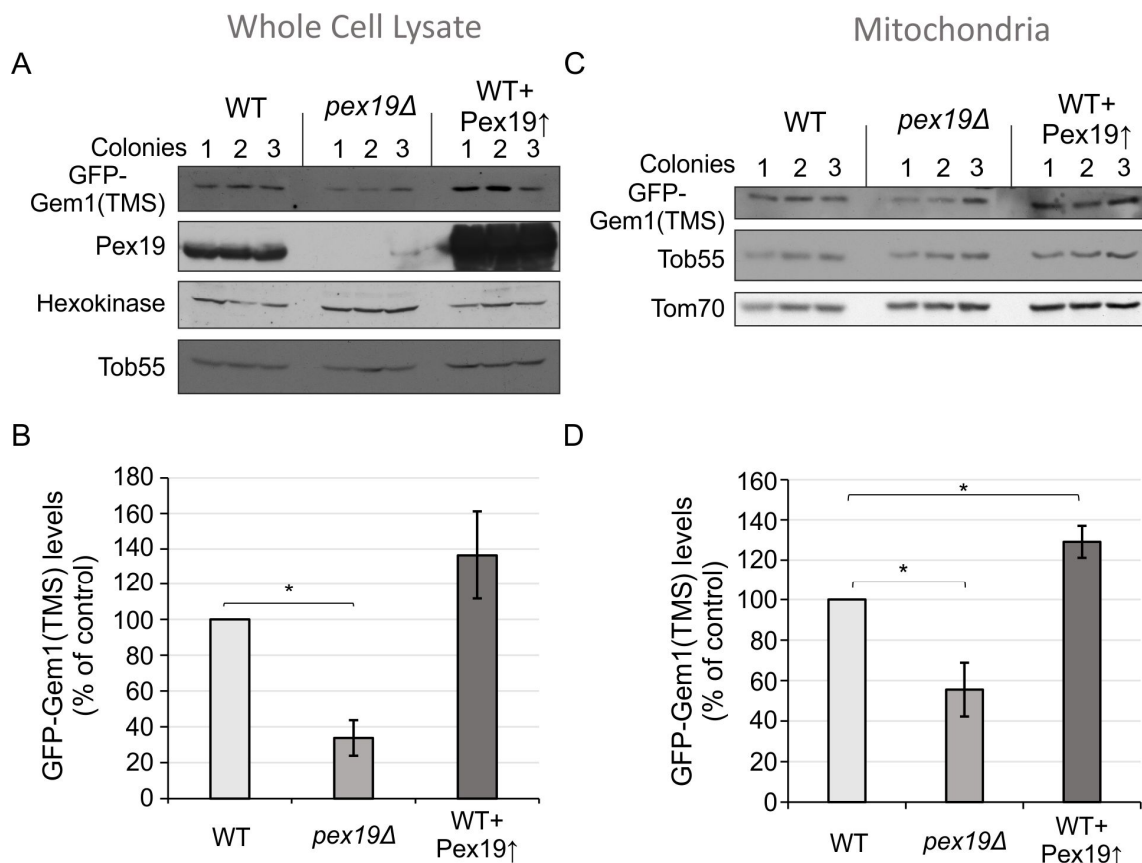


Figure 5.16: Alterations of the levels of Pex19 affect the cellular amounts of GFP-Gem1(TMS). (A, C) WT, *pex19* Δ , and WT+Pex19 \uparrow cells were transformed with a plasmid encoding GFP-Gem1(TMS). Whole cell lysates (A) or crude mitochondria fractions (C) of three colonies of these cells were analyzed by SDS-PAGE and immunodecoration with the indicated antibodies. (B and D) The intensities of the GFP-Gem1(TMS) signal from three independent experiments as in (A) and (B) are presented as mean percentage of WT cells in whole cell lysate (B) and mitochondria (D) (n=9). Error bars represent \pm s.d. *, $p < 0.005$.

The importance of Pex19 in the biogenesis of Gem1 is substantiated by the elevated levels of the fusion protein upon overexpression of Pex19. As a control, the levels of eGFP alone in whole cell extract were not affected by the deletion or *PEX19* (Fig. 5.17A and B).

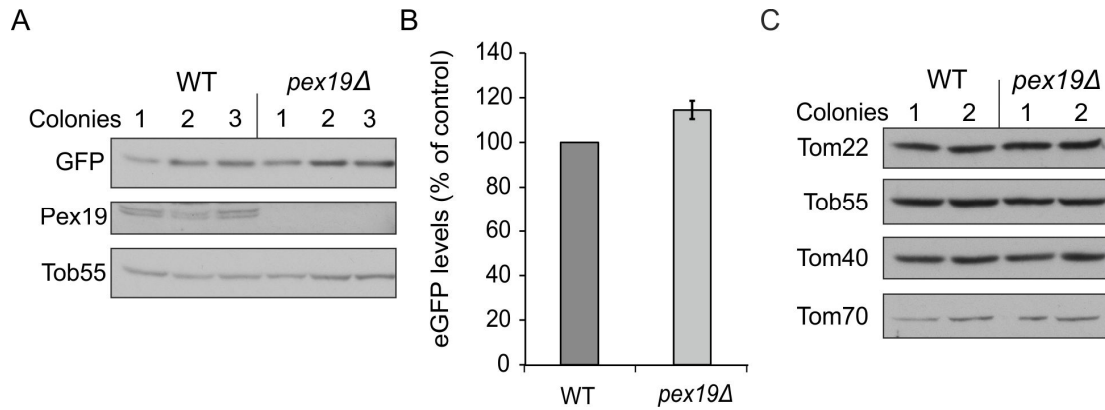


Figure 5.17 eGFP and Tom22 levels are unaffected in *pex19Δ* cells. (A) Whole cell lysates of three colonies of WT or *pex19Δ* cells expressing eGFP were analysed by SDS-PAGE and immunodecoration with the indicated antibodies (n=6). (B) The intensity of the eGFP from three independent experiments as those presented in (A) are depicted as mean percentage of its levels in control cells (n=9). Error bars represent \pm s.d. (C) Crude mitochondria fractions of 2 colonies of WT or *pex19Δ* strain were analysed by SDS-PAGE and immunodecoration with the indicated antibodies.

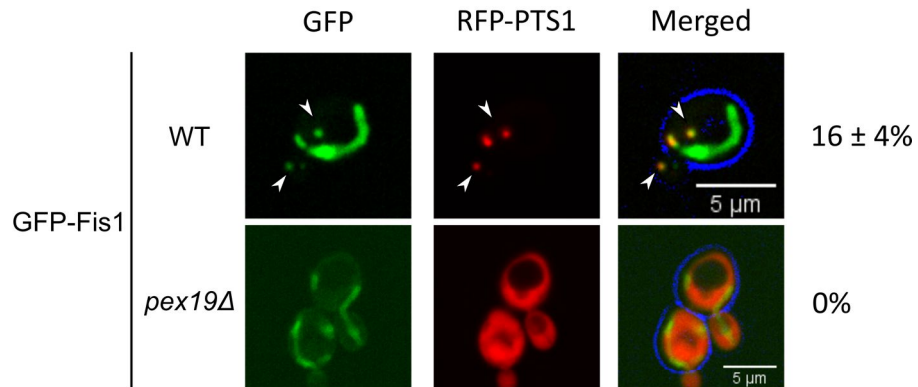
These results imply that the TMS of Gem1 together with its flanking regions is sufficient to be recognized by Pex19. Our findings are also in line with previous works demonstrating that Pex19 can recognize the peroxisomal targeting sequence at the TMS and CTE of peroxisomal TA proteins (Delille and Schrader, 2008; Halbach, 2006).

5.9 GFP-Gem1 and GFP-Gem1(TMS) are dually localized to mitochondria and peroxisomes

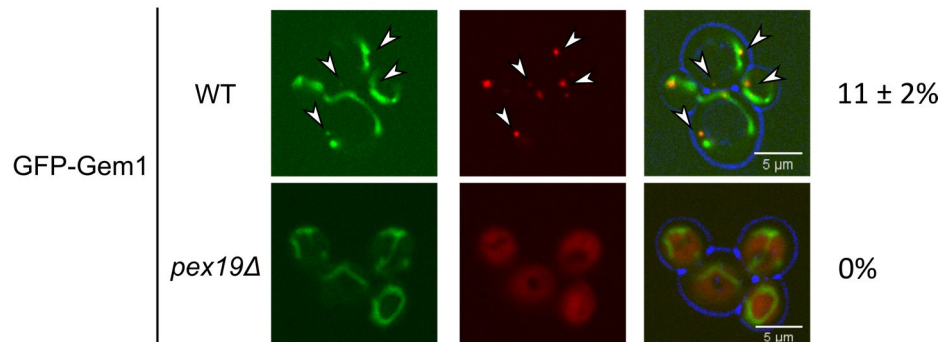
The significant effect of Pex19 on the steady state levels of Gem1 led us to ask if Gem1, similarly to Fis1, shares a dual localization in mitochondria and peroxisomes (Koch et al., 2005). During the course of this study, the human homologs of Gem1 – Miro1/2 were found to be located also in peroxisomes (Costello et al., 2017). To address this point, GFP-Gem1 and GFP-Gem1(TMS)

were expressed in WT or *pex19* Δ cells together with the peroxisomal marker PTS1-mCherry. As a comparison, GFP-Fis1 was also examined. The localization of these proteins was examined using fluorescent microscopy. When analyzing the distribution of GFP-Fis1, GFP-Gem1 and GFP-Gem1(TMS), large tubular structures of mitochondria could be detected but also small punctual structure co-localizing with the PTS1 marker (Fig. 5.18A, B and C).

A



B



C

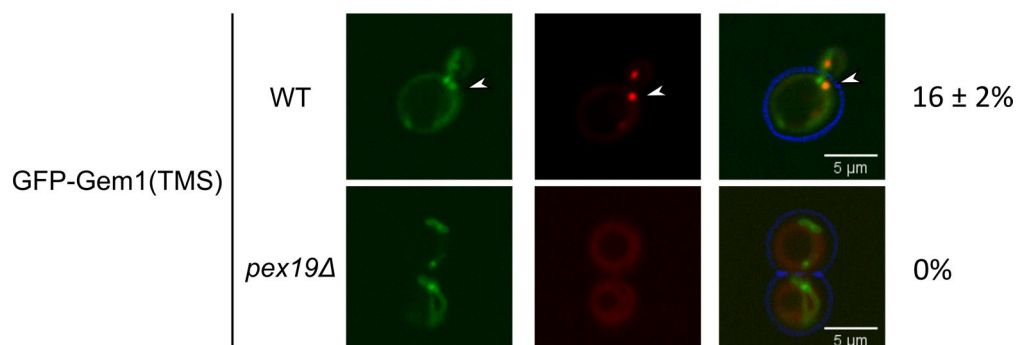


Figure 5.18: Fis1, Gem1 and GFP-Gem1(TMS) dual-localize to mitochondria and peroxisomes. WT or *pex19* Δ cells harboring peroxisomal-targeted RFP and expressing GFP-Fis1 (A), GFP-Gem1 (B), or GFP-Gem1(TMS) (C) were visualized by fluorescence microscopy. The percentage of cells with peroxisomal location of the GFP-tagged proteins is indicated to the right \pm s.d. The numbers reflect three independent experiments with at least 100 cells in each.

This co-localization vanished in the *pex19Δ* strain when the PTS1-mCherry signal was dispersed in the cell due to lack of functional peroxisomes. Furthermore, the co-localization points resembled the ones of GFP-Fis1 with the PTS1-mCherry (Fig. 5.18A). Hence, we conclude that the observed structures are peroxisomes and that both GFP-Gem1 and GFP-Gem1(TMS) are dual-localized to mitochondria and peroxisomes. The co-localized structures cover only a minority of the total signal in the population (data not shown) and are present in 11-16% of the cells in the population (Fig. 5.18A, B and C). Of note, many co-localization structures could be found on mitochondrial tubules representing most likely peroxisome-mitochondria contact sites. This co-localization foci were not part of the quantifications.

5.10 Pex19 is required for import of Fis1 and Gem1 into mitochondria

Since Fis1 levels are reduced in mitochondria *pex19Δ* cells, but neither are its levels reduced on the whole cell level nor is its stability significantly affected, we hypothesized that Pex19 might directly import TA proteins to the MOM like it does for peroxisomal proteins (Fang et al., 2004). However, inconsistently with this observation, Gem1 whole cell extract levels of all of the Gem1 hybrid constructs were altered when *PEX19* was deleted or overexpressed. In order to test if Pex19 can participate directly in import of MOM TA proteins, we performed an *in vitro* import assay for Gem1 or Fis1-TMC into isolated mitochondria in presence or absence of Pex19. To achieve this, radiolabelled proteins were expressed in yeast extract from either WT or *pex19Δ* cells. Afterwards, the radiolabeled proteins were mixed with isolated mitochondria and Fis1-TMC was modified with IASD whereas Gem1 was carbonate extracted to measure the TA protein incorporation into the membrane.

When Fis1-TMC was imported into mitochondria from WT cells, no significant difference in import efficiency could be observed between the proteins translated either in WT or *pex19Δ* extract (data not shown). Interestingly, when the identical experiment was performed with import of TA proteins expressed in WT extract into WT mitochondria and TA proteins expressed in *pex19Δ* extract into *pex19Δ* mitochondria, the import efficiency of Fis1-TMC was significantly

impaired for the protein pool coming from the *pex19* Δ extract in comparison to the WT extract (Fig. 5.19A). Similarly, import of Gem1 expressed in the *pex19* Δ extract was impaired when imported into *pex19* Δ mitochondria (Fig. 5.19B) whereas import of matrix precursor protein pSu9-DHFR was not affected (Fig. 5.19C).

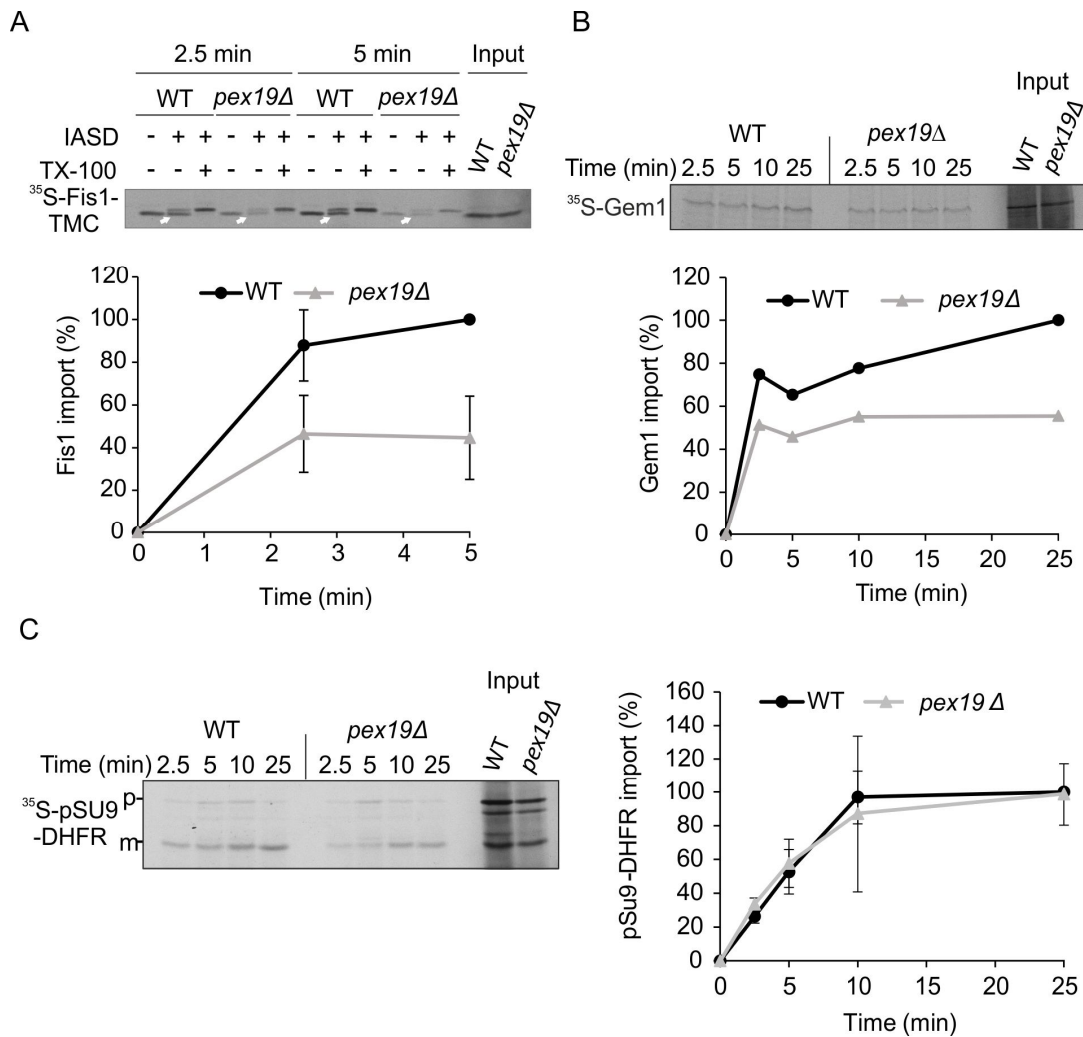


Figure 5.19: In vitro import of TA proteins into mitochondria is inhibited in the absence of Pex19. (A, B) Mitochondria isolated from WT or *pex19* Δ cells were incubated with radiolabelled Fis1-TMC (A) or Gem1 (B) synthesized *in vitro* in yeast extract of either WT or *pex19* Δ cells. After import for the indicated time periods, mitochondria were subjected to either an IASD assay, (A) or alkaline extraction (B). In both cases, samples were analysed by SDS-PAGE and autoradiography. Lower panels: Bands corresponding to the IASD unmodified form (A) or present in the alkaline pellets (B) were quantified and import into control mitochondria after 5 min was set to 100%. The mean \pm s.d. is depicted ($n = 3$). White arrow head, IASD unmodified band (C) Radiolabelled pSu9-DHFR was synthesized and imported as in (A) and (B) for the indicated time points. After import, mitochondria were treated by PK to remove unimported molecules, re-isolated, and analysed by SDS-PAGE and autoradiography. p and m, precursor and mature forms, respectively. Bands corresponding to the mature form were quantified and import into control mitochondria for 25 min was set to 100%. The mean \pm s.d. is depicted ($n = 3$).

We conclude therefore that Pex19 assists the import of Fis1 and Gem1 into the MOM. Additionally, we speculate that Pex19 is most likely attached to mitochondria membrane since import competence was indistinguishable for TA proteins from *pex19* Δ and WT yeast extract when imported to mitochondria from WT cells.

5.11 Pex19 is localized to mitochondria

To check if indeed Pex19 can be bound to mitochondria, we performed an immunodetection assay of Pex19 in isolated mitochondria. To purify the mitochondrial fraction to a grade free from peroxisome contamination, we separated an organelle pellet, using a sucrose gradient, into mitochondria and peroxisome fractions (Distel and Kragt, 2006). All the fractions were analyzed by SDS-PAGE and immunodecorated for Pex19 and Pex14 as a peroxisome marker and Tom20 as a mitochondrial one.

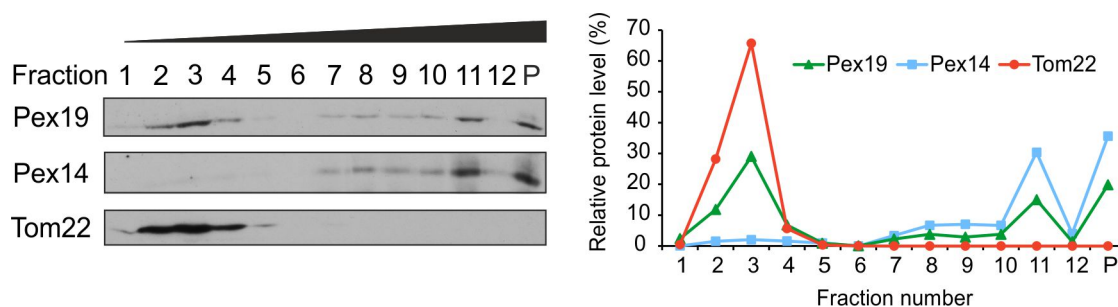


Figure 5.20: Pex19 is bound to the mitochondrial membrane. Isolated membrane fraction was subjected to sucrose density gradient centrifugation. Fractions of the gradient were collected and analyzed by SDS-PAGE and immunodecorated with antibodies against the indicated proteins. Right panel: the intensities of the various bands were quantified and depicted. The sum of all intensities of each protein was set to 100%.

Surprisingly, we were able to identify a substantial fraction of Pex19 in mitochondria that were free from Pex14 contamination (Fig. 5.20). Moreover, the ratio of Pex19 to Pex14 signal in peroxisomes when compared to the one in mitochondria clearly indicates that the detected pool of Pex19 in the mitochondrial fractions cannot be originated from peroxisomes. Thus, we conclude that Pex19 is partially localized to mitochondria.

5.12 Mim1 and Tom20 are involved in the biogenesis of Atg32-HA

Since a population of Pex19 is bound to mitochondria we speculated that membrane binding could be facilitated through an interaction of Pex19 with a dedicated receptor. The MIM complex is known to import MOM helical proteins including signal-anchored proteins. Additionally, unpublished work from Daniela Vitali in the group demonstrated involvement of the MIM complex as well as Tom20 and Tom70/71 receptors in biogenesis of Atg32-HA. Thus we asked if Pex19 effects on the biogenesis of MOM TA proteins are dependent on the MIM complex and the cooperation of MIM with TOM subunits.

To that end, we compared the aforementioned increase of Atg32-HA protein levels upon Pex19 overexpression in WT cells to the situation in a Mim1 deletion strain. As expected, we observed substantial reduction of steady states levels of MOM proteins in Mim1 deletion strains. Similarly to Tom40, Atg32-HA levels were reduced in *mim1* Δ mitochondria (Fig. 5.21B and D). The same observation could be made for the Atg32-HA levels in whole cell extract (Fig. 5.21A and C). Surprisingly, upon overexpression of Pex19 in *mim1* Δ cells, Atg32-HA levels remained completely unchanged in mitochondria and whole cell extract (Fig. 5.21A, B, C and D). This is in contrast to the increase of Atg32-HA levels upon Pex19 overexpression in WT cells. These results indicate that Pex19 cannot assist import of Atg32-HA without the presence of Mim1.

Next, we tested the influence of Pex19 overexpression on Atg32-HA levels when the Tom receptors Tom20 or Tom70/71 were missing. Atg32-HA levels were reduced in mitochondria from $\Delta tom20$ cells, although not as much as in the *MIM1* deletion strain. The levels of Atg32-HA did not display any changes in the whole cell extract of the deletion cells. When Pex19 was overexpressed, Atg32-HA levels did not increase in $\Delta tom20$ strain (Fig. 5.22A, B, C, and D). Of note, deletion of *TOM20* resulted in slight decrease of mitochondrial Mim1 levels (Fig. 5.22B).

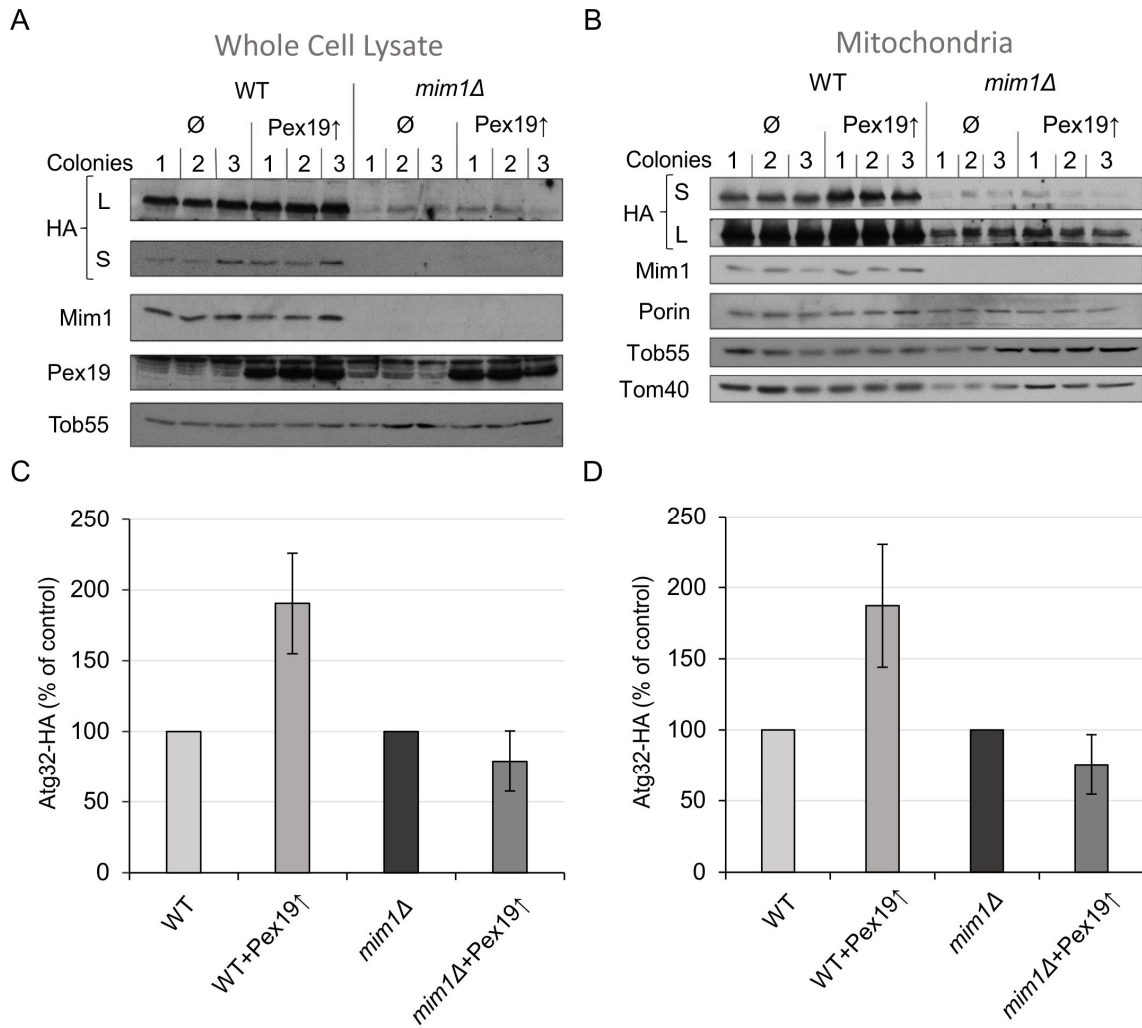


Figure 5.21: Protein levels of Atg32-HA are not increased upon Pex19 overexpression in *mim1Δ* mitochondria. The whole cell lysates (**A**) or crude mitochondria fractions (**B**) of three colonies of WT, WT overexpressing Pex19 (WT+Pex19↑), *mim1Δ*, and *mim1Δ* overexpressing Pex19 (*mim1Δ*+Pex19↑) cells were analyzed by SDS-PAGE and immunodecoration with the indicated antibodies. For HA, long (L) and short (S) exposures are presented (HA = Atg32-HA). (**C and D**) The intensity of the Atg32-HA from three independent experiments as those illustrated in (A and B) are represented as mean percentages of their levels in whole cell lysate (C) and mitochondria (D). Atg32-HA levels in WT and *mim1Δ* cells without overexpression of Pex19 were set as 100%. Error bars represent \pm s.d. (n=9).

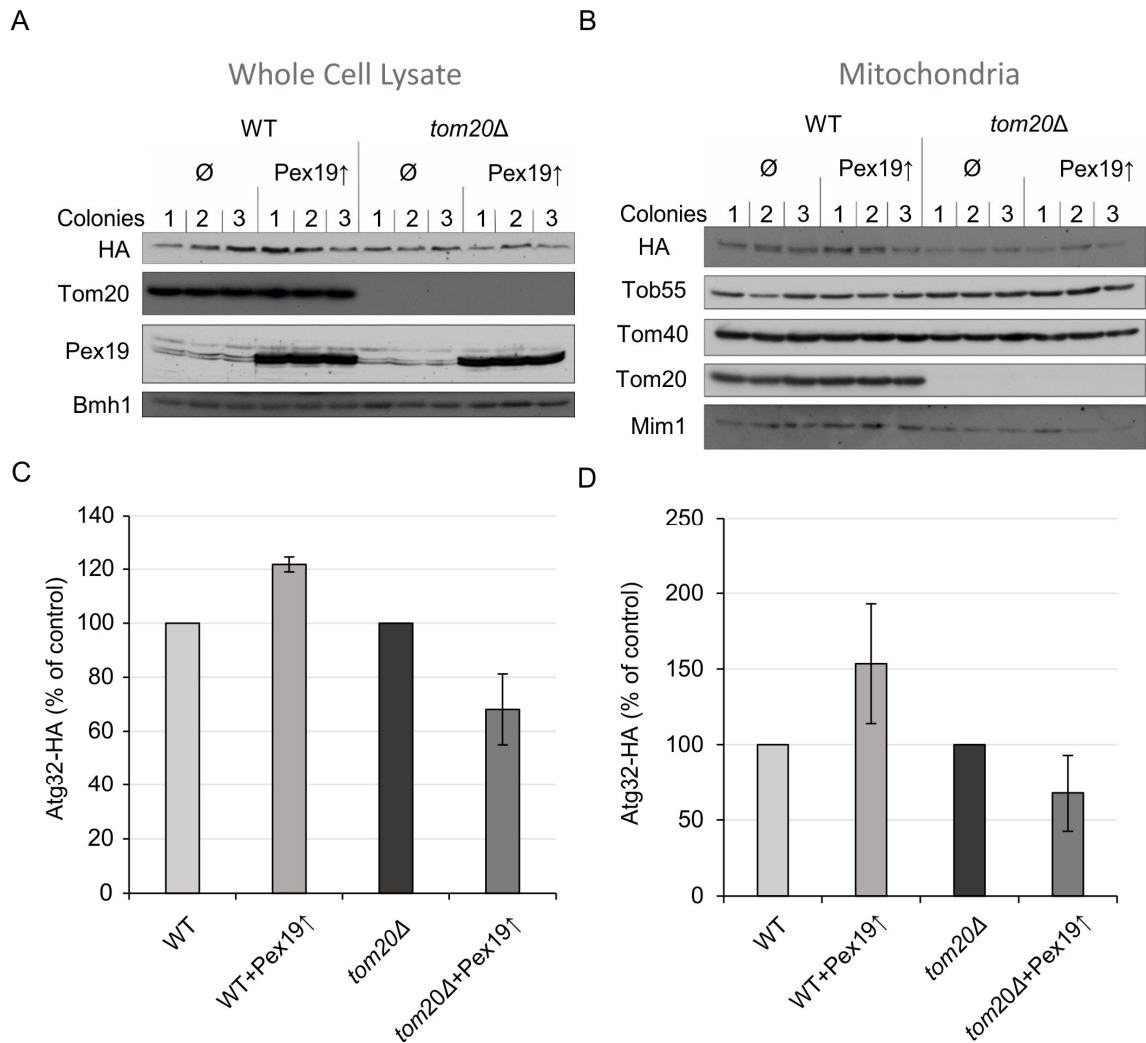


Figure 5.22: Accumulation of Atg32-HA upon Pex19 overexpression cannot be observed in mitochondria from $\Delta tom20$ cells. Whole cell lysates (**A**) or crude mitochondria fractions (**B**) of three colonies of WT, WT overexpressing Pex19 (WT+Pex19 \uparrow), *tom20Δ*, and *tom20Δ* overexpressing Pex19 (*tom20Δ*+Pex19 \uparrow) cells were analyzed by SDS-PAGE and immunodecoration with the indicated antibodies (HA = Atg32-HA). (**C and D**) The intensity of the Atg32-HA from three independent experiments as those illustrated in A and B are represented as mean percentages of their levels in whole cell lysate (C) and mitochondria (D). Atg32-HA levels in WT and *tom20Δ* cells without overexpression of Pex19 were set as 100%. Error bars represent \pm s.d. (n=9).

In contrast, double deletion of the genes encoding Tom70 and Tom71 receptors, lead to reduction of Atg32-HA levels in mitochondria and whole cell extract but did not prevent partial restoration of Atg32-HA steady state levels in mitochondria when Pex19 was overexpressed (Fig. 5.23A, B, C and D). However, the effect of Pex19 on Atg32-HA levels cannot be observed in the $\Delta tom70/71$ whole cell extract (Fig. 5.23A and C). To exclude that Atg32-HA levels are increased in mitochondria due to increased levels of Mim1 upon overexpression

of Pex19, Mim1 levels in mitochondrial fractions were quantified. Interestingly, Mim1 levels were reduced twofold in $\Delta tom70/71$ +Pex19 \uparrow strain when compared to $\Delta tom70/71$ strains (Fig. 5.23B and D). This excludes the possibility that increased Atg32-HA levels are resulted from higher levels of Mim1.

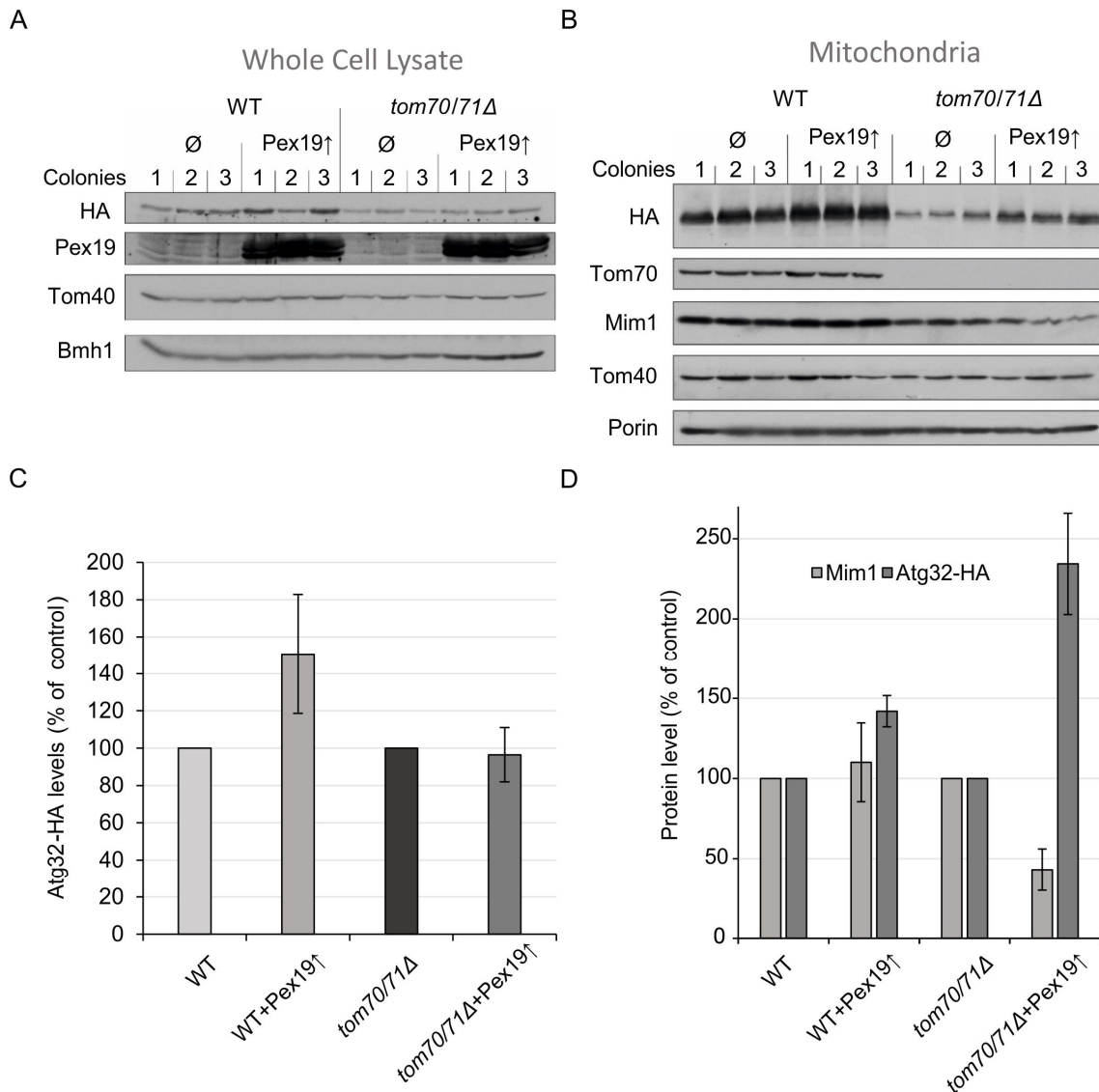


Figure 5.23: Double deletion of Tom70 and Tom71 receptors does not affect accumulation of Atg32-HA in mitochondria upon Pex19 overexpression. The whole cell lysates (A) or crude mitochondria fractions (B) of three colonies of WT, WT overexpressing Pex19 (WT+Pex19 \uparrow), $tom70/71\Delta$, and $tom70/71\Delta$ overexpressing Pex19 ($tom70/71\Delta$ +Pex19 \uparrow) cells were analyzed by SDS-PAGE and immunodecoration with the indicated antibodies (HA = Atg32-HA). (C and D) The intensity of the Atg32-HA from three independent experiments as those illustrated in A and B are represented as mean percentages of their levels in whole cell lysate (C) and mitochondria (D). Panel D: additionally Mim1 levels from three independent experiments as in B are represented. Atg32-HA and Mim1 levels in WT and $mim1\Delta$ cells without overexpression of Pex19 were set as 100%. Error bars represent \pm s.d. (n=9).

We concluded therefore that Pex19 requires Mim1 and Tom20 but not Tom70/71 to assist biogenesis of Atg32-HA. Collectively, this could indicate that Mim1 serves as the receptor for Pex19 mediated MOM TA import.

5.13 The effects of deletion of Pex19 and Sti1 are not cumulative

Biochemical analysis of *pex19Δ* and *sti1Δ* strains demonstrated that both deletions have a negative effect on the biogenesis of MOM TA but do not lead to complete abolishment of import of TA proteins. Loss of function of chaperones is often compensated by another functionally related chaperone. Thus, we tested if Pex19 and Sti1 can compensate each other's deletion.

We constructed a double deletion of *STI1* and *PEX19* (*sti1Δ/pex19Δ*) and compared Fis1 levels in mitochondria and whole cell extract of this double deletion strain with Fis1 levels in the single deletions or WT cells. Although the levels of the protein controls Bmh1, Tob55, Tom40 and Tom20 remained unaltered, the levels of Fis1 in mitochondria and whole cell extract were reduced in *sti1Δ* (as expected) and *sti1Δ/pex19Δ* when compared to WT (Fig. 5.24). However, Fis1 steady state levels were not reduced in the double mutant when compared to the single mutant *sti1Δ*, in contrary they exhibited a slight increase. Therefore, deletion of Pex19 and Sti1 does not lead to a cumulative effect on Fis1 levels.

These findings might indicate that Pex19 and Sti1 lie in the same pathway of biogenesis of TA proteins and thus cannot compensate for each other. Alternatively, a third unknown factor can rescue the biogenesis of TA proteins in the double deletion *sti1Δ/pex19Δ* strain.

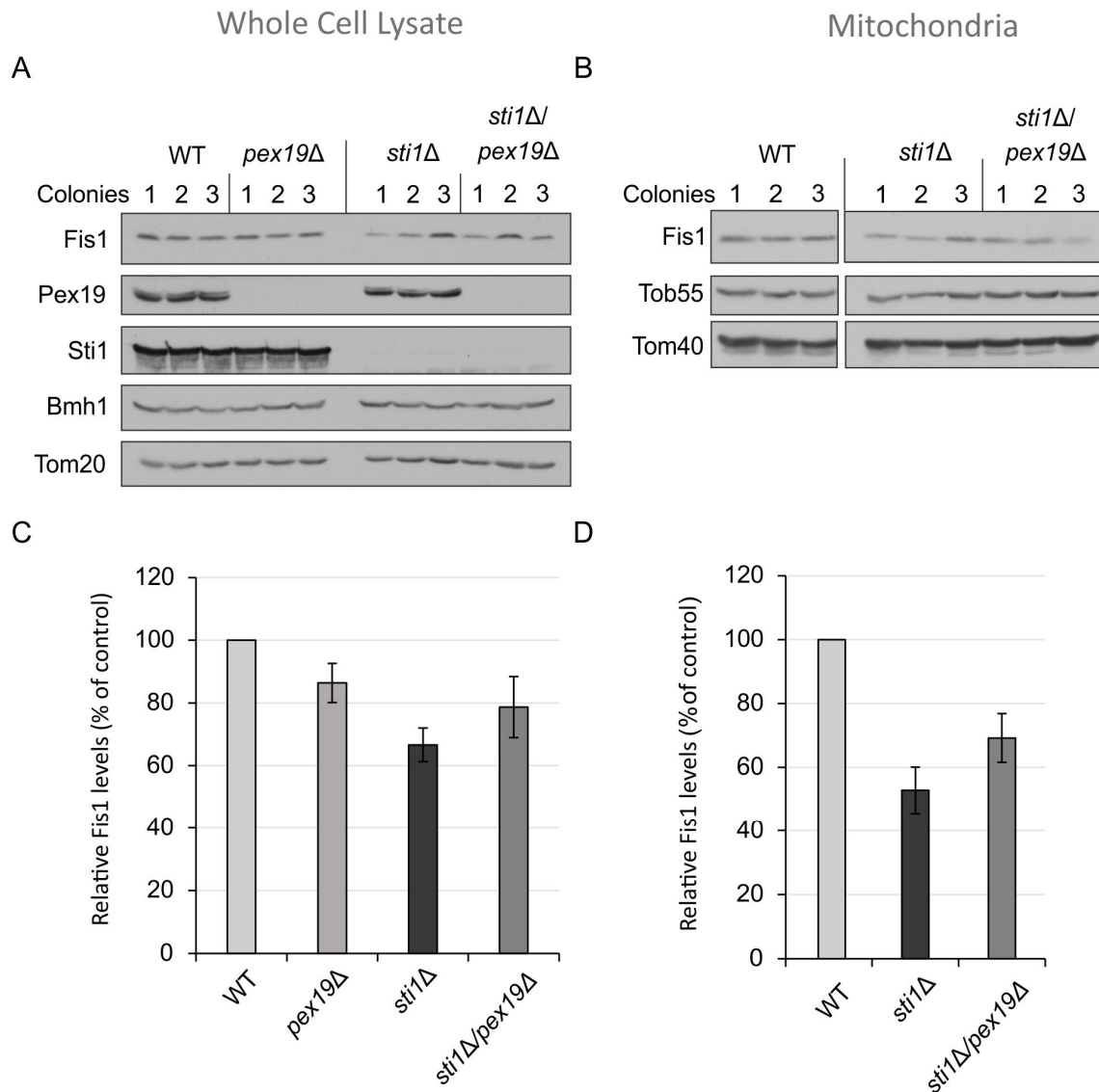


Figure 5.24: The influence of *Sti1* and *Pex19* on mitochondrial levels of *Fis1* does not accumulate. Whole cell lysates (**A**) or crude mitochondria fractions (**B**) of 3 colonies of WT, *pex19Δ* (only whole cell lysates), *sti1Δ*, and double deletion *sti1Δ/pex19Δ* cells were analysed by SDS-PAGE and immunodecoration with the indicated antibodies. The intensity of the *Fis1* bands from two independent experiments as those presented in (A and B) are presented as mean percentages of their levels in whole cell lysate (**C**) (n=6) and mitochondria (**D**) (n=6). Error bars represent mean \pm s.d.

6. Discussion

The delivery and insertion of cytosolically synthesized proteins into specific compartments is believed to require chaperones, guiding factors, receptors and/or insertases. Such factors have been characterized for most cellular compartments and substrates. However, to date, no factors involved in the import of mitochondrial TA proteins were identified. Here, we report that cytosolic chaperones of the Hsp70 family and Pex19 are required for the optimal biogenesis of the mitochondrial TA proteins Fis1 and Gem1.

6.1 Hsp70 chaperone complex involved in Fis1 biogenesis.

The contribution of cytosolic factors to the mitochondrial import of TA proteins became evident when Setoguchi et al. demonstrated that, in semi-permeabilized HeLa cells, the import of Bak is dependent on addition of reticulocyte lysate (Setoguchi et al., 2006). However, further studies could not identify a dedicated chaperone and/or guiding factor for the MOM TA proteins. Since some other mitochondrial proteins are known to require Hsp70/90 chaperones (only Hsp70 in yeast) for import (Deshaies et al., 1988, Young et al., 2003), it was hypothesized that Hsp70 chaperone complexes might fulfill this role (Borgese and Fasana, 2011). Here, we show that the yeast cytosolic Hsp70 family chaperones Ssa1/Ssa2 are indeed required for the proper biogenesis of the TA protein Fis1.

The exact composition of the chaperone complex interacting with Fis1 is unknown, but we could identify some possible members. Fis1 mitochondrial levels are affected upon deactivating cytosolic Hsp70 pointing out that Ssa1 is required for its biogenesis. Accordingly, mass spectrometry analysis of Fis1 crosslink adducts identified binding to Ssa1/2. Considering the high redundancy of the four Ssa family chaperones (Werner-Washburne et al., 1987), all four could be considered as potential Fis1 interactors.

The fact that the *in vitro* integration of Fis1 to mitochondria is hampered by an inhibitor of Hsp40/Hsp70 activity suggests a direct involvement of Hsp70 and possibly of its Hsp40 co-chaperones in the import process. Hsp40 co-chaperones

regulate the ATPase activity of Hsp70 chaperones and thereby, influence its substrate binding cycle (Wall et al., 1994). Furthermore, such co-chaperones were also suggested to function as fine tuner of the capacity of Hsp70s to participate in various cellular processes (Craig and Marszalek, 2017; Cyr and Ramos, 2015). Since Hsp70 chaperones often work in close cooperation with Hsp40 co-chaperones, it is possible that such co-chaperones are also involved in the biogenesis of mitochondrial TA proteins.

Moreover, Hsp40 co-chaperones can drive the function of the Hsp70 complex by narrowing the functional specificity of the complex (Fan et al., 2003). One such example can be found for the mitochondrial importer Mim1, which is topologically similar to TA proteins. The co-chaperone Djp1, and no other Hsp40 co-chaperone, specifically affects the levels of Mim1 in mitochondria (Papić et al., 2013). It is tempting to speculate that just like Mim1, some MOM TA proteins can be regulated and targeted by specific Hsp40/Hsp70 factors. Such a variety is in line with the high diversity of exclusive import factors in the MOM identified for specific TA proteins like VDAC2 for Bak, Tom40 for Tom5 in mammalian cells, or the Mim1, Mas37/Sam37 and Tom receptors for the small Tom subunits in yeast (Horie et al., 2002; Setoguchi et al., 2006; Stojanovski et al., 2007; Becker et al., 2008; Thornton et al., 2010).

We analyzed if Sti1 is involved in the mitochondrial biogenesis of Fis1 and found that both dysfunction of Ssa family chaperones and deletion of *STI1* have similar hampering effect on the mitochondrial level of Fis1. Hence, it is likely that both proteins are part of a chaperone complex that mediates the biogenesis of Fis1. Sti1 specifically interacts with Ssa chaperones to form a ternary multi-chaperone complex and greatly stimulates the ATPase activity of the Hsp70 chaperones (Wegele et al., 2003). Chaperones of the Hsp90 family are also part of this multi-chaperone complex and Sti1 facilitates the transfer of the protein substrate from Hsp70 to Hsp90 chaperones (Alvira et al., 2014). Whether Hsp90 chaperones are required for the biogenesis of mitochondrial TA proteins is thus an interesting question for future studies.

Altogether, we propose that, in yeast cells the chaperone complex involved in the mitochondrial import of TA proteins is composed of at least one of the four

Ssa family chaperones, the Sti1 co-chaperone and an Hsp40 co-chaperone (Fig. 6.1). Further studies are required to investigate whether Hsp90 chaperones are also part of this complex and to identify which Hsp40 co-chaperones interact with mitochondrial TA proteins.

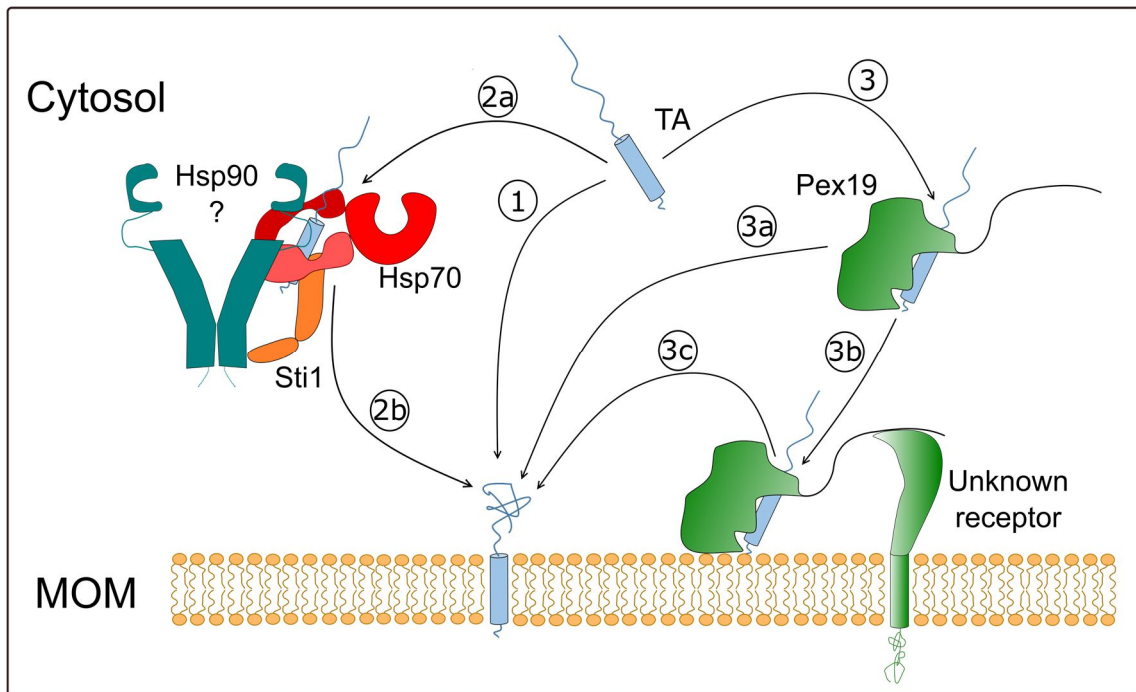


Figure 6.1: Insertion pathway of MOM TA proteins. TA proteins can either incorporate to mitochondria in an unassisted pathway via spontaneous insertion (1) or with the help of the ternary multi-chaperone complex (2a and 2b) or Pex19 chaperone (3). Pex19 keeps proteins in an import competent state till their reach the membrane (3a) however an alternate pathway is possible where Pex19 binds to mitochondria through a MOM receptor (3b) which then leads to insertion of the MOM TA into the lipid bilayer (3c).

6.2 Possible roles of Pex19 in the biogenesis of MOM TA proteins

Interestingly, only a part of the Fis1 population was affected by inhibition of Hsp70 chaperones and co-chaperones. Therefore, we hypothesize that the remaining pool of Fis1 is either integrated into the MOM by spontaneous insertion or that additional chaperones are involved. Redundancy among several parallel potential pathways was demonstrated lately for the insertion pathway of ER TA proteins. The newly discovered SND pathway (hSND in humans) can complement the loss of the Get/TRC40 or SRP pathway and most likely even the disruption of both pathways together (Aviram et al., 2016; Casson et al., 2017; Haßdenteufel et al., 2017).

As a putative alternative route for the Hsp70-mediated pathway, we investigated the involvement of Pex19. This cytosolic protein was shown to interact and guide the peroxisomes/mitochondria dual-localized proteins ATAD1, GDAP1, Miro1 and Fis1 to peroxisomes in mammalian cells (Delille and Schrader, 2008; Huber et al., 2013; Liu et al., 2016; Okumoto et al., 2018).

Here, we demonstrate that Pex19 is interacting directly with the yeast mitochondrial TA proteins Fis1 and Gem1 and facilitate their correct integration into the MOM. Furthermore, we identified Gem1 as a novel substrate of Pex19 and accordingly, found the former to be dual-localized in mitochondria and peroxisomes. We could demonstrate that its TMS is sufficient for its dual targeting and deduced that this region of the protein is most likely the binding segment for Pex19. These results are in accordance with the findings that the position of the guiding signal of peroxisomal TA proteins is identical to the mitochondrial targeting sequence. The Pex19 binding site is probably located in both cases at the TMS and its flanking regions (Kuroda et al., 1998; Beilharz et al., 2003; Costello et al., 2017).

A previous study in mammalian cells with knock-down of Pex19 questioned its involvement in the mitochondrial biogenesis of Fis1 (Delille and Schrader, 2008). However, the significant impact of Pex19 on the levels of TA proteins in mitochondria, and the fact that the mitochondrial levels of Fis1 is affected even when the total amount in the cell is not influenced, point towards a direct effect of Pex19 on the mitochondrial biogenesis of yeast TA proteins. It might be that yeast and mammalian cells behave differently in this respect.

During the course of this study the Gem1 human homologs Miro1 and Miro2 were as well identified to be dual-localized to peroxisomes and mitochondria (Costello et al., 2017). Subsequent work suggested that the Miro isoforms are involved in motility and proliferation of peroxisomes (Castro et al., 2018; Okumoto et al., 2018). Thus, it seems plausible that in yeast, Gem1 would mediate peroxisomal proliferation, similar like for mitochondria, either by tethering peroxisomes to the ER during fission or supporting scission and distribution of the organelle by its elongation and movement.

Pex19 does not only affect the biogenesis of MOM TA proteins but expands its function also to a topologically similar protein Atg32. Atg32 TMS is located closer to the C-terminus but its IMS segment (100 a.a. residues) is significantly longer compared to canonical TA proteins. Mechanistically, this long IMS fragment could prevent spontaneous insertion and thus places Atg32 in a different class of membrane proteins than the classical TA proteins. Nevertheless, Atg32 possesses two putative mPTS1 sequences potentially allowing it to be a Pex19 interactor. Accordingly, Atg32-HA levels are affected by both Pex19 overexpression and deletion pointing out that Pex19 participates also in biogenesis of receptor dependent proteins. This effect seems to be exclusive for Atg32 as the biogenesis of other MOM protein with similar topology, Tom22 and Mim1, does not seem to be influenced by Pex19. Furthermore, Mim1 import is dependent on Tom70/71 receptors (Papić et al., 2013) whereas Pex19 induced TA biogenesis is not. However, further interaction studies are necessary to determine if Pex19 indeed binds Atg32.

Strikingly, although Pex19 functions as a known chaperone for its substrates neither deletion of *PEX19* nor overexpression did affect the stability of the MOM TA proteins or Atg32-HA. This is either because TA proteins are too unstable and they are degraded too fast to detect any change after translation inhibition or another redundant chaperone ensures the stability of TA proteins. Indeed, overexpressed Atg32-HA and Gem1-HA are extremely unstable compared to other OM proteins and are degraded, independently of Pex19 level alteration, to the same basal level. However, native Fis1 is more stable than Atg32-HA or Gem1-HA and it is neither degraded to a basal level nor its stability is significantly changed by *PEX19* deletion. Hence, we cannot exclude the possibility that the HA tag contributes to the de-stabilization of the tagged proteins. Pex19 might not stabilize MOM proteins which would indicate that Pex19, rather than keeping TA proteins import competent, functions in the biogenesis of TA proteins by directly delivering them to the mitochondrial membrane. In such a case, the different half-life of TA proteins could be a regulatory factor, which ensures higher ratio of membrane insertion for stable proteins as compared to the unstable ones. Recently, a similar principle was

demonstrated for the import of the ER TA proteins syntaxins in mouse (Rivera-Monroy et al., 2016).

6.3 Pex19 has impact on mitochondrial functionality

In addition to the lowered mitochondrial levels of TA proteins, *pex19*Δ cells display an altered mitochondrial morphology compared to WT cells. In some cases, the mitochondrial morphology is similar to that of *fis1*Δ cells. This indicates that at least some of the mitochondrial morphology changes caused by the deletion of *PEX19* could be linked to the reduced levels of Fis1 in mitochondria.

Furthermore, growth of *pex19*Δ cells under respiratory conditions is slightly impaired and this growth phenotype becomes more severe at elevated temperatures. Thus, we conclude that Pex19 is required for optimal mitochondrial function, especially upon heat stress when proteins require chaperones as the danger of aggregation is higher (Verghese et al., 2012). Alternatively, the impaired growth phenotype on non-fermentable carbon sources could be a consequence of impairment in peroxisomal metabolic processes since peroxisomes are lacking in *pex19*Δ strains. A recent study on *Drosophila melanogaster* and human fibroblasts has linked mitochondrial dysfunctionality in *PEX19* deletion cells with a vicious cycle of transcriptionally activated constant fatty acid synthesis and mitochondrial β-oxidation. It was suggested that the cycle is responsible for the toxic effect of *PEX19* deletion. (Bülow et al., 2018).

Although this study suggests an interesting link between peroxisomes/lipid droplets and mitochondria, a similar conclusion cannot be drawn for yeast cells since they do not possess a homologous transcriptional regulation mechanism responsible for the vicious cycle and yeast mitochondria do not perform β-oxidation. Moreover in the described here growth assay we used two non-fermentable carbon sources (glycerol and lactate), which are mainly linked to mitochondria metabolism, to reduce the possibility of observing indirect effects on mitochondrial functionality. Collectively, although currently it is unclear how Pex19 supports mitochondrial functionality in yeast, it is tempting to speculate that this happens due to its contribution to import of TA proteins into the MOM.

6.4 Pex19 is bound to the mitochondrial membrane

Several options can be envisaged how Pex19 supports the import of Fis1 and Gem1 into the MOM. Pex19 can either keep TA proteins in an import-competent conformation till they are targeted to the MOM in a Pex19-independent manner (Yagita et al., 2013; Chen et al., 2014a) or it can deliver them directly to the membrane and thus participates in their actual membrane insertion (Fig. 6.1). The latter possibility is supported by our observation that Pex19 is partially associated with the mitochondrial surface.

Membrane binding of Pex19 to mitochondria could be achieved either by direct lipid binding or through interaction with a receptor protein. A favorable mechanism for direct binding to the membrane is the farnesylation modification of Pex19 since the hydrophobic character of the farnesyl group makes it suitable for mediation of membrane-protein interactions (Novelli and D'Apice, 2012). Similarly, the Hsp40 chaperone Ydj1 binding to ER membranes has been demonstrated to be dependent on farnesylation (Caplan et al., 1992). However, currently Pex19 farnesylation has been associated with increase of substrate specificity and function switching and thus further studies are required to clarify if it could support mitochondrial membrane binding (Emmanouilidis et al., 2017; Schrul and Kopito, 2016).

Recently, a study in mammalian cells discovered that the peroxisomal receptors Pex3 and Pex14 are partially targeted to mitochondria and can induce there formation of mitochondria derived pre-peroxisomes (Sugiura et al., 2017). However, so far Pex3 was not found in yeast mitochondria. Thus, the mechanism by which Pex19 can be delivered to yeast mitochondria remains to be discovered.

Another suitable candidate for a receptor would be the MIM complex, which has been proven to mediate the import of single span membrane proteins like signal-anchored proteins and was suggested to support membrane incorporation of the small Tom subunits. Unpublished data from a laboratory colleague Daniela Vitali demonstrated that Mim1, Tom20 and Tom70 deletion leads to reduced steady state levels of HA-Gem1 and Atg32-HA. Since similar effects can be observed for *PEX19* deletion, we wondered if Pex19 could function

in cooperation with these receptors. Surprisingly, deletion of Mim1 and Tom20 abolished the Atg32-HA accumulation in whole cell extract and mitochondria when Pex19 was overexpressed. However, this was not the case when Tom70/71 receptors were deleted. Thus, it appears that Pex19 needs Mim1 and Tom20 to support the biogenesis of Atg32-HA. The reduction of Atg32-HA levels in the *tom70/71Δ* strain might be an indirect effect of hampered Mim1 import when its receptor is lacking. Interestingly, Mim1 and Tom20 were previously shown to interact with each other which, together with our data, suggests that both proteins could be involved in the import of TA proteins and points out towards MIM complex as a possible receptor for Pex19. Along this line, the N-terminal cytosolic domain of Mim1 is dispensable for its function which could explain published observations where PK treatment of isolated mitochondria did not interfere with import of TA proteins (Kemper et al., 2008; Popov-Celeketić et al., 2008; Setoguchi et al., 2006).

6.5 The specificity of recognition by Pex19

Pex19 is a chaperone, which was believed to be dedicated nearly completely to peroxisome biogenesis. Here we demonstrate that it is also responsible for import of TA proteins to mitochondria. However, regardless of the actual mode of its function, it seems that Pex19 does not bind all MOM TA proteins. Interestingly, the non-canonical MOM TA protein Tom22 does not interact with Pex19. Accordingly, neither the mitochondrial level of Tom22 nor its stability is affected by *PEX19* deletion. These observations are in line with the recently published findings that the interaction of mammalian Pex19 with TA proteins is mediated through positively charged amino acids at the CTE (Costello et al., 2017). In contrast to Fis1 and Gem1 that harbor four charged residues, Tom22 possess only one such residue in the proximity of its TMS (Fig. 6.2). The targeting signal of peroxisomal TA proteins is conserved between mammals and yeast (Buentzel et al., 2015), suggesting similar recognition pattern by Pex19 in both systems. Thus, Tom22 is presumably not an appropriate substrate of Pex19 in yeast. Tom6 and Tom7, two additional solely mitochondrial TA proteins, also do not possess a highly charged tail necessary for Pex19 interaction (Costello et al., 2017)

(Fig. 6.2). Along the same line, the charges of the third mitochondrial TA protein Tom5 are dispensable for its targeting and insertion in yeast, whereas the opposite could be demonstrated for Fis1 (Horie et al., 2003). Hence, the TA proteins that are targeted exclusively to mitochondria seem to follow a Pex19-independent biogenesis pathway.

Accordingly, Atg32-HA, which currently is believed to be a solely mitochondrial protein, does not possess a charged tail after the TMS. However, it contains a super charged region on the cytosolic side close to the TMS, which encompasses 17 charged residues. We speculate that these residues together with the mPTS1 motifs could “overwrite” the tail charge signal necessary for Pex19 recognition turning it into the only Pex19 substrate being a solely mitochondrial protein.

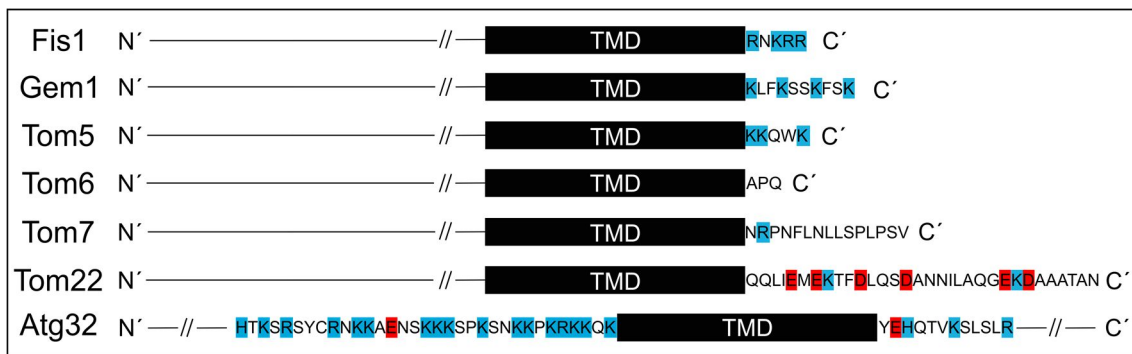


Figure 6.2: Charges of MOM TA C-terminal tail. Positively charged amino acids are marked with blue-whereas negatively charged ones are marked with red. The flanking regions of the TMS of Atg32 are displayed.

It is possible that Atg32 could be dual localized, like the rest of mitochondrial Pex19 targets, to peroxisomes and mitochondria. This is especially likely because the pexophagy and mitophagy processes share major similarities, including the autophagosome machinery composed of Atg32 interactors (Atg8, Atg11 and PAS), the formation of the phagosome and relation of both processes to the fission machinery, which is shared between both compartments (Müller et al., 2015; Schrader et al., 2015). The exact cellular location of Atg32 as well as the connection of mito/pexophagy to contact sites between both organelles (Mao et al., 2014) requires further investigation.

6.6 The biogenesis pathway of MOM TA proteins

Despite identifying cytosolic factors that are involved in the biogenesis of TA proteins, the import route of those proteins remains elusive. Both Hsp70 and Pex19 affect mitochondrial Fis1 biogenesis, however their position in the import pathways and relation to each other could not be clarified. Since deletion of both Pex19 and Sti1 does not lead to further decrease in Fis1 levels, we cannot deduce if the two proteins function in the same pathway or in parallel ones.

However, the slight increase of Fis1 steady state levels in the *PEX19/STI1* double deletion points toward the existence of a third factor important for TA biogenesis which might be upregulated when Pex19 and Sti1 are missing. This is not surprising concerning that similar redundancy could be demonstrated for import of ER TA proteins in mammals when the SRP and GET pathway have been disrupted. In this case, the increase of the ER TA protein levels was explained by a compensation effect from the SND pathway (Casson et al., 2017). What could be the third import factor for mitochondrial TA import remains to be investigated.

Alternatively, both Pex19 and Hsp70 complex are the only chaperones for mitochondria TA proteins and function in the same TA biogenesis pathway. Nevertheless they affect only 40% of the total mitochondria TA pool because the rest of the TA proteins inserts spontaneously into the MOM.

6.7 Evolution of the dual-localized TA proteome

The origins of the MOM and peroxisome proteome are currently under debate. Some views suggest that part of the peroxisome proteome or even the peroxisomes themselves originate from mitochondria (Mohanty and McBride, 2013). Nevertheless, strong evidence suggest that peroxisomes appeared after uptake of the pre-mitochondrial endosymbiont possibly as a host response for the changed metabolic environment (Speijer, 2017). Our findings that biogenesis of dual-localized TA proteins is dependent on the same cytosolic factor, Pex19, strengthens the concept of mitochondria-peroxisome cooperation, coevolution and the common origin of their proteome.

6.8 Summary

In summary, we propose a working model in which the biogenesis of MOM TA proteins is assisted by the Hsp70 chaperone complex and Pex19 (Fig. 6.2, 3). Disruption of neither one nor of both chaperones leads to complete abolishment of TA integration suggesting that other cytosolic factors might support the import of TA proteins. The remaining pool of MOM TA proteins could also incorporate into mitochondria via spontaneous insertion in an unassisted pathway (Fig. 6.2, 1).

7. References

- Abell, B.M., Pool, M.R., Schlenker, O., Sinning, I., and High, S. (2004). Signal recognition particle mediates post-translational targeting in eukaryotes. *EMBO J.* *23*, 2755–2764.
- Ahn, C.S., and Metallo, C.M. (2015). Mitochondria as biosynthetic factories for cancer proliferation. *Cancer Metab.* *3*.
- Alvira, S., Cuéllar, J., Röhl, A., Yamamoto, S., Itoh, H., Alfonso, C., Rivas, G., Buchner, J., and Valpuesta, J.M. (2014). Structural characterization of the substrate transfer mechanism in Hsp70/Hsp90 folding machinery mediated by Hop. *Nat. Commun.* *5*, 5484.
- Aranovich, A., Hua, R., Rutenberg, A.D., and Kim, P.K. (2014). PEX16 contributes to peroxisome maintenance by constantly trafficking PEX3 via the ER. *J. Cell Sci.* *127*, 3675–3686.
- Asai, T., Takahashi, T., Esaki, M., Nishikawa, S., Ohtsuka, K., Nakai, M., and Endo, T. (2004). Reinvestigation of the Requirement of Cytosolic ATP for Mitochondrial Protein Import. *J. Biol. Chem.* *279*, 19464–19470.
- Ast, J., Stiebler, A.C., Freitag, J., and Böcker, M. (2013). Dual targeting of peroxisomal proteins. *Front. Physiol.* *4*.
- Aviram, N., Ast, T., Costa, E.A., Arakel, E.C., Chuartzman, S.G., Jan, C.H., Haßdenteufel, S., Dudek, J., Jung, M., Schorr, S., et al. (2016). The SND proteins constitute an alternative targeting route to the endoplasmic reticulum. *Nature* *540*, 134–138.
- Baumgart, E., Vanhorebeek, I., Grabenbauer, M., Borgers, M., Declercq, P.E., Fahimi, H.D., and Baes, M. (2001). Mitochondrial alterations caused by defective peroxisomal biogenesis in a mouse model for Zellweger syndrome (PEX5 knockout mouse). *Am. J. Pathol.* *159*, 1477–1494.
- Becker, J., Walter, W., Yan, W., and Craig, E.A. (1996). Functional interaction of cytosolic hsp70 and a DnaJ-related protein, Ydj1p, in protein translocation in vivo. *Mol. Cell. Biol.* *16*, 4378–4386.
- Becker, T., Pfannschmidt, S., Guiard, B., Stojanovski, D., Milenkovic, D., Kutik, S., Pfanner, N., Meisinger, C., and Wiedemann, N. (2008). Biogenesis of the mitochondrial TOM complex: Mim1 promotes insertion and assembly of signal-anchored receptors. *J. Biol. Chem.* *283*, 120–127.
- Becker, T., Guiard, B., Thornton, N., Zufall, N., Stroud, D.A., Wiedemann, N., and Pfanner, N. (2010). Assembly of the mitochondrial protein import channel: role of Tom5 in two-stage interaction of Tom40 with the SAM complex. *Mol. Biol. Cell* *21*, 3106–3113.

- Becker, T., Wenz, L.-S., Krüger, V., Lehmann, W., Müller, J.M., Goroncy, L., Zufall, N., Lithgow, T., Guiard, B., Chacinska, A., et al. (2011). The mitochondrial import protein Mim1 promotes biogenesis of multispanning outer membrane proteins. *J. Cell Biol.* 194, 387–395.
- Beilharz, T., Egan, B., Silver, P.A., Hofmann, K., and Lithgow, T. (2003). Bipartite signals mediate subcellular targeting of tail-anchored membrane proteins in *Saccharomyces cerevisiae*. *J. Biol. Chem.* 278, 8219–8223.
- Birnboim, H.C., and Doly, J. (1979). A rapid alkaline extraction procedure for screening recombinant plasmid DNA. *Nucleic Acids Res.* 7, 1513–1523.
- van der Blik, A.M., Shen, Q., and Kawajiri, S. (2013). Mechanisms of mitochondrial fission and fusion. *Cold Spring Harb. Perspect. Biol.* 5.
- Borgese, N., and Fasana, E. (2011). Targeting pathways of C-tail-anchored proteins. *Biochim. Biophys. Acta* 1808, 937–946.
- Bradford, M.M. (1976). A rapid and sensitive method for the quantitation of microgram quantities of protein utilizing the principle of protein-dye binding. *Anal. Biochem.* 72, 248–254.
- Brambillasca, S., Yabal, M., Soffientini, P., Stefanovic, S., Makarow, M., Hegde, R.S., and Borgese, N. (2005). Transmembrane topogenesis of a tail-anchored protein is modulated by membrane lipid composition. *EMBO J.* 24, 2533–2542.
- Buentzel, J., Vilardi, F., Lotz-Havla, A., Gärtner, J., and Thoms, S. (2015). Conserved targeting information in mammalian and fungal peroxisomal tail-anchored proteins. *Sci. Rep.* 5, 17420.
- Bülow, M.H., Wingen, C., Senyilmaz, D., Gosejacob, D., Sociale, M., Bauer, R., Schulze, H., Sandhoff, K., Teleman, A.A., Hoch, M., et al. (2018). Unbalanced lipolysis results in lipotoxicity and mitochondrial damage in peroxisome-deficient Pex19 mutants. *Mol. Biol. Cell* 29, 396–407.
- Caplan, A.J., Tsai, J., Casey, P.J., and Douglas, M.G. (1992). Farnesylation of YDJ1p is required for function at elevated growth temperatures in *Saccharomyces cerevisiae*. *J. Biol. Chem.* 267, 18890–18895.
- Casson, J., McKenna, M., Haßdenteufel, S., Aviram, N., Zimmerman, R., and High, S. (2017). Multiple pathways facilitate the biogenesis of mammalian tail-anchored proteins. *J. Cell Sci.* 130, 3851–3861.
- Castro, I.G., Richards, D.M., Metz, J., Costello, J.L., Passmore, J.B., Schrader, T.A., Gouveia, A., Ribeiro, D., and Schrader, M. (2018). A role for Mitochondrial Rho GTPase 1 (MIRO1) in motility and membrane dynamics of peroxisomes. *Traffic Cph. Den.* 19, 229–242.
- Chacinska, A., Pfannschmidt, S., Wiedemann, N., Kozjak, V., Sanjuán Szklarz, L.K., Schulze-Specking, A., Truscott, K.N., Guiard, B., Meisinger, C., and

- Pfanner, N. (2004). Essential role of Mia40 in import and assembly of mitochondrial intermembrane space proteins. *EMBO J.* *23*, 3735–3746.
- Chacinska, A., Lind, M., Frazier, A.E., Dudek, J., Meisinger, C., Geissler, A., Sickmann, A., Meyer, H.E., Truscott, K.N., Guiard, B., et al. (2005). Mitochondrial presequence translocase: switching between TOM tethering and motor recruitment involves Tim21 and Tim17. *Cell* *120*, 817–829.
- Chacinska, A., Koehler, C.M., Milenkovic, D., Lithgow, T., and Pfanner, N. (2009). Importing Mitochondrial Proteins: Machineries and Mechanisms. *Cell* *138*, 628–644.
- Chan, D.C. (2012). Fusion and fission: interlinked processes critical for mitochondrial health. *Annu. Rev. Genet.* *46*, 265–287.
- Chen, X.J., and Butow, R.A. (2005). The organization and inheritance of the mitochondrial genome. *Nat. Rev. Genet.* *6*, 815–825.
- Chen, Y., Pieuchot, L., Loh, R.A., Yang, J., Kari, T.M.A., Wong, J.Y., and Jedd, G. (2014a). Hydrophobic handoff for direct delivery of peroxisome tail-anchored proteins. *Nat. Commun.* *5*, 5790.
- Chen, Y.-C., Umanah, G.K.E., Dephoure, N., Andrabi, S.A., Gygi, S.P., Dawson, T.M., Dawson, V.L., and Rutter, J. (2014b). Msp1/ATAD1 maintains mitochondrial function by facilitating the degradation of mislocalized tail-anchored proteins. *EMBO J.* *33*, 1548–1564.
- Chio, U.S., Cho, H., and Shan, S.-O. (2017). Mechanisms of Tail-Anchored Membrane Protein Targeting and Insertion. *Annu. Rev. Cell Dev. Biol.* *33*, 417–438.
- Costello, J.L., Castro, I.G., Camões, F., Schrader, T.A., McNeill, D., Yang, J., Giannopoulou, E.-A., Gomes, S., Pogenberg, V., Bonekamp, N.A., et al. (2017). Predicting the targeting of tail-anchored proteins to subcellular compartments in mammalian cells. *J. Cell Sci.* *130*, 1675–1687.
- Daum, G., Böhni, P.C., and Schatz, G. (1982). Import of proteins into mitochondria. Cytochrome b2 and cytochrome c peroxidase are located in the intermembrane space of yeast mitochondria. *J. Biol. Chem.* *257*, 13028–13033.
- Delille, H.K., and Schrader, M. (2008). Targeting of hFis1 to Peroxisomes Is Mediated by Pex19p. *J. Biol. Chem.* *283*, 31107–31115.
- Dembowski, M., Kunkele, K.P., Nargang, F.E., Neupert, W., and Rapaport, D. (2001). Assembly of Tom6 and Tom7 into the TOM core complex of *Neurospora crassa*. *J. Biol. Chem.* *276*, 17679–17685.
- Deshaies, R.J., Koch, B.D., Werner-Washburne, M., Craig, E.A., and Schekman, R. (1988). A subfamily of stress proteins facilitates translocation of secretory and mitochondrial precursor polypeptides. *Nature* *332*, 800–805.

- Dimitrov, L., Lam, S.K., and Schekman, R. (2013). The Role of the Endoplasmic Reticulum in Peroxisome Biogenesis. *Cold Spring Harb. Perspect. Biol.* 5.
- Dimmer, K.S., and Rapaport, D. (2017). Mitochondrial contact sites as platforms for phospholipid exchange. *Biochim. Biophys. Acta* 1862, 69–80.
- Dimmer, K.S., Papić, D., Schumann, B., Sperl, D., Krumpe, K., Walther, D.M., and Rapaport, D. (2012). A crucial role for Mim2 in the biogenesis of mitochondrial outer membrane proteins. *J. Cell Sci.* 125, 3464–3473.
- Dirkx, R., Vanhorebeek, I., Martens, K., Schad, A., Grabenbauer, M., Fahimi, D., Declercq, P., Van Veldhoven, P.P., and Baes, M. (2005). Absence of peroxisomes in mouse hepatocytes causes mitochondrial and ER abnormalities. *Hepatology* 41, 868–878.
- Distel, B., and Kragt, A. (2006). Purification of yeast peroxisomes. *Methods Mol. Biol.* Clifton NJ 313, 21–26.
- Dixit, E., Boulant, S., Zhang, Y., Lee, A.S.Y., Odendall, C., Shum, B., Hacohen, N., Chen, Z.J., Whelan, S.P., Fransen, M., et al. (2010). Peroxisomes are signaling platforms for antiviral innate immunity. *Cell* 141, 668–681.
- de Duve, C. (1969). Evolution of the Peroxisome. *Ann. N. Y. Acad. Sci.* 168, 369–381.
- Dyall, S.D., Brown, M.T., and Johnson, P.J. (2004). Ancient invasions: from endosymbionts to organelles. *Science* 304, 253–257.
- Ellis, J. (1987). Proteins as molecular chaperones. *Nature* 328, 378–379.
- Emmanouilidis, L., Schütz, U., Tripsianes, K., Madl, T., Radke, J., Rucktäschel, R., Wilmanns, M., Schliebs, W., Erdmann, R., and Sattler, M. (2017). Allosteric modulation of peroxisomal membrane protein recognition by farnesylation of the peroxisomal import receptor PEX19. *Nat. Commun.* 8, 14635.
- Fan, C.-Y., Lee, S., and Cyr, D.M. (2003). Mechanisms for regulation of Hsp70 function by Hsp40. *Cell Stress Chaperones* 8, 309–316.
- Fang, Y., Morrell, J.C., Jones, J.M., and Gould, S.J. (2004). PEX3 functions as a PEX19 docking factor in the import of class I peroxisomal membrane proteins. *J. Cell Biol.* 164, 863–875.
- Ferrer, I., Kapfhammer, J.P., Hindelang, C., Kemp, S., Troffer-Charlier, N., Broccoli, V., Callyzot, N., Mooyer, P., Selhorst, J., Vreken, P., et al. (2005). Inactivation of the peroxisomal ABCD2 transporter in the mouse leads to late-onset ataxia involving mitochondria, Golgi and endoplasmic reticulum damage. *Hum. Mol. Genet.* 14, 3565–3577.
- Fewell, S.W., Smith, C.M., Lyon, M.A., Dumitrescu, T.P., Wipf, P., Day, B.W., and Brodsky, J.L. (2004). Small molecule modulators of endogenous and co-

- chaperone-stimulated Hsp70 ATPase activity. *J. Biol. Chem.* **279**, 51131–51140.
- Fransson, S., Ruusala, A., and Aspenström, P. (2006). The atypical Rho GTPases Miro-1 and Miro-2 have essential roles in mitochondrial trafficking. *Biochem. Biophys. Res. Commun.* **344**, 500–510.
- Freel, K.C., Friedrich, A., and Schacherer, J. (2015). Mitochondrial genome evolution in yeasts: an all-encompassing view. *FEMS Yeast Res.* **15**, fov023.
- Friedman, J.R., and Nunnari, J. (2014). Mitochondrial form and function. *Nature* **505**, 335.
- Friedman, J.R., Lackner, L.L., West, M., DiBenedetto, J.R., Nunnari, J., and Voeltz, G.K. (2011). ER tubules mark sites of mitochondrial division. *Science* **334**, 358–362.
- Fujiki, Y., Hubbard, A.L., Fowler, S., and Lazarow, P.B. (1982). Isolation of intracellular membranes by means of sodium carbonate treatment: application to endoplasmic reticulum. *J. Cell Biol.* **93**, 97–102.
- Gabaldón, T., Snel, B., van Zimmeren, F., Hemrika, W., Tabak, H., and Huynen, M.A. (2006). Origin and evolution of the peroxisomal proteome. *Biol. Direct* **1**, 8.
- Gadir, N., Haim-Vilmovsky, L., Kraut-Cohen, J., and Gerst, J.E. (2011). Localization of mRNAs coding for mitochondrial proteins in the yeast *Saccharomyces cerevisiae*. *RNA N. Y. N* **17**, 1551–1565.
- Gandre-Babbe, S., and van der Blik, A.M. (2008). The novel tail-anchored membrane protein Mff controls mitochondrial and peroxisomal fission in mammalian cells. *Mol. Biol. Cell* **19**, 2402–2412.
- Gautschi, M., Lilie, H., Fünfschilling, U., Mun, A., Ross, S., Lithgow, T., Rücknagel, P., and Rospert, S. (2001). RAC, a stable ribosome-associated complex in yeast formed by the DnaK-DnaJ homologs Ssz1p and zuotin. *Proc. Natl. Acad. Sci. U. S. A.* **98**, 3762–3767.
- Giannopoulou, E.A., Emmanouilidis, L., Sattler, M., Dodt, G., and Wilmanns, M. (2016). Towards the molecular mechanism of the integration of peroxisomal membrane proteins. *Biochim. Biophys. Acta* **1863**, 863–869.
- Gietz, R.D., Schiestl, R.H., Willems, A.R., and Woods, R.A. (1995). Studies on the transformation of intact yeast cells by the LiAc/SS-DNA/PEG procedure. *Yeast Chichester Engl.* **11**, 355–360.
- Gold, V.A., Chroscicki, P., Bragoszewski, P., and Chacinska, A. (2017). Visualization of cytosolic ribosomes on the surface of mitochondria by electron cryo-tomography. *EMBO Rep.* **18**, 1786–1800.

- Gong, Y., Kakihara, Y., Krogan, N., Greenblatt, J., Emili, A., Zhang, Z., and Houry, W.A. (2009). An atlas of chaperone-protein interactions in *Saccharomyces cerevisiae*: implications to protein folding pathways in the cell. *Mol. Syst. Biol.* 5, 275.
- Gould, S.J., and Valle, D. (2000). Peroxisome biogenesis disorders: genetics and cell biology. *Trends Genet.* TIG 16, 340–345.
- Gray, M.W. (2012). Mitochondrial Evolution. *Cold Spring Harb. Perspect. Biol.* 4.
- Greene, M.K., Maskos, K., and Landry, S.J. (1998). Role of the J-domain in the cooperation of Hsp40 with Hsp70. *Proc. Natl. Acad. Sci. U. S. A.* 95, 6108–6113.
- Halbach, A. (2006). Targeting of the tail-anchored peroxisomal membrane proteins PEX26 and PEX15 occurs through C-terminal PEX19-binding sites. *J. Cell Sci.* 119, 2508–2517.
- Haßdenteufel, S., Sicking, M., Schorr, S., Aviram, N., Fecher-Trost, C., Schuldiner, M., Jung, M., Zimmermann, R., and Lang, S. (2017). hSnd2 protein represents an alternative targeting factor to the endoplasmic reticulum in human cells. *FEBS Lett.* 591, 3211–3224.
- Hegde, R.S., and Keenan, R.J. (2011). Tail-anchored membrane protein insertion into the endoplasmic reticulum. *Nat. Rev. Mol. Cell Biol.* 12, 787–798.
- Hoepfner, D., Schildknegt, D., Braakman, I., Philippsen, P., and Tabak, H.F. (2005). Contribution of the Endoplasmic Reticulum to Peroxisome Formation. *Cell* 122, 85–95.
- Honsho, M., and Fujiki, Y. (2001). Topogenesis of peroxisomal membrane protein requires a short, positively charged intervening-loop sequence and flanking hydrophobic segments. study using human membrane protein PMP34. *J. Biol. Chem.* 276, 9375–9382.
- Horie, C., Suzuki, H., Sakaguchi, M., and Mihara, K. (2002). Characterization of signal that directs C-tail-anchored proteins to mammalian mitochondrial outer membrane. *Mol. Biol. Cell* 13, 1615–1625.
- Horie, C., Suzuki, H., Sakaguchi, M., and Mihara, K. (2003). Targeting and Assembly of Mitochondrial Tail-anchored Protein Tom5 to the TOM Complex Depend on a Signal Distinct from That of Tail-anchored Proteins Dispersed in the Membrane. *J. Biol. Chem.* 278, 41462–41471.
- Hoseini, H., Pandey, S., Jores, T., Schmitt, A., Franz-Wachtel, M., Macek, B., Buchner, J., Dimmer, K.S., and Rapaport, D. (2016). The cytosolic cochaperone Sti1 is relevant for mitochondrial biogenesis and morphology. *FEBS J.* 283, 3338–3352.

- Huber, N., Guimaraes, S., Schrader, M., Suter, U., and Niemann, A. (2013). Charcot-Marie-Tooth disease-associated mutants of GDAP1 dissociate its roles in peroxisomal and mitochondrial fission. *EMBO Rep.* *14*, 545–552.
- Humphries, A.D., Streimann, I.C., Stojanovski, D., Johnston, A.J., Yano, M., Hoogenraad, N.J., and Ryan, M.T. (2005). Dissection of the mitochondrial import and assembly pathway for human Tom40. *J. Biol. Chem.* *280*, 11535–11543.
- Itakura, E., Zavodszky, E., Shao, S., Wohlever, M.L., Keenan, R.J., and Hegde, R.S. (2016). Ubiquilins Chaperone and Triage Mitochondrial Membrane Proteins for Degradation. *Mol. Cell* *63*, 21.
- James, P., Pfund, C., and Craig, E.A. (1997). Functional specificity among Hsp70 molecular chaperones. *Science* *275*, 387–389.
- Jones, J.M., Morrell, J.C., and Gould, S.J. (2001). Multiple distinct targeting signals in integral peroxisomal membrane proteins. *J. Cell Biol.* *153*, 1141–1150.
- Jones, J.M., Morrell, J.C., and Gould, S.J. (2004). PEX19 is a predominantly cytosolic chaperone and import receptor for class 1 peroxisomal membrane proteins. *J. Cell Biol.* *164*, 57–67.
- Jores, T., Klinger, A., Groß, L.E., Kawano, S., Flinner, N., Duchardt-Ferner, E., Wöhnert, J., Kalbacher, H., Endo, T., Schleiff, E., et al. (2016). Characterization of the targeting signal in mitochondrial β -barrel proteins. *Nat. Commun.* *7*.
- Joshi, A.S., Choudhary, V., Levine, T.P., and Prinz, W.A. (2017). Lipid droplet and peroxisome biogenesis occur at the same ER subdomains. *BioRxiv* 188433.
- Kang, P.J., Ostermann, J., Shilling, J., Neupert, W., Craig, E.A., and Pfanner, N. (1990). Requirement for hsp70 in the mitochondrial matrix for translocation and folding of precursor proteins. *Nature* *348*, 137–143.
- Kemper, C., Habib, S.J., Engl, G., Heckmeyer, P., Dimmer, K.S., and Rapaport, D. (2008). Integration of tail-anchored proteins into the mitochondrial outer membrane does not require any known import components. *J. Cell Sci.* *121*, 1990–1998.
- Koch, J., and Brocard, C. (2012). PEX11 proteins attract Mff and human Fis1 to coordinate peroxisomal fission. *J. Cell Sci.* *125*, 3813–3826.
- Koch, A., Yoon, Y., Bonekamp, N.A., McNiven, M.A., and Schrader, M. (2005). A Role for Fis1 in Both Mitochondrial and Peroxisomal Fission in Mammalian Cells. *Mol. Biol. Cell* *16*, 5077–5086.
- Kondo-Okamoto, N., Ohkuni, K., Kitagawa, K., McCaffery, J.M., Shaw, J.M., and Okamoto, K. (2006). The novel F-box protein Mfb1p regulates

- mitochondrial connectivity and exhibits asymmetric localization in yeast. *Mol. Biol. Cell* **17**, 3756–3767.
- Kondo-Okamoto, N., Noda, N.N., Suzuki, S.W., Nakatogawa, H., Takahashi, I., Matsunami, M., Hashimoto, A., Inagaki, F., Ohsumi, Y., and Okamoto, K. (2012). Autophagy-related protein 32 acts as autophagic degron and directly initiates mitophagy. *J. Biol. Chem.* **287**, 10631–10638.
- Kornmann, B., Osman, C., and Walter, P. (2011). The conserved GTPase Gem1 regulates endoplasmic reticulum-mitochondria connections. *Proc. Natl. Acad. Sci. U. S. A.* **108**, 14151–14156.
- Krüger, V., Becker, T., Becker, L., Montilla-Martinez, M., Ellenrieder, L., Vögtle, F.-N., Meyer, H.E., Ryan, M.T., Wiedemann, N., Warscheid, B., et al. (2017). Identification of new channels by systematic analysis of the mitochondrial outer membrane. *J. Cell Biol.* **216**, 3485–3495.
- Krumpe, K., Frumkin, I., Herzig, Y., Rimon, N., Özbalci, C., Brügger, B., Rapaport, D., and Schuldiner, M. (2012). Ergosterol content specifies targeting of tail-anchored proteins to mitochondrial outer membranes. *Mol. Biol. Cell* **23**, 3927–3935.
- Kuroda, R., Ikenoue, T., Honsho, M., Tsujimoto, S., Mitoma, J.Y., and Ito, A. (1998). Charged amino acids at the carboxyl-terminal portions determine the intracellular locations of two isoforms of cytochrome b5. *J. Biol. Chem.* **273**, 31097–31102.
- Kyhse-Andersen, J. (1984). Electrophoretic transfer of multiple gels: a simple apparatus without buffer tank for rapid transfer of proteins from polyacrylamide to nitrocellulose. *J. Biochem. Biophys. Methods* **10**, 203–209.
- van der Laan, M., Meinecke, M., Dudek, J., Hutu, D.P., Lind, M., Perschil, I., Guiard, B., Wagner, R., Pfanner, N., and Rehling, P. (2007). Motor-free mitochondrial presequence translocase drives membrane integration of preproteins. *Nat. Cell Biol.* **9**, 1152–1159.
- Lazarow, P.B., and Fujiki, Y. (1985). Biogenesis of peroxisomes. *Annu. Rev. Cell Biol.* **1**, 489–530.
- Lill, R. (2009). Function and biogenesis of iron-sulphur proteins. *Nature* **460**, 831–838.
- Liu, Y., Yagita, Y., and Fujiki, Y. (2016). Assembly of Peroxisomal Membrane Proteins via the Direct Pex19p-Pex3p Pathway. *Traffic Cph. Den.* **17**, 433–455.
- Mao, K., Wang, K., Liu, X., and Klionsky, D.J. (2013). The scaffold protein Atg11 recruits fission machinery to drive selective mitochondria degradation by autophagy. *Dev. Cell* **26**, 9–18.

- Mao, K., Liu, X., Feng, Y., and Klionsky, D.J. (2014). The progression of peroxisomal degradation through autophagy requires peroxisomal division. *Autophagy* 10, 652–661.
- Martin, W.F., Garg, S., and Zimorski, V. (2015). Endosymbiotic theories for eukaryote origin. *Philos. Trans. R. Soc. B Biol. Sci.* 370.
- Matsuzono, Y., and Fujiki, Y. (2006). In vitro transport of membrane proteins to peroxisomes by shuttling receptor Pex19p. *J. Biol. Chem.* 281, 36–42.
- Matsuzono, Y., Kinoshita, N., Tamura, S., Shimozawa, N., Hamasaki, M., Ghaedi, K., Wanders, R.J.A., Suzuki, Y., Kondo, N., and Fujiki, Y. (1999). Human PEX19: cDNA cloning by functional complementation, mutation analysis in a patient with Zellweger syndrome, and potential role in peroxisomal membrane assembly. *Proc. Natl. Acad. Sci.* 96, 2116–2121.
- Mattoo, R.U.H., and Goloubinoff, P. (2014). Molecular chaperones are nanomachines that catalytically unfold misfolded and alternatively folded proteins. *Cell. Mol. Life Sci.* 71, 3311–3325.
- Mayer, M.P., and Bukau, B. (2005). Hsp70 chaperones: Cellular functions and molecular mechanism. *Cell. Mol. Life Sci.* 62, 670–684.
- Mayer, A., Lill, R., and Neupert, W. (1993). Translocation and insertion of precursor proteins into isolated outer membranes of mitochondria. *J. Cell Biol.* 121, 1233–1243.
- Mayerhofer, P.U. (2016). Targeting and insertion of peroxisomal membrane proteins: ER trafficking versus direct delivery to peroxisomes. *Biochim. Biophys. Acta* 1863, 870–880.
- Meijer, W.H., Gidijala, L., Fekken, S., Kiel, J.A.K.W., van den Berg, M.A., Lascaris, R., Bovenberg, R.A.L., and van der Klei, I.J. (2010). Peroxisomes Are Required for Efficient Penicillin Biosynthesis in *Penicillium chrysogenum*. *Appl. Environ. Microbiol.* 76, 5702–5709.
- Merz, S., Hammermeister, M., Altmann, K., Dürr, M., and Westermann, B. (2007). Molecular machinery of mitochondrial dynamics in yeast. *Biol. Chem.* 388, 917–926.
- Mohanty, A., and McBride, H.M. (2013). Emerging roles of mitochondria in the evolution, biogenesis, and function of peroxisomes. *Front. Physiol.* 4, 268.
- Morgenstern, M., Stiller, S.B., Lübbert, P., Peikert, C.D., Dannenmaier, S., Drepper, F., Weill, U., Höß, P., Feuerstein, R., Gebert, M., et al. (2017). Definition of a High-Confidence Mitochondrial Proteome at Quantitative Scale. *Cell Rep.* 19, 2836–2852.
- Motley, A.M., Ward, G.P., and Hettema, E.H. (2008). Dnm1p-dependent peroxisome fission requires Caf4p, Mdv1p and Fis1p. *J. Cell Sci.* 121, 1633–1640.

- Motley, A.M., Nuttall, J.M., and Hettema, E.H. (2012). Pex3-anchored Atg36 tags peroxisomes for degradation in *Saccharomyces cerevisiae*. *EMBO J.* *31*, 2852–2868.
- Mozdy, A.D., McCaffery, J.M., and Shaw, J.M. (2000). Dnm1p GTPase-mediated mitochondrial fission is a multi-step process requiring the novel integral membrane component Fis1p. *J. Cell Biol.* *151*, 367–380.
- Müller, M., Lu, K., and Reichert, A.S. (2015). Mitophagy and mitochondrial dynamics in *Saccharomyces cerevisiae*. *Biochim. Biophys. Acta* *1853*, 2766–2774.
- Murley, A., Lackner, L.L., Osman, C., West, M., Voeltz, G.K., Walter, P., and Nunnari, J. (2013). ER-associated mitochondrial division links the distribution of mitochondria and mitochondrial DNA in yeast. *ELife* *2*, e00422.
- Neupert, W., and Herrmann, J.M. (2007). Translocation of proteins into mitochondria. *Annu. Rev. Biochem.* *76*, 723–749.
- Novelli, G., and D'Apice, M.R. (2012). Protein farnesylation and disease. *J. Inherit. Metab. Dis.* *35*, 917–926.
- Nunnari, J., and Suomalainen, A. (2012). Mitochondria: in sickness and in health. *Cell* *148*, 1145–1159.
- Nyathi, Y., Wilkinson, B.M., and Pool, M.R. (2013). Co-translational targeting and translocation of proteins to the endoplasmic reticulum. *Biochim. Biophys. Acta* *1833*, 2392–2402.
- Okamoto, K., Kondo-Okamoto, N., and Ohsumi, Y. (2009). Mitochondria-anchored receptor Atg32 mediates degradation of mitochondria via selective autophagy. *Dev. Cell* *17*, 87–97.
- Okreglak, V., and Walter, P. (2014). The conserved AAA-ATPase Msp1 confers organelle specificity to tail-anchored proteins. *Proc. Natl. Acad. Sci. U. S. A.* *111*, 8019–8024.
- Okumoto, K., Ono, T., Toyama, R., Shimomura, A., Nagata, A., and Fujiki, Y. (2018). New splicing variants of mitochondrial Rho GTPase-1 (Miro1) transport peroxisomes. *J. Cell Biol.* *217*, 619–633.
- Osellame, L.D., Blacker, T.S., and Duchon, M.R. (2012). Cellular and molecular mechanisms of mitochondrial function. *Best Pract. Res. Clin. Endocrinol. Metab.* *26*, 711–723.
- Palmer, C.S., Osellame, L.D., Laine, D., Koutsopoulos, O.S., Frazier, A.E., and Ryan, M.T. (2011). MiD49 and MiD51, new components of the mitochondrial fission machinery. *EMBO Rep.* *12*, 565–573.
- Palmfeldt, J., and Bross, P. (2017). Proteomics of human mitochondria. *Mitochondrion* *33*, 2–14.

- Papic, D., Krumpke, K., Dukanovic, J., Dimmer, K.S., and Rapaport, D. (2011). Multispan mitochondrial outer membrane protein Ugo1 follows a unique Mim1-dependent import pathway. *J. Cell Biol.* *194*, 397–405.
- Papić, D., Elbaz-Alon, Y., Koerdts, S.N., Leopold, K., Worm, D., Jung, M., Schuldiner, M., and Rapaport, D. (2013). The role of Djp1 in import of the mitochondrial protein Mim1 demonstrates specificity between a cochaperone and its substrate protein. *Mol. Cell. Biol.* *33*, 4083–4094.
- Pfanner, N., Müller, H.K., Harmey, M.A., and Neupert, W. (1987). Mitochondrial protein import: involvement of the mature part of a cleavable precursor protein in the binding to receptor sites. *EMBO J.* *6*, 3449–3454.
- Pfund, C., Lopez-Hoyo, N., Ziegelhoffer, T., Schilke, B.A., Lopez-Buesa, P., Walter, W.A., Wiedmann, M., and Craig, E.A. (1998). The molecular chaperone Ssb from *Saccharomyces cerevisiae* is a component of the ribosome-nascent chain complex. *EMBO J.* *17*, 3981–3989.
- Popov-Celeketić, J., Waizenegger, T., and Rapaport, D. (2008). Mim1 functions in an oligomeric form to facilitate the integration of Tom20 into the mitochondrial outer membrane. *J. Mol. Biol.* *376*, 671–680.
- Rabu, C., Wipf, P., Brodsky, J.L., and High, S. (2008). A Precursor-specific Role for Hsp40/Hsc70 during Tail-anchored Protein Integration at the Endoplasmic Reticulum. *J. Biol. Chem.* *283*, 27504–27513.
- Rao, M., Okreglak, V., Chio, U.S., Cho, H., Walter, P., and Shan, S.-O. (2016). Multiple selection filters ensure accurate tail-anchored membrane protein targeting. *ELife* *5*.
- Rivera-Monroy, J., Musiol, L., Unthan-Fechner, K., Farkas, Á., Clancy, A., Coy-Vergara, J., Weill, U., Gockel, S., Lin, S.-Y., Corey, D.P., et al. (2016). Mice lacking WRB reveal differential biogenesis requirements of tail-anchored proteins in vivo. *Sci. Rep.* *6*.
- Rucktäschel, R., Thoms, S., Sidorovitch, V., Halbach, A., Pechlivanis, M., Volkmer, R., Alexandrov, K., Kuhlmann, J., Rottensteiner, H., and Erdmann, R. (2009). Farnesylation of pex19p is required for its structural integrity and function in peroxisome biogenesis. *J. Biol. Chem.* *284*, 20885–20896.
- Sacksteder, K.A., Jones, J.M., South, S.T., Li, X., Liu, Y., and Gould, S.J. (2000). PEX19 binds multiple peroxisomal membrane proteins, is predominantly cytoplasmic, and is required for peroxisome membrane synthesis. *J. Cell Biol.* *148*, 931–944.
- Sahi, C., and Craig, E.A. (2007). Network of general and specialty J protein chaperones of the yeast cytosol. *Proc. Natl. Acad. Sci. U. S. A.* *104*, 7163–7168.

- Schliebs, W., Girzalsky, W., and Erdmann, R. (2010). Peroxisomal protein import and ERAD: variations on a common theme. *Nat. Rev. Mol. Cell Biol.* *11*, 885–890.
- Schmidt, F., Dietrich, D., Eylenstein, R., Groemping, Y., Stehle, T., and Dodt, G. (2012). The role of conserved PEX3 regions in PEX19-binding and peroxisome biogenesis. *Traffic Cph. Den.* *13*, 1244–1260.
- Schrader, M., Costello, J., Godinho, L.F., and Islinger, M. (2015). Peroxisome-mitochondria interplay and disease. *J. Inherit. Metab. Dis.* *38*, 681–702.
- Schrader, M., Costello, J.L., Godinho, L.F., Azadi, A.S., and Islinger, M. (2016). Proliferation and fission of peroxisomes - An update. *Biochim. Biophys. Acta* *1863*, 971–983.
- Schrul, B., and Kopito, R.R. (2016). Peroxin-Dependent Targeting of a Lipid Droplet-Destined Membrane Protein to ER-subdomains. *Nat. Cell Biol.* *18*, 740–751.
- Schuldiner, M., Metz, J., Schmid, V., Denic, V., Rakwalska, M., Schmitt, H.D., Schwappach, B., and Weissman, J.S. (2008). The GET Complex Mediates Insertion of Tail-Anchored Proteins into the ER Membrane. *Cell* *134*, 634–645.
- Setoguchi, K., Otera, H., and Mihara, K. (2006). Cytosolic factor- and TOM-independent import of C-tail-anchored mitochondrial outer membrane proteins. *EMBO J.* *25*, 5635–5647.
- Sherman, E.L., Go, N.E., and Nargang, F.E. (2005). Functions of the Small Proteins in the TOM Complex of *Neurospora crassa*. *Mol. Biol. Cell* *16*, 4172–4182.
- Smith, J.J., and Aitchison, J.D. (2013). Peroxisomes take shape. *Nat. Rev. Mol. Cell Biol.* *14*, 803–817.
- Speijer, D. (2017). Evolution of peroxisomes illustrates symbiogenesis. *BioEssays News Rev. Mol. Cell. Dev. Biol.* *39*.
- Stojanovski, D., Guiard, B., Kozjak-Pavlovic, V., Pfanner, N., and Meisinger, C. (2007). Alternative function for the mitochondrial SAM complex in biogenesis of α -helical TOM proteins. *J. Cell Biol.* *179*, 881–893.
- Sugiura, A., Mattie, S., Prudent, J., and McBride, H.M. (2017). Newly born peroxisomes are a hybrid of mitochondrial and ER-derived pre-peroxisomes. *Nature* *542*, 251–254.
- Tanabe, Y., Maruyama, J., Yamaoka, S., Yahagi, D., Matsuo, I., Tsutsumi, N., and Kitamoto, K. (2011). Peroxisomes are involved in biotin biosynthesis in *Aspergillus* and *Arabidopsis*. *J. Biol. Chem.* *286*, 30455–30461.
- Thornton, N., Stroud, D.A., Milenkovic, D., Guiard, B., Pfanner, N., and Becker, T. (2010). Two modular forms of the mitochondrial sorting and assembly

- machinery are involved in biogenesis of alpha-helical outer membrane proteins. *J. Mol. Biol.* **396**, 540–549.
- Towbin, H., Staehelin, T., and Gordon, J. (1979). Electrophoretic transfer of proteins from polyacrylamide gels to nitrocellulose sheets: procedure and some applications. *Proc. Natl. Acad. Sci. U. S. A.* **76**, 4350–4354.
- Vergheze, J., Abrams, J., Wang, Y., and Morano, K.A. (2012). Biology of the Heat Shock Response and Protein Chaperones: Budding Yeast (*Saccharomyces cerevisiae*) as a Model System. *Microbiol. Mol. Biol. Rev.* **MMBR 76**, 115–158.
- Vogel, M., Mayer, M.P., and Bukau, B. (2006a). Allosteric regulation of Hsp70 chaperones involves a conserved interdomain linker. *J. Biol. Chem.* **281**, 38705–38711.
- Vogel, M., Bukau, B., and Mayer, M.P. (2006b). Allosteric regulation of Hsp70 chaperones by a proline switch. *Mol. Cell* **21**, 359–367.
- Vögtle, F.-N., Wortelkamp, S., Zahedi, R.P., Becker, D., Leidhold, C., Gevaert, K., Kellermann, J., Voos, W., Sickmann, A., Pfanner, N., et al. (2009). Global analysis of the mitochondrial N-proteome identifies a processing peptidase critical for protein stability. *Cell* **139**, 428–439.
- Wach, A., Brachat, A., Pöhlmann, R., and Philippsen, P. (1994). New heterologous modules for classical or PCR-based gene disruptions in *Saccharomyces cerevisiae*. *Yeast Chichester Engl.* **10**, 1793–1808.
- Waizenegger, T., Schmitt, S., Zivkovic, J., Neupert, W., and Rapaport, D. (2005). Mim1, a protein required for the assembly of the TOM complex of mitochondria. *EMBO Rep.* **6**, 57–62.
- Wall, D., Zylicz, M., and Georgopoulos, C. (1994). The NH₂-terminal 108 amino acids of the *Escherichia coli* DnaJ protein stimulate the ATPase activity of DnaK and are sufficient for lambda replication. *J. Biol. Chem.* **269**, 5446–5451.
- Waterham, H.R., Ferdinandusse, S., and Wanders, R.J.A. (2016). Human disorders of peroxisome metabolism and biogenesis. *Biochim. Biophys. Acta BBA - Mol. Cell Res.* **1863**, 922–933.
- Wegele, H., Haslbeck, M., Reinstein, J., and Buchner, J. (2003). Sti1 is a novel activator of the Ssa proteins. *J. Biol. Chem.* **278**, 25970–25976.
- Werner-Washburne, M., Stone, D.E., and Craig, E.A. (1987). Complex interactions among members of an essential subfamily of hsp70 genes in *Saccharomyces cerevisiae*. *Mol. Cell. Biol.* **7**, 2568–2577.
- Wessel, D., and Flügge, U.I. (1984). A method for the quantitative recovery of protein in dilute solution in the presence of detergents and lipids. *Anal. Biochem.* **138**, 141–143.

- Westermann, B. (2014). Mitochondrial inheritance in yeast. *Biochim. Biophys. Acta* 1837, 1039–1046.
- Whitley, D., Goldberg, S.P., and Jordan, W.D. (1999). Heat shock proteins: a review of the molecular chaperones. *J. Vasc. Surg.* 29, 748–751.
- Wiedemann, N., and Pfanner, N. (2017). Mitochondrial Machineries for Protein Import and Assembly. *Annu. Rev. Biochem.* 86, 685–714.
- Williams, C., Opalinski, L., Landgraf, C., Costello, J., Schrader, M., Krikken, A.M., Knoops, K., Kram, A.M., Volkmer, R., and van der Klei, I.J. (2015). The membrane remodeling protein Pex11p activates the GTPase Dnm1p during peroxisomal fission. *Proc. Natl. Acad. Sci. U. S. A.* 112, 6377–6382.
- Williams, C.C., Jan, C.H., and Weissman, J.S. (2014). Targeting and plasticity of mitochondrial proteins revealed by proximity-specific ribosome profiling. *Science* 346, 748–751.
- Wright, C.M., Chovatiya, R.J., Jameson, N.E., Turner, D.M., Zhu, G., Werner, S., Huryn, D.M., Pipas, J.M., Day, B.W., Wipf, P., et al. (2008). Pyrimidinone-peptoid hybrid molecules with distinct effects on molecular chaperone function and cell proliferation. *Bioorg. Med. Chem.* 16, 3291–3301.
- Yagita, Y., Hiromasa, T., and Fujiki, Y. (2013). Tail-anchored PEX26 targets peroxisomes via a PEX19-dependent and TRC40-independent class I pathway. *J. Cell Biol.* 200, 651–666.
- Yamamoto, Y., and Sakisaka, T. (2018). The peroxisome biogenesis factors posttranslationally target reticulon homology domain-containing proteins to the endoplasmic reticulum membrane. *Sci. Rep.* 8, 2322.
- Yamano, K., Yatsukawa, Y.-I., Esaki, M., Hobbs, A.E.A., Jensen, R.E., and Endo, T. (2008). Tom20 and Tom22 share the common signal recognition pathway in mitochondrial protein import. *J. Biol. Chem.* 283, 3799–3807.
- Yamano, K., Tanaka-Yamano, S., and Endo, T. (2010). Tom7 regulates Mdm10-mediated assembly of the mitochondrial import channel protein Tom40. *J. Biol. Chem.* 285, 41222–41231.
- Yoshida, Y., Niwa, H., Honsho, M., Itoyama, A., and Fujiki, Y. (2015). Pex11 mediates peroxisomal proliferation by promoting deformation of the lipid membrane. *Biol. Open* 4, 710–721.
- Youle, R.J., and Karbowski, M. (2005). Mitochondrial fission in apoptosis. *Nat. Rev. Mol. Cell Biol.* 6, 657–663.
- Young, J.C., Hoogenraad, N.J., and Hartl, F.U. (2003). Molecular chaperones Hsp90 and Hsp70 deliver preproteins to the mitochondrial import receptor Tom70. *Cell* 112, 41–50.

- van der Zand, A., Braakman, I., and Tabak, H.F. (2010). Peroxisomal Membrane Proteins Insert into the Endoplasmic Reticulum. *Mol. Biol. Cell* 21, 2057–2065.
- van der Zand, A., Gent, J., Braakman, I., and Tabak, H.F. (2012). Biochemically distinct vesicles from the endoplasmic reticulum fuse to form peroxisomes. *Cell* 149, 397–409.

Acknowledgments

First I would like to express my sincere gratitude to Prof. Dr. Doron Rapaport for the opportunity of doing my PhD thesis in his laboratory. I especially would like to thank him for introducing me to the field of mitochondrial proteomics, his supervision and scientific approach.

I would like to thank Prof. Dr. Gabriele Dodt for being my supervisor, and her and Prof. Dr. Ralph Jansen and Dr. Christopher Grefen for their valuable time and effort to be members of my doctoral examination committee.

I would like to thank all the lab members, colleagues and friends from student to postdoc which I had the opportunity to meet in the last four years. Elena, for the good jokes and help, Tobias for all the enormous scientific input, Kai for his help and advices, Daniela and Enzo for all the pick-ups and because TAMPTing rules, Janani for being kind of a maternal figure in the lab, Diana for being the best neighbor I ever had, Ravi and Lena for all the cooking and great holidays, Thomas for the calm attitude, Moni for showing me Tübingen for the first time, Hoda for halva, Jailin for offering me constantly water and cookies, Fenia for the solo voice, Johannes for really good jokes and Layla for taking over the closing duty of the lab.

I would also like to deeply thank Patrycja for the exhaustive critical reading of my thesis, for her patience, for cheering me up when I needed it and especially for all the trust she had in me.

A very special thank you goes to my family because they never stopped believing in me. To my parents for the invaluable advices and for supporting me during this time and before, even when I was far away from home. To my sister and my nephew for giving me the opportunity to be a child again. And to my brother for constantly asking me when the thesis will be ready. And now it is done.

Curriculum Vitae

Personal information:

Name: Bogdan

Last Name: Cichocki

Date and place of birth: 26.12.88 Aachen

Address: Moltkestr.55/50, 72072 Tübingen

Nationality: Polish

School education:

- 1994-1999 - Willy Brandt Schule Warschau
- 1999-2001 - Ground school nr.56 im. Księcia Adama Czartoryskiego
- 2001-2004 - Gymnasium nr.56 im. Księcia Adama Czartoryskiego
- 2004-2007 - Liceum nr.64 im. Stanisława Witkacego
- Juni 2007 - Abitur/Matura

Academical education:

- 2007 – 2010 - Bachelor studies. Biotechnology studies at the Warsaw University
- August 2010- Bachelor of science
- 2010 – 2012- Master studies. Biotechnology studies at the Warsaw University
- September 2012 - Master of science
- 2013 - 2018- PhD research in the laboratory of Prof. Doron Rapaport at the Interfaculty Institute of Biochemistry, University of Tübingen, Germany